Groundwater Availability of the Trinity Aquifer, Hill Country Area, Texas: Numerical Simulations through 2050

Report 353

by
Robert E. Mace
Ali H. Chowdhury
Roberto Anaya
Shao-Chih (Ted) Way

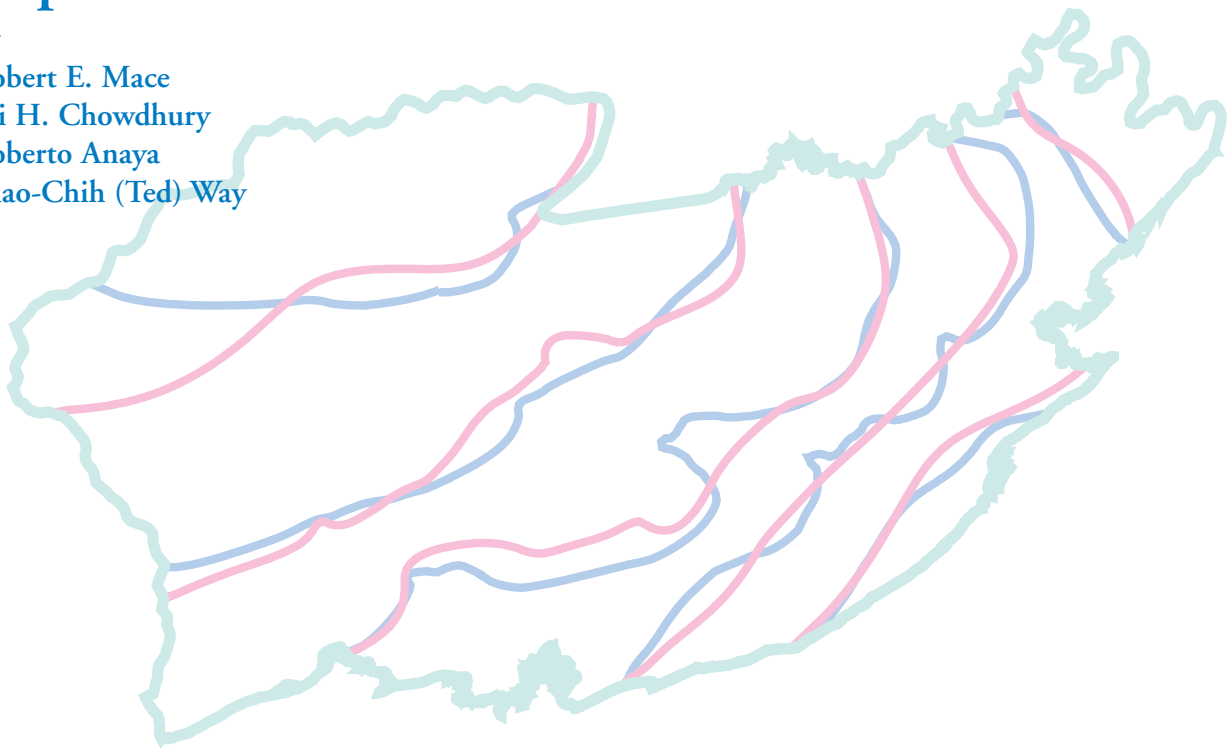

Texas Water Development Board
P.O. Box 13231
Austin, Texas 78711-3231
1(512) 936-0861, robert.mace@twdb.state.tx.us

September 2000

Table of Contents

List of Figures

List of Figures *(cont'd.)*

List of Tables

Groundwater Availability of the Trinity Aquifer, Hill Country Area, Texas: Numerical Simulations through 2050

Abstract

A three-dimensional, numerical groundwater flow model of the Middle Trinity aquifer in the Hill Country area of south-central Texas was developed to help estimate groundwater availability and water levels in response to pumping and potential future droughts. The model includes historical information on the aquifer and incorporates results of new studies on water levels, structure, hydraulic properties, and recharge rates. A steady-state model was calibrated for 1975 hydrologic conditions when water levels in the aquifer were near equilibrium, and a transient model was calibrated for 1996 through 1997 when the climate transitioned from a dry to a wet period. Using the model, values of recharge, hydraulic conductivity, specific storage, and specific yield were calibrated for the aquifer. The model was used to predict future water levels and saturated thickness under drought-of-record conditions using estimates of future groundwater demands based on demand numbers from the Regional Water Planning Groups. The model predicts that the area near Cibolo Creek in northern Bexar, southern Kendall, and western Comal counties is the most susceptible to future water-level declines due to increased demand and potential droughts. If a drought similar to the drought-of-record occurs in the future, the model suggests that water levels may decrease as much as 100 ft in this area by 2010 and that a large part of the aquifer may be depleted in this area by 2030. The model suggests that water levels may decline nearly 100 ft in the Dripping Springs area by 2040. Hays, Blanco, Travis, southeastern Kerr, and eastern Bandera counties may experience moderate water-level declines (50 to 100 ft) in response to projected demands and potential drought as early as 2010. The model suggests that major rivers may continue to flow seasonally even with increased pumping and under drought conditions.

Introduction

The Trinity aquifer in south-central Texas is an important source of groundwater to municipalities, industries, and landowners in the Hill Country area. New development and recent droughts have increased interest in the Trinity aquifer and have heightened concerns about groundwater availability in the aquifer. Many landowners want to know how pumping and drought affect water levels and impact groundwater resources and the environment. Regional Water Planning Groups are required by Senate Bill 1 to plan for future water needs under drought conditions and are similarly interested in future groundwater availability in the Hill Country.

Although the Trinity aquifer is recognized by the State as a major aquifer (Ashworth and Hopkins, 1995), yields in the aquifer can be comparatively lower than other major aquifers.

For example, average yields in the Trinity aquifer in the Hill Country are about 250 times lower than average yields in the Edwards (Balcones Fault Zone [BFZ]) aquifer immediately to the south. Lower yields combined with water-level fluctuations and greater pumping decrease the reliability of the Trinity aquifer in the Hill Country as a source of water in times of drought.

Several studies have noted the vulnerability of the Trinity aquifer to drought and increased pumping. Ashworth (1983) concluded that heavy pumping is resulting in rapid water-level declines in certain areas and that continued growth would result in continued water-level declines. Bluntzer (1992) noted that concentrated withdrawals of water had caused water-level declines, decreased well yields, and increased the potential for the encroachment of poorer quality water and the depletion of base flow in nearby streams. Simpson and others (1993) noted that groundwater withdrawals exceeding the groundwater availability would result in water-level declines, reduced well yields, and a possible deterioration of water quality in northern Bexar County. Kalaswad and Mills (2000) agreed with these conclusions in a later report.

A numerical groundwater flow model is a tool that can help predict how an aquifer might respond to increased pumping and drought. A groundwater flow model is a numerical representation of the aquifer in a computer. Information about the aquifer (such as aquifer properties and water-level changes) is used to constrain the numerical model so that the model is a realistic approximation of the actual aquifer. Once an aquifer model is completed, it can be a valuable tool to evaluate the effects of pumping, drought, and different aquifer-management scenarios on water resources in an aquifer.

In this study, we developed a three-dimensional finite-difference groundwater flow model for the Trinity aquifer in the Hill Country as a tool to (1) improve our conceptual understanding of groundwater flow in the region; (2) develop a management tool to support water-planning efforts for Regional Water Planning Groups, Groundwater Conservation Districts, and River Authorities in the area; and (3) evaluate groundwater availability under drought-of-record conditions. This report describes the construction and calibration of the numerical model and presents results of predictive simulations of water levels for the next 50 years based on projected demands from Regional Water Planning Groups. This final report supercedes an interim report published earlier on the construction and calibration of the model (Mace and others, 2000). Besides results from predictive simulations, this final report includes additional details on model construction and calibration and addresses some errors and omissions in the interim report.

Our general approach involved (1) developing the conceptual model, (2) organizing and distributing aquifer information for entering into the model, (3) calibrating a steady-state model for 1975, (4) calibrating and verifying a transient model for 1996 and 1997, and (5) making predictive simulations. This report describes (1) the study area, previous work, and hydrogeologic setting used to develop the conceptual model; (2) the code, grid, and model parameters assigned during model construction; (3) the calibration and sensitivity analysis of steady-state and transient models; (4) predictions of water-level changes; (5) the limitations of the current model; and (6) suggestions for future improvements.

Study Area

The study area is located in the Hill Country of south-central Texas and includes all or parts of Bandera, Bexar, Blanco, Comal, Gillespie, Hays, Kendall, Kerr, Medina, Travis, and Uvalde counties (fig. 1). Hydrologic boundaries define the boundaries of the study area. These boundaries include (1) major faults in the Balcones Fault Zone to the east and south,

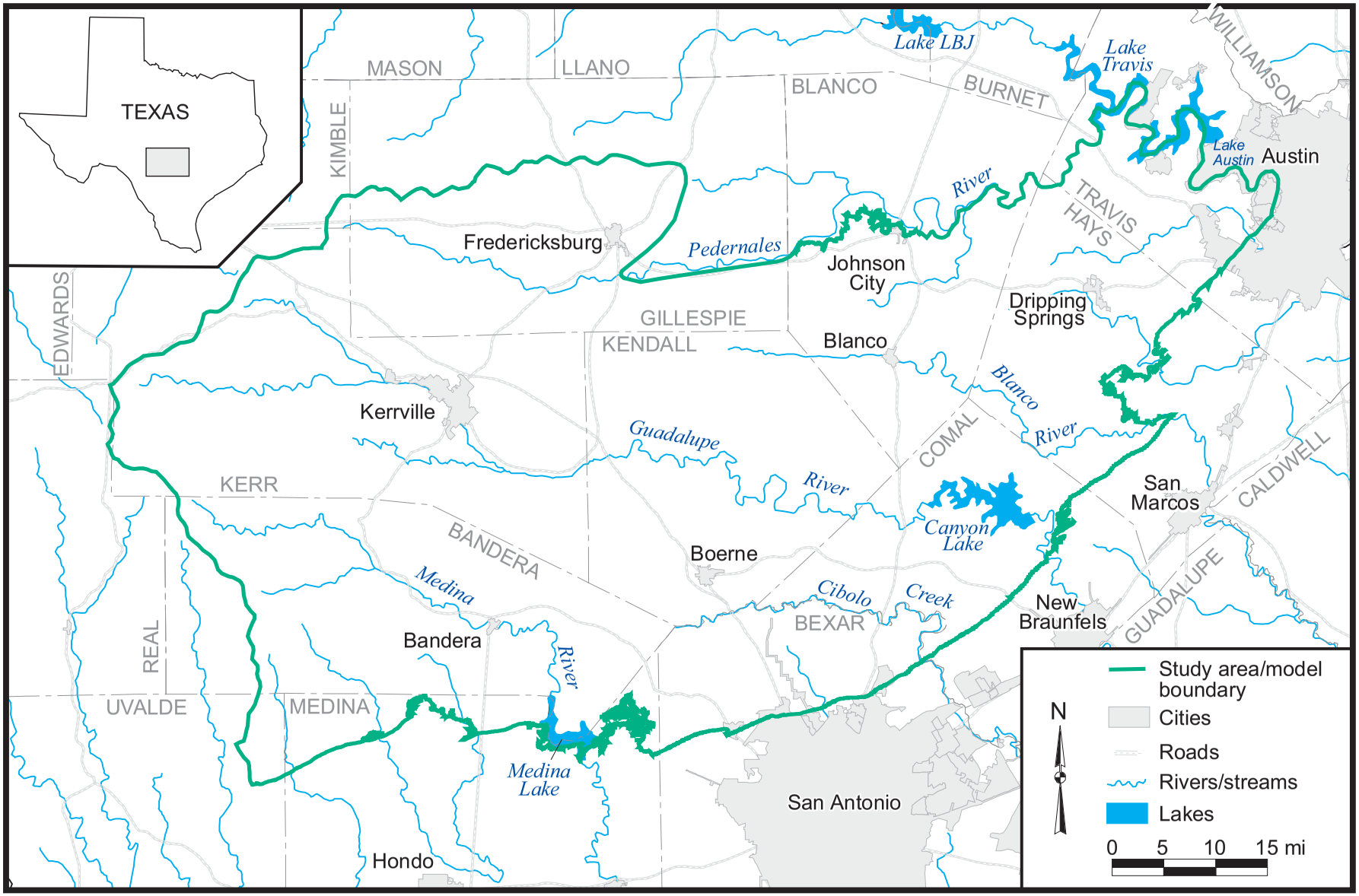

Figure 1: Location of the study area relative to roads, major cities and towns, lakes, and rivers.

(2) presumed groundwater flow paths to the west, and (3) outcrop or rivers to the north (fig. 1). Because we chose groundwater flow paths to the west, the study area does not include the entire Hill Country area (i.e. parts of Bandera and Uvalde counties) and includes the easternmost parts of the Edwards-Trinity (Plateau) aquifer (see Ashworth and Hopkins, 1995) in Bandera, Gillespie, Kendall, and Kerr counties (fig. 2).

The study area includes parts of three regional water-planning areas: (1) the Lower Colorado Region (Region K), (2) the South Central Texas Region (Region L), and (3) the Plateau Region (Region J) (fig. 3). The study area includes all or parts of several Groundwater Conservation Districts including (1) Hill Country Underground Water Conservation District, (2) Headwaters Underground Water Conservation District, (3) Springhills Water Management District, (4) Cow Creek Groundwater Conservation District, (5) Southeast Trinity Groundwater Conservation District, (6) Hays Trinity Groundwater Conservation District, (7) Medina County Groundwater Conservation District, and (8) Uvalde County Underground Water Conservation District (fig. 4). The study area overlies parts of the Edwards Aquifer Authority, particularly in northern Bexar County (fig. 4). Hays Trinity Groundwater Conservation District, Southeast Trinity Groundwater Conservation District, and Cow Creek Groundwater Conservation District are Senate Bill 1911 districts awaiting confirmation by the Texas Legislature in the 2001 session. The study area also overlies four River Authorities: (1) the Lower Colorado River Authority (which includes Blanco and Travis counties in the study area), (2) the Guadalupe-Blanco River Authority (which includes Comal, Hays, and Kendall counties in the study area), (3) the Upper Guadalupe River Authority (which includes Kerr County), and (4) the Nueces River Authority (which includes Bandera, Medina, and Uvalde counties in the study area).

Physiography and Climate

The study area is located along the southeastern margin of the Edwards Plateau region commonly referred to as the Texas Hill Country. The Texas Hill Country is also known as the Balcones Canyonlands sub-region, a terrain deeply dissected by the head-ward erosion of major streams with steep gradients from the plateau to the base of the Balcones Escarpment. The Balcones Escarpment was formed during the Tertiary period by faulting along the Balcones Fault Zone, a zone of northeast-southwest trending normal faults parallel to the Texas Gulf Coast. Land-surface elevations across the study area range from 2,400 feet above sea level in the west to about 800 feet along the Balcones Fault Zone (fig. 5).

The more massive and resistant carbonate members of the Edwards Group form the nearly flat uplands of the Edwards Plateau in the west and the topographic divides in the central portion of the study area. The differential weathering of alternating beds of hard limestones and dolomites with soft marls and shales of the Glen Rose Limestone form the characteristic stair-step topography of the Balcones Canyonlands. In general, the Glen Rose Limestone is much less resistant to erosion than the Edwards Group caprock.

The study area is characterized by a subhumid to semi-arid climate. A gradual decrease in mean annual precipitation occurs from east to west (35 inches to 25 inches) due to an increase in topographic elevation and increasing distance from the Gulf of Mexico (Carr, 1967). Historical annual precipitation varies from less than 10 inches to more than 60 inches (fig. 6). Precipitation has a bimodal distribution during the year with most of the rainfall occurring in the spring and fall. During the spring, weak cool fronts begin to stall and mix with warm moist air from the Gulf of Mexico. During the summer, sparse rainfall is due to infrequent convectional thunderstorms. In early fall, rainfall is due to more frequent convectional thunderstorms and occasional tropical cyclones that make landfall along the Texas coast. Rainfall

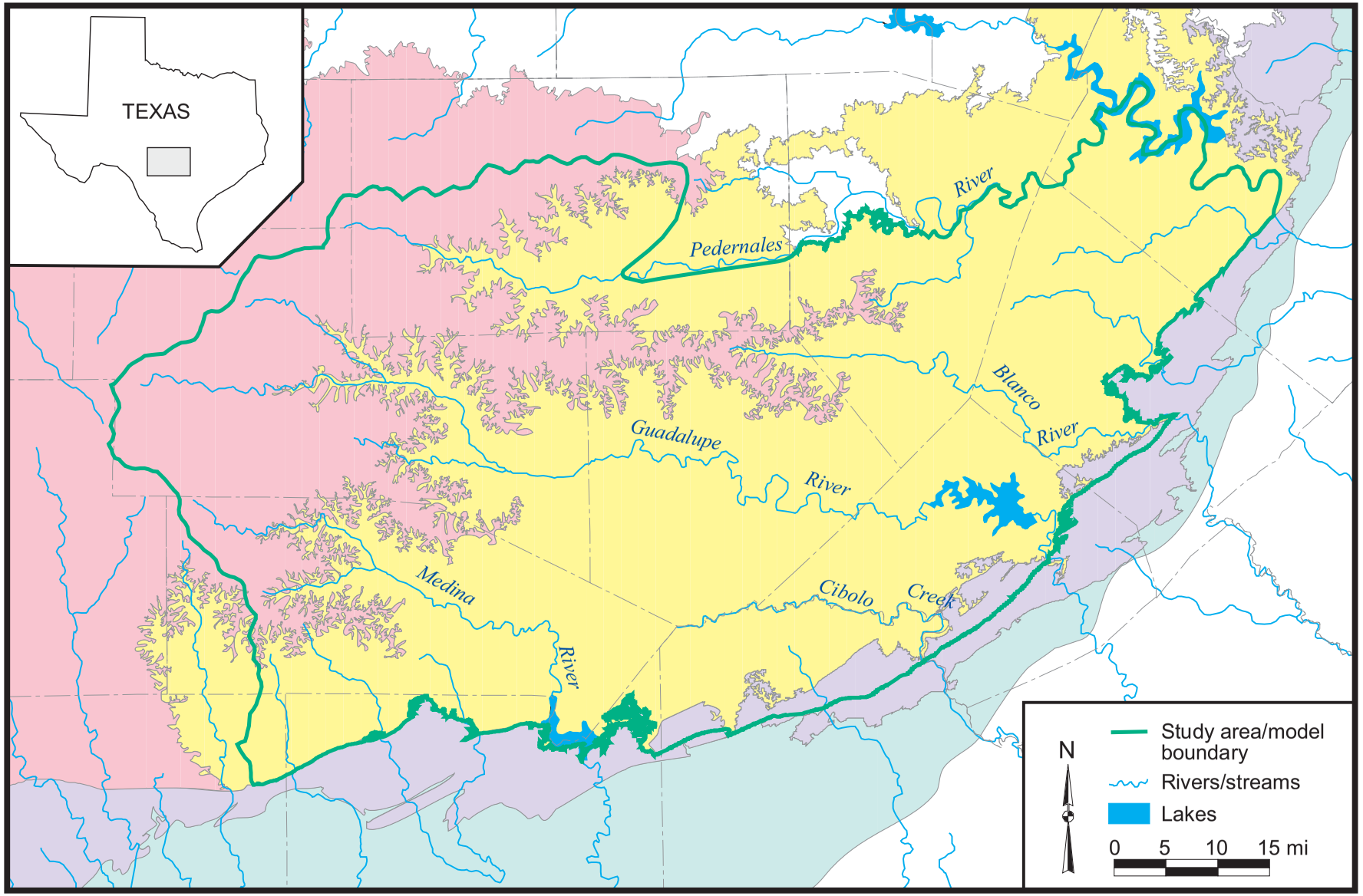

Figure 2. Location of the outcrops of major aquifers in the study area. Sediments of the Trinity aquifer are part of the Edwards-Trinity Plateau aquifer to the west and underlay the Edwards (BFZ) aquifer to the south and east.

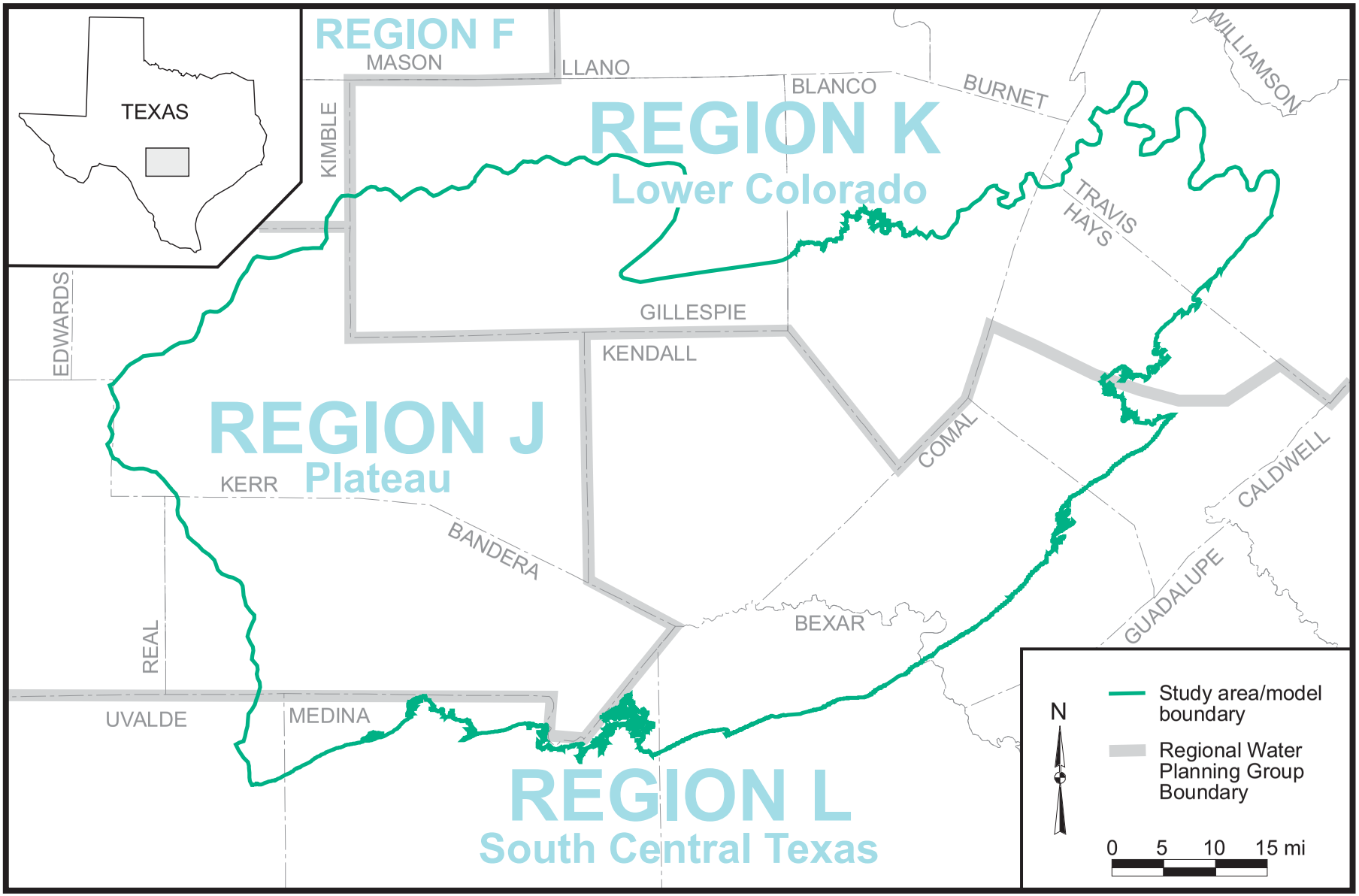

Figure 3. Location of Regional Water Planning Group boundaries in the study area.

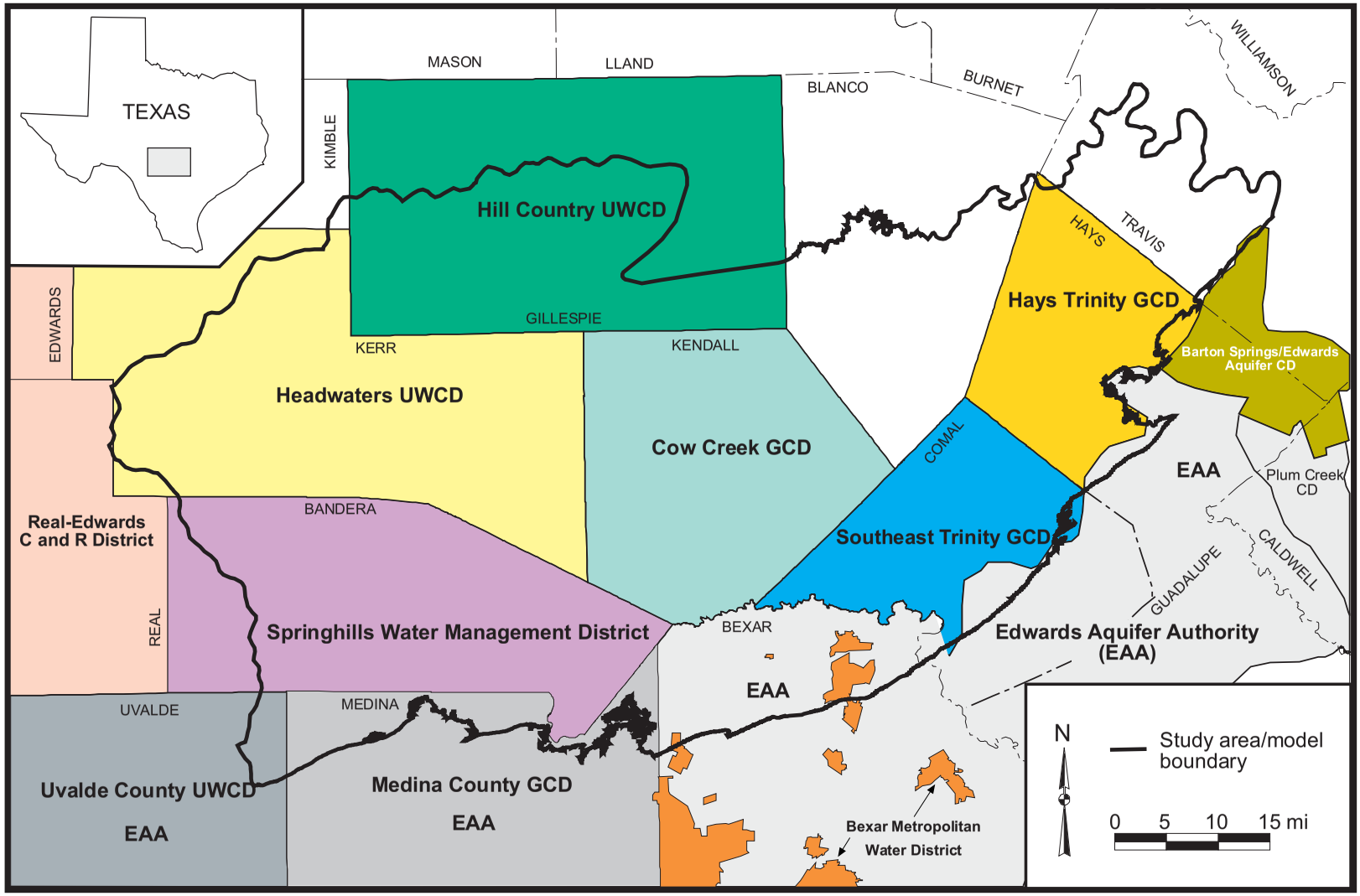

C and R District = Conservation and Reclamation District
UWCD = Underground Water Conservation District
GCD = Groundwater Conservation District
CD = Conservation District

Figure 4. Location of Groundwater Conservation Districts in the study area, Hays Trinity GCD, Southeast Trinity GCD, and Cow Creek GCD are SB 1911 districts awaiting confirmation in the 2001 legislative session.

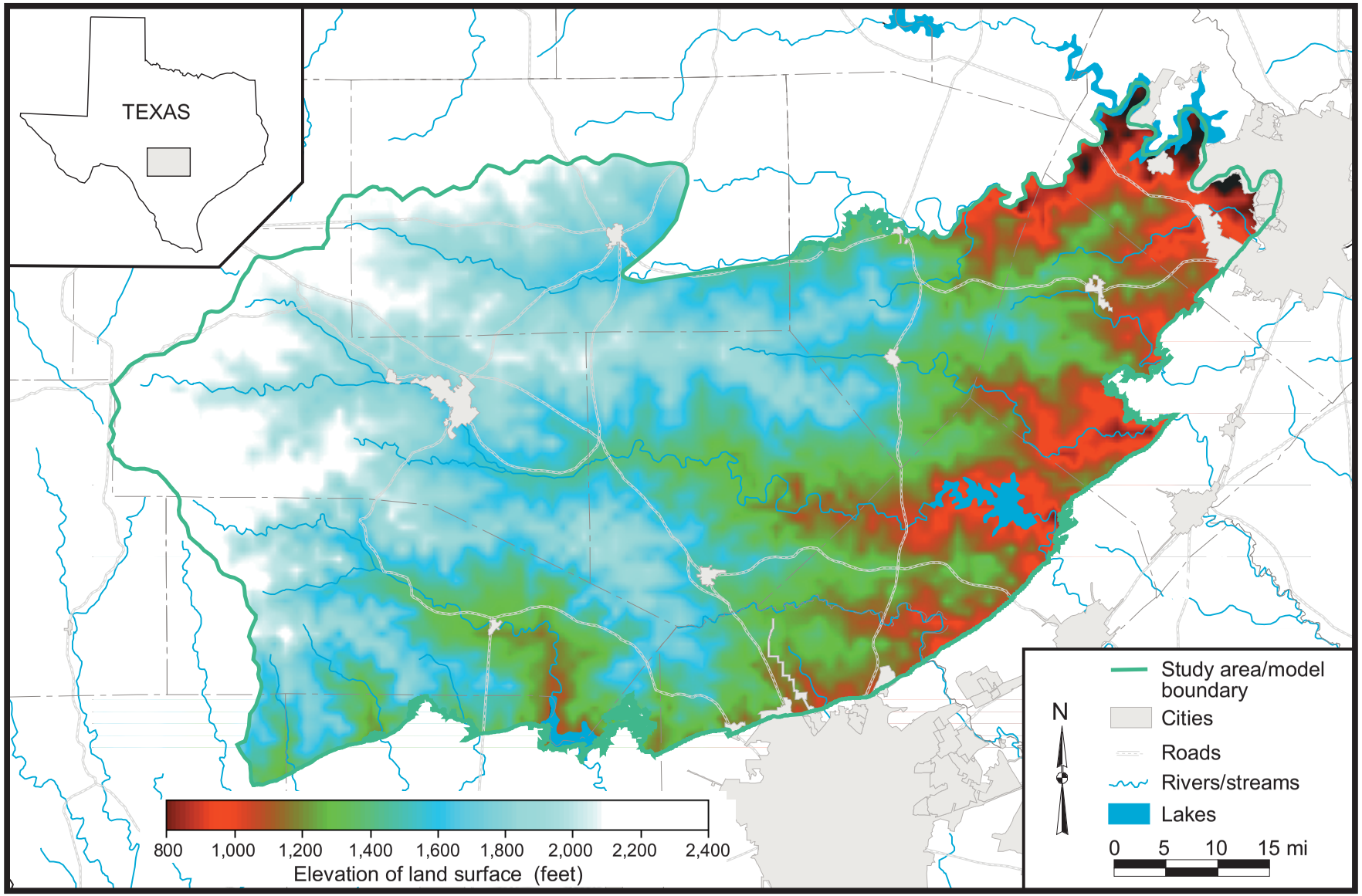

Figure 5. Land-surface elevation in the study area.

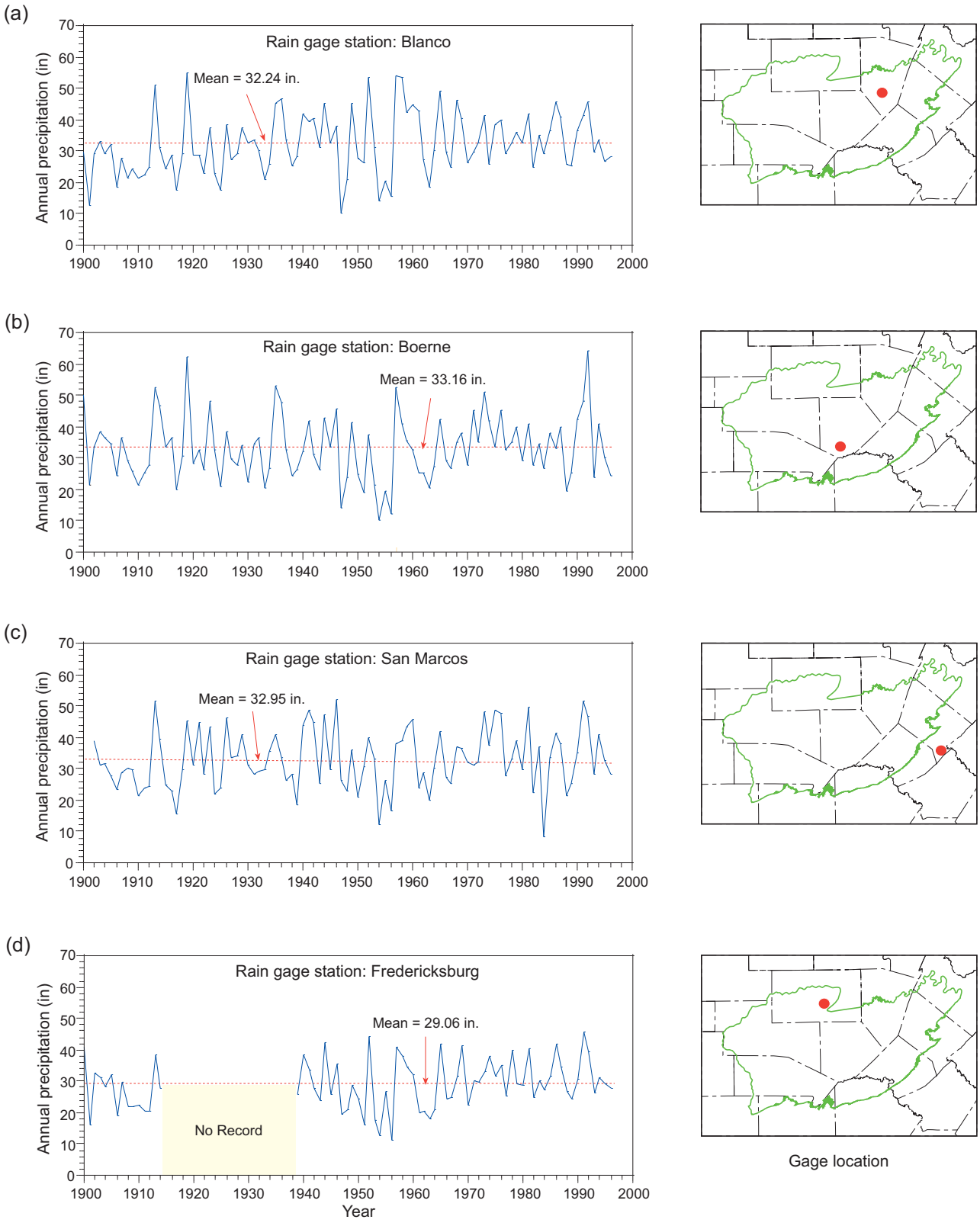

Figure 6. Historical annual precipitation for rain gage stations at (a) Blanco, (b) Boerne, (c) San Marcos, and (d) Fredericksburg.

frequency continues to increase in late fall as cool fronts once again begin to strengthen and mix with the warm moist air masses of the Gulf of Mexico.

Mean annual temperature ranges from 69°F in the west to 63°F in the east (Kuniansky and Holligan, 1994). The average annual (1940-1965) gross lake surface evaporation is more than twice the mean annual precipitation and ranges from 65 inches in the east to 73 inches in the west (Ashworth, 1983).

Geology

Cretaceous rocks unconformably overlie Paleozoic rocks in the study area (fig. 7). The Cretaceous rocks in the study area consist of, from oldest to youngest, the Hosston Formation (Sycamore Sand in outcrop), the Sligo Formation (Sycamore Sand in outcrop), the Hammett Shale, the Cow Creek Limestone, the Hensel Sand, the Lower and Upper Members of the Glen Rose Limestone, and the Fort Terrett and Segovia Formations of the Edwards Group (fig. 7). The Hosston Formation, Sligo Formation, Hammett Shale, Cow Creek Limestone, and Hensel Sand form the Travis Peak equivalent. The formations of the Travis Peak equivalent and the Glen Rose Limestone together form the Trinity Group. Cretaceous sediments are locally covered by Quaternary alluvium along streams and rivers.

The Hensel Sand crops out in the northern part of the study area in Gillespie County (fig. 8). The Upper Member of the Glen Rose Limestone is exposed at land surface in most of the study area except where the Lower Member of the Glen Rose Limestone is exposed owing to erosion and where the Edwards Group is exposed on the Edwards-Trinity Plateau to the west and in the Balcones Fault Zone to the east (fig. 8). Details of the geology in the region can be found in Ashworth (1983) and Barker and others (1994).

There is a downdip lateral gradation of the Hensel Sand, Cow Creek Limestone, and Hammet Shale portion of the Travis Peak equivalent into the Pearsall Formation along the southeastern margin of the Balcones Fault Zone. The Pine Island Shale Member, which is the downdip lateral equivalent of the Hammet Shale, forms the base of the Pearsall Formation. The Cow Creek Limestone Member of the Pearsall Formation overlies the Pine Island Shale Member. The shallow marine deposits of the Bexar Shale Member forms the top of the Pearsall Formation and is the downdip equivalent of the Hensel Sand (Barker and others, 1994).

Previous Work

The Texas Water Development Board (TWDB) and the United States Geologic Survey (USGS) have conducted a number of hydrogeologic studies in the Hill Country area. Ashworth (1983), Bluntzer (1992), and Barker and others (1994) review much of the previous geologic and hydrogeologic work done in the area.

One other regional numerical groundwater flow model has been developed and published for the area: a super-regional model developed by the USGS (Kuniansky and Holligan, 1994). Besides the Trinity aquifer in the Hill Country, the USGS model included the Edwards-Trinity (Plateau) and Edwards (BFZ) aquifers and extends almost 400 miles across the State. The purpose of the USGS model was to better understand and describe the regional groundwater flow system. Using the model, Kuniansky and Holligan (1994) defined transmissivity ranges, estimated total flow through the aquifer system, estimated recharge to aquifer, and simulated groundwater flow from the Trinity aquifer into Edwards (BFZ) aquifer. The two-dimensional, finite element, steady-state model was developed as the simplest approximation of the regional flow system. Because the model (1) covers such a large area, (2) lumps many different formations into one layer, and (3) does not simulate water-level changes with time, it is inappropriate for regional water planning.

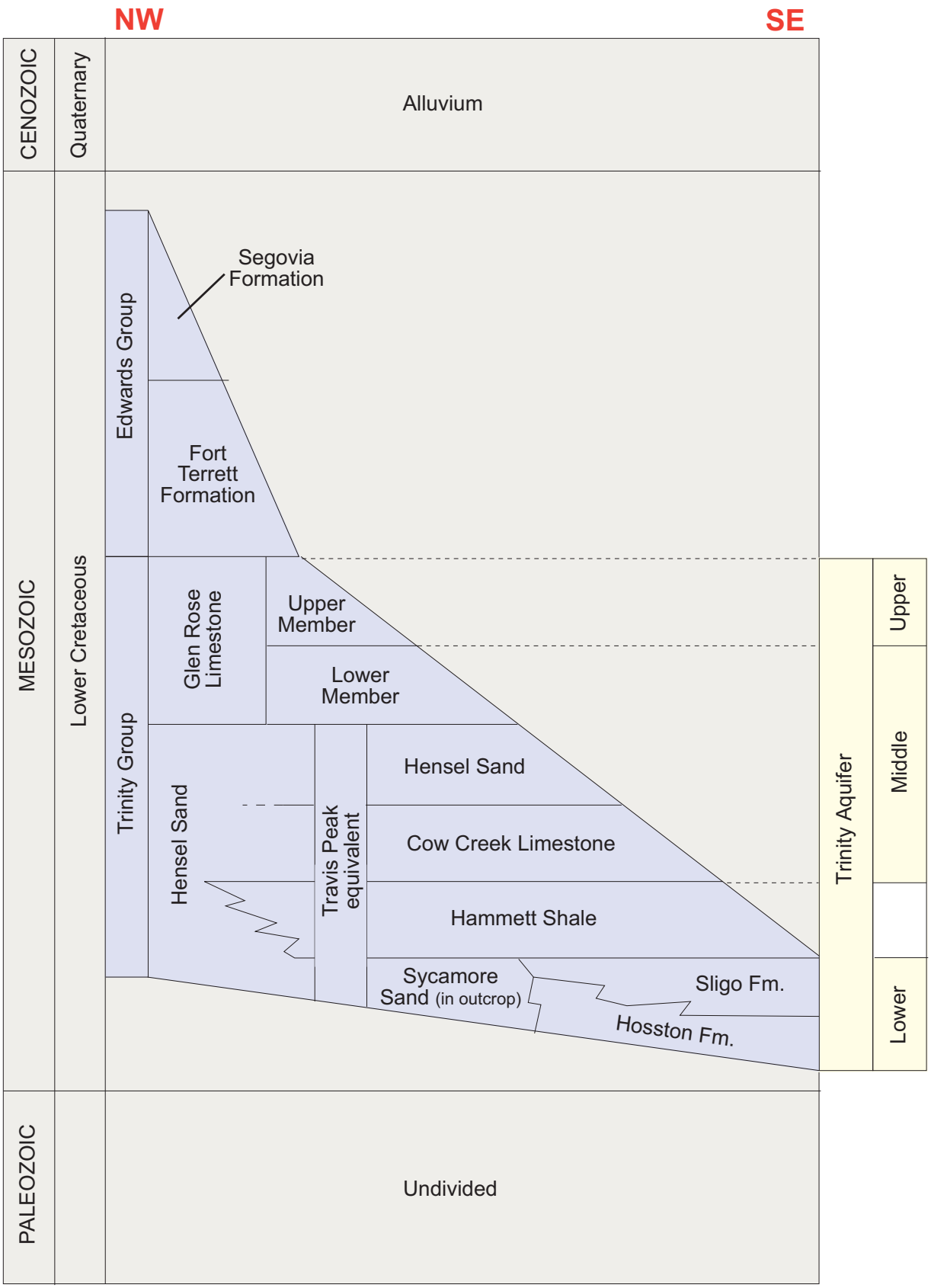

Figure 7. Stratigraphic and hydrostratigraphic section of the Hill Country area (after Ashworth, 1983; Barker and others, 1994).

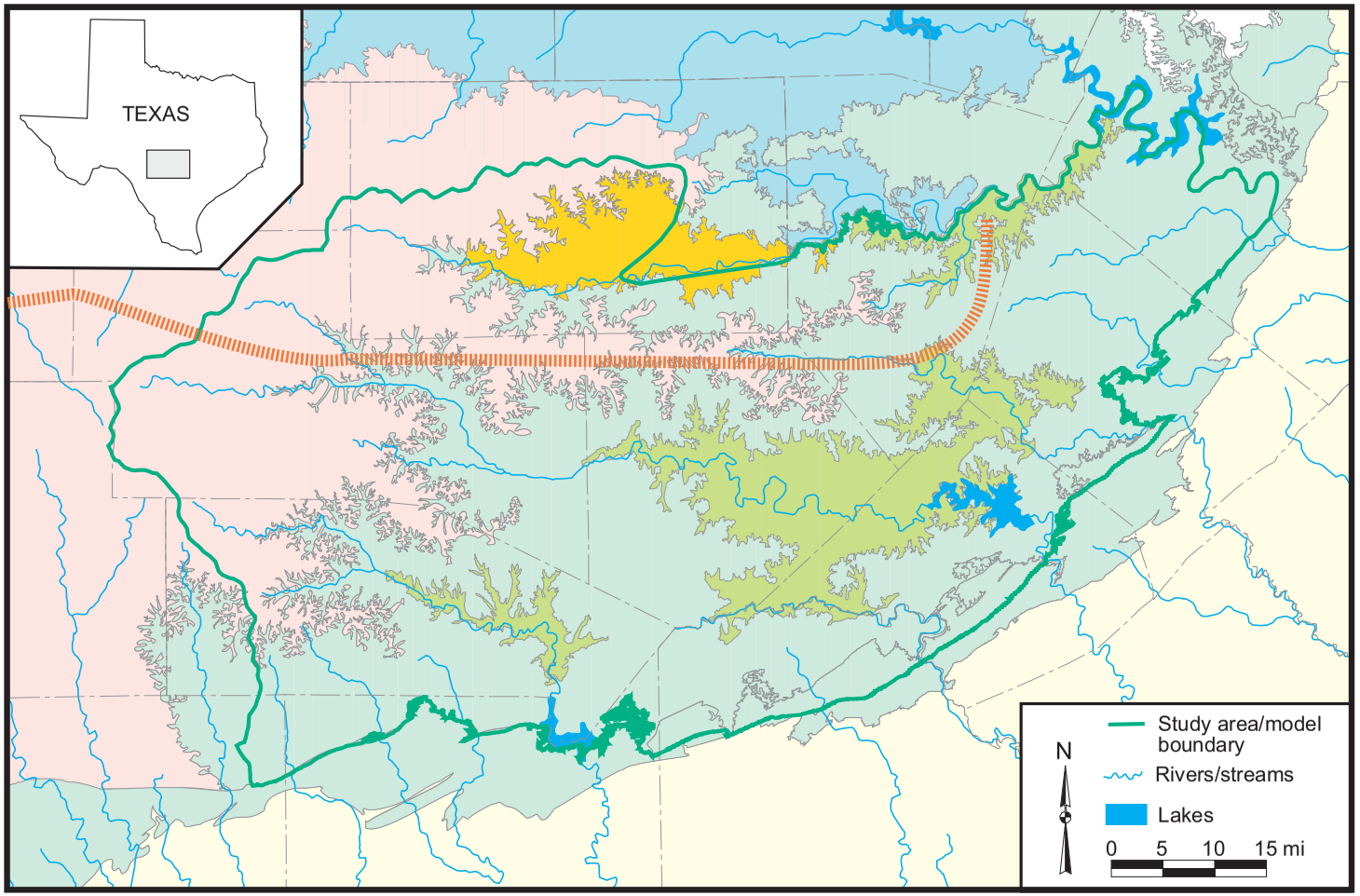

Figure 8. Surface geology in the study area.

Hydrogeologic Setting

The hydrogeologic setting describes the aquifer and the hydrologic features and hydraulic properties that influence groundwater flow in the aquifer. We based the hydrogeologic setting for the Trinity aquifer on previous work (e.g. Ashworth, 1983; Bluntzer, 1992; Barker and others, 1994; Kuniansky and Holligan, 1994) and additional studies we conducted in support of the modeling effort. These additional studies included assembling structure maps, developing water-level maps and hydrographs, quantifying baseflow to streams, investigating recharge rates, conducting aquifer tests, and assembling pumping information.

Hydrostratigraphy

The Trinity aquifer in the Hill Country is comprised of sediments of the Trinity Group and is divided into lower, middle, and upper aquifers (fig. 7) based on hydraulic characteristics of the sediments (Barker and others, 1994). The Lower Trinity aquifer consists of the Hosston and Sligo Formations in the subsurface and the Sycamore Sand in outcrop; the Middle Trinity aquifer consists of the Cow Creek Limestone, the Hensel Sand, and the Lower Member of the Glen Rose Limestone; and the Upper Trinity aquifer consists of the Upper Member of the Glen Rose Limestone. Low-permeability sediments in the middle and upper parts of the Glen Rose Limestone separate the Middle and Upper Trinity aquifers. The Lower and Middle Trinity aquifers are separated by the low permeability Hammett Shale except where the Hammett Shale pinches out in the northern part of the study area (Amsbury, 1974; Barker and Ardis, 1996) (fig. 8).

The basal parts of the Hosston Formation, the Sycamore Sand, and updip parts of the Hensel Sand are mostly sand and contain some of the most permeable sediments in the Hill Country (Barker and others, 1994). The Cow Creek Limestone is highly permeable in outcrop but has relatively lower permeability in the subsurface due to the precipitation of calcitic cements (Barker and others, 1994). Similarly, the lower parts of the Glen Rose Limestone have higher permeabilities in outcrop and lower permeabilities at depth (Barker and others, 1994). The Sligo Formation is a sandy dolomitic limestone that may yield small to large quantities of water (Ashworth, 1983).

Our study area is completely underlain by sediments of the Middle Trinity aquifer (fig. 8). The Upper Trinity aquifer exists in most of the study area except where it has been eroded along and near the lower reaches of the Pedernales, Blanco, Guadalupe, Cibolo, and Medina streams (fig. 8). In the western part of the study area, the Fort Terrett and Segovia Formations of the Edwards Group (fig. 8) cap the Trinity aquifer sediments. The Edwards Group may produce large amounts of water where it is saturated and has high transmissivity.

Structure

The structural geometry of Lower Cretaceous sediments in the study area are characterized by (1) a southeast regional dip, (2) an uneven surface of pre-Cretaceous rocks at the base of the Trinity Group sediments, (3) the San Marcos arch in the south-east, (4) the Llano Uplift to the north, and (5) the Balcones Fault Zone to the south and east. Both Trinity and Edwards Group sediments have a regional dip to the south and southeast. The dip increases from a rate of about 10 to 15 feet per mile near the Llano Uplift to about 100 feet per mile near the Balcones Fault Zone (Ashworth, 1983). These Lower Cretaceous sediments may be described as a series of stacked wedges that pinch out against the Llano Uplift and thicken down-dip towards the Gulf of Mexico (fig. 9). At the base of Trinity Group sediments, underlying Paleozoic rocks have been moderately folded, uplifted, and eroded to form an unconformable surface upon which the Trinity Group

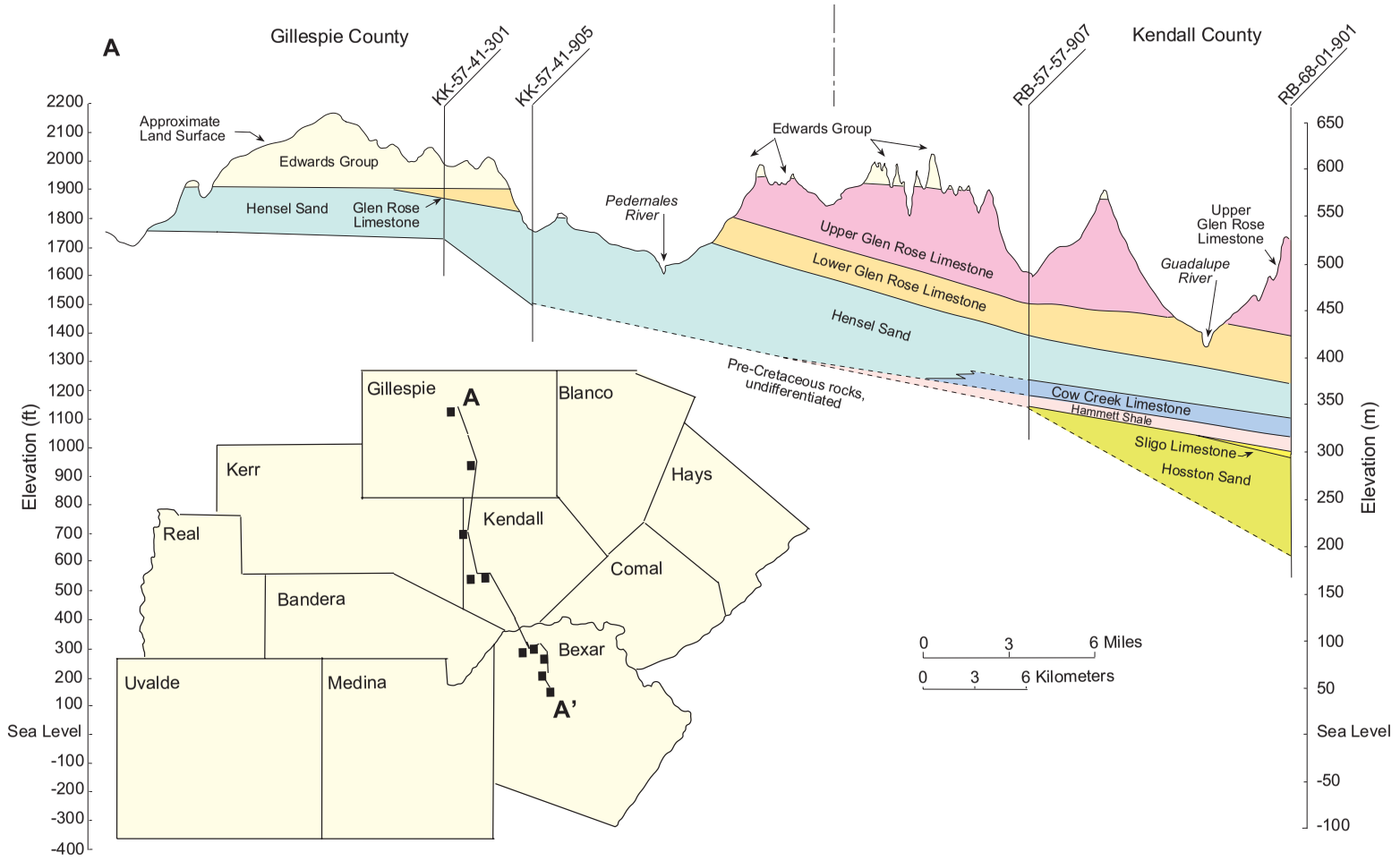

Figure 9. Geologic cross section through the study area (after Ashworth, 1983, fig. 6).

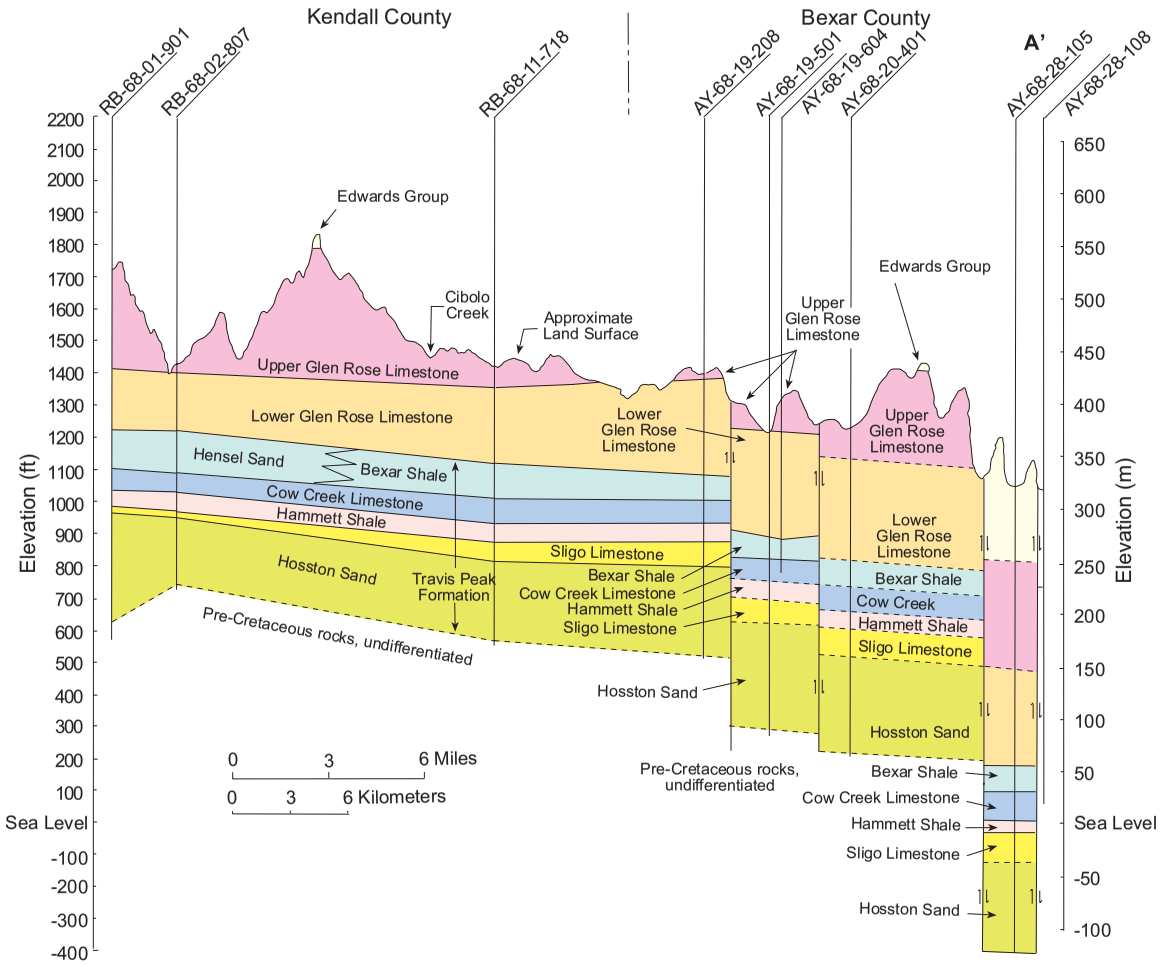

Figure 9. Geologic cross section through the study area (after Ashworth, 1983, fig. 6) *Continued*

sediments were deposited (fig. 9). Along the northern margin of the study area, the Middle and Upper Trinity sediments directly overlay pre-Cretaceous rocks (fig. 9).

The Llano Uplift (fig. 10) is a regional dome formed by a massive pre-Cambrian granitic pluton. The uplift remained a structural high throughout the Quachita orogeny that folded and uplifted the Paleozoic rocks of this area. The Llano Uplift provided a source of sediments for terrigenous and near-shore facies during the deposition of the Trinity Group sediments (Ashworth, 1983; Barker and others, 1994). The San Marcos arch is a broad anticlinal extension of the Llano Uplift with a southeast plunging axis through central Blanco and southwest Hays counties (Ashworth, 1983) (fig. 10). This arch contributed to the formation of a carbonate platform with thinning sediments along the structural ridge of the anticlinal axis. The Balcones Fault Zone is a northeast-southwest trending system of high-angle normal faults with down-thrown blocks towards the Gulf of Mexico (fig. 10). The faulting occurred during the Tertiary Period along the sub-surface axis of the Quachita fold belt as a result of extensional forces created by the subsidence of basin sediments in the Gulf of Mexico. The last episode of movement in the fault zone is thought to have occurred in the late Early Miocene approximately 15 million years ago (Young, 1972). The Balcones Fault Zone is a primary structural feature that laterally juxtaposes Trinity Group sediments against Edwards Group sediments.

Building on the structural interpretations of Ashworth (1983), drilling logs from the Hill Country Underground Water Conservation District, geophysical logs, and locations of outcrop areas, we developed structural elevation maps for the base of the Edwards Group and the Upper and Middle Trinity aquifers (fig. 11, 12, 13). We collected geophysical logs from TWDB files, Edwards Aquifer Authority, Springhills Water Management District, and private collections and used the natural gamma logs to locate (1) the base of the Edwards Group, (2) the contact between the Upper and Lower Members of the Glen Rose Limestone (as defined by the lower evaporite beds just above the "Corbula bed" or correlated equivalent), and (3) the base of the Middle Trinity sediments. Resistivity logs were used to add control in parts of the study area where gamma logs were not available.

To further enhance the control of our structural elevation point data, we supplemented our well log based data with outcrop elevation points (fig. 14). We digitized the appropriate formation contacts for the base of the Edwards Group, Upper Trinity, and Middle Trinity sediments from 1:250,000 scale maps of surface geology in the area (Brown and others, 1974; Proctor and others, 1974a,b; Barnes, 1981;) using AutoCAD® (Autodesk, 1997) and converted the digitized contacts into an ArcInfo® (ESRI, 1991) geographical information system (GIS) line coverage. The line coverage was then georeferenced, converted into a point coverage from the arc vertices, and intersected with a triangulated irregular network (TIN) constructed from a USGS 3-arc second digital elevation model (DEM) to determine their point elevations. The structural elevation information was compiled and organized into ArcInfo® for the base of the Middle Trinity aquifer, the base of the Upper Trinity aquifer, and the base of the Edwards Group sediments. We then exported the point elevations from ArcInfo® into point coordinates and imported them into Surfer® (Golden Software, 1995) for spatial interpolation (fig. 11, 12, 13). We then developed thickness maps with the surface analysis tools provided by Surfer® (fig. 15, 16, 17).

The thickness of the Edwards Group is controlled by relatively flat lying beds and the dendritic erosional pattern of the surface topography (figs. 11, 15). Although mostly masked by the dendritic erosional pattern of the surface topography in the central and eastern portions of the study area, sediments of the Upper Trinity aquifer thicken towards the Balcones Fault Zone (fig. 16). Sediments of the Middle Trinity aquifer also generally increase in thickness towards the Balcones Fault Zone (fig 17).

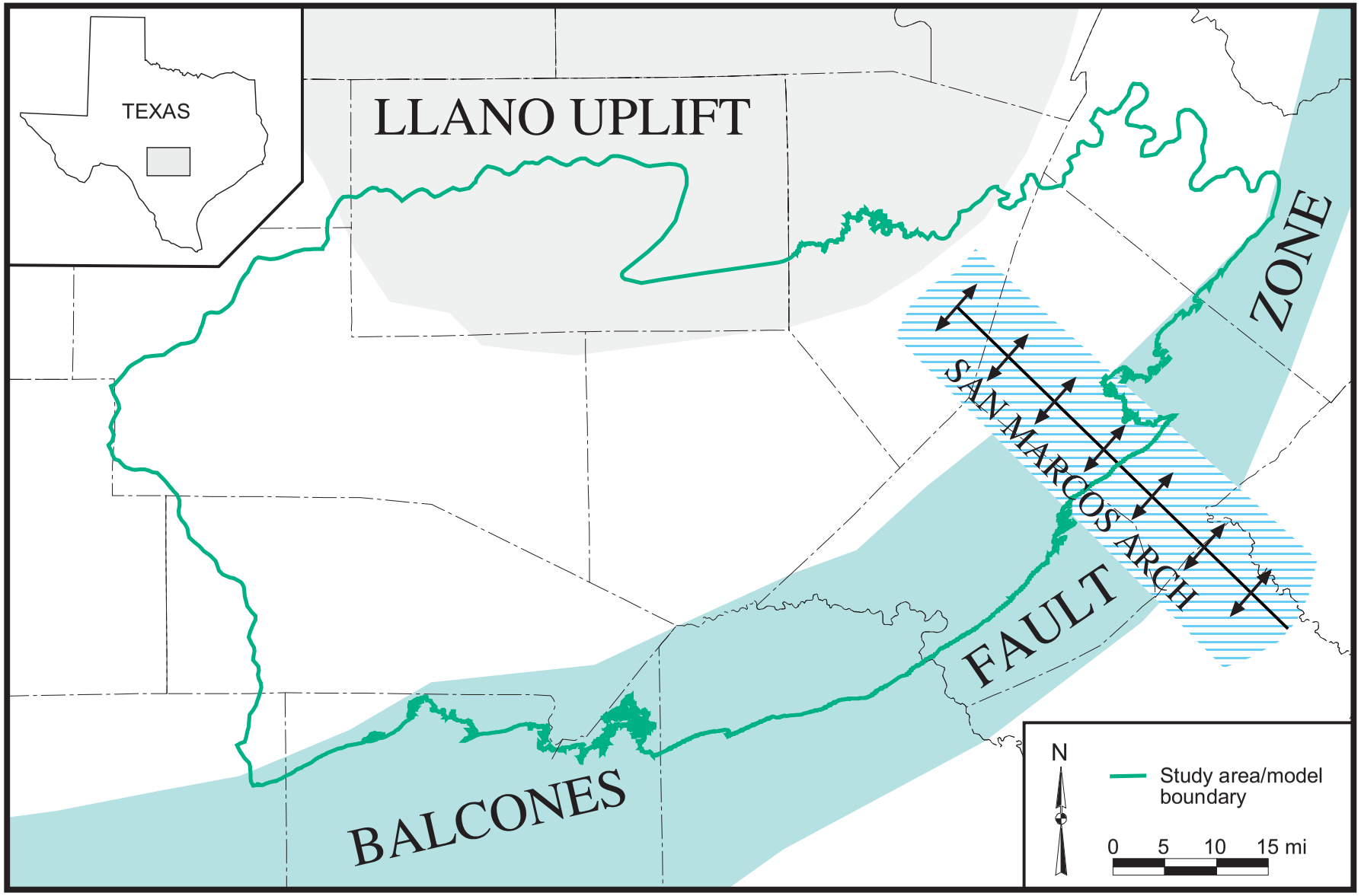

Figure 10. General structural setting in the study area.

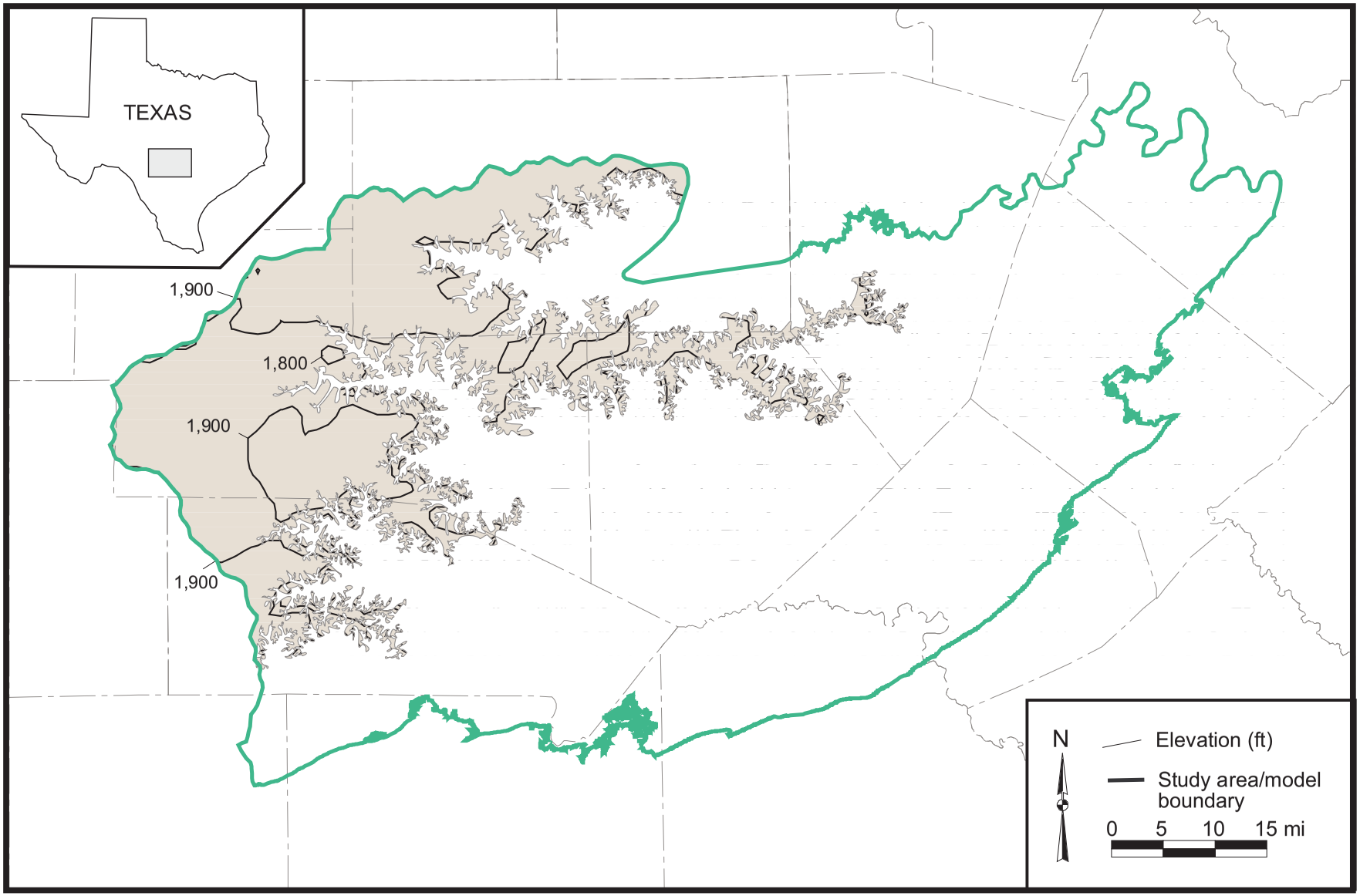

Figure 11. Elevation of the base of the Edwards Group. Figure 14 shows the control points.

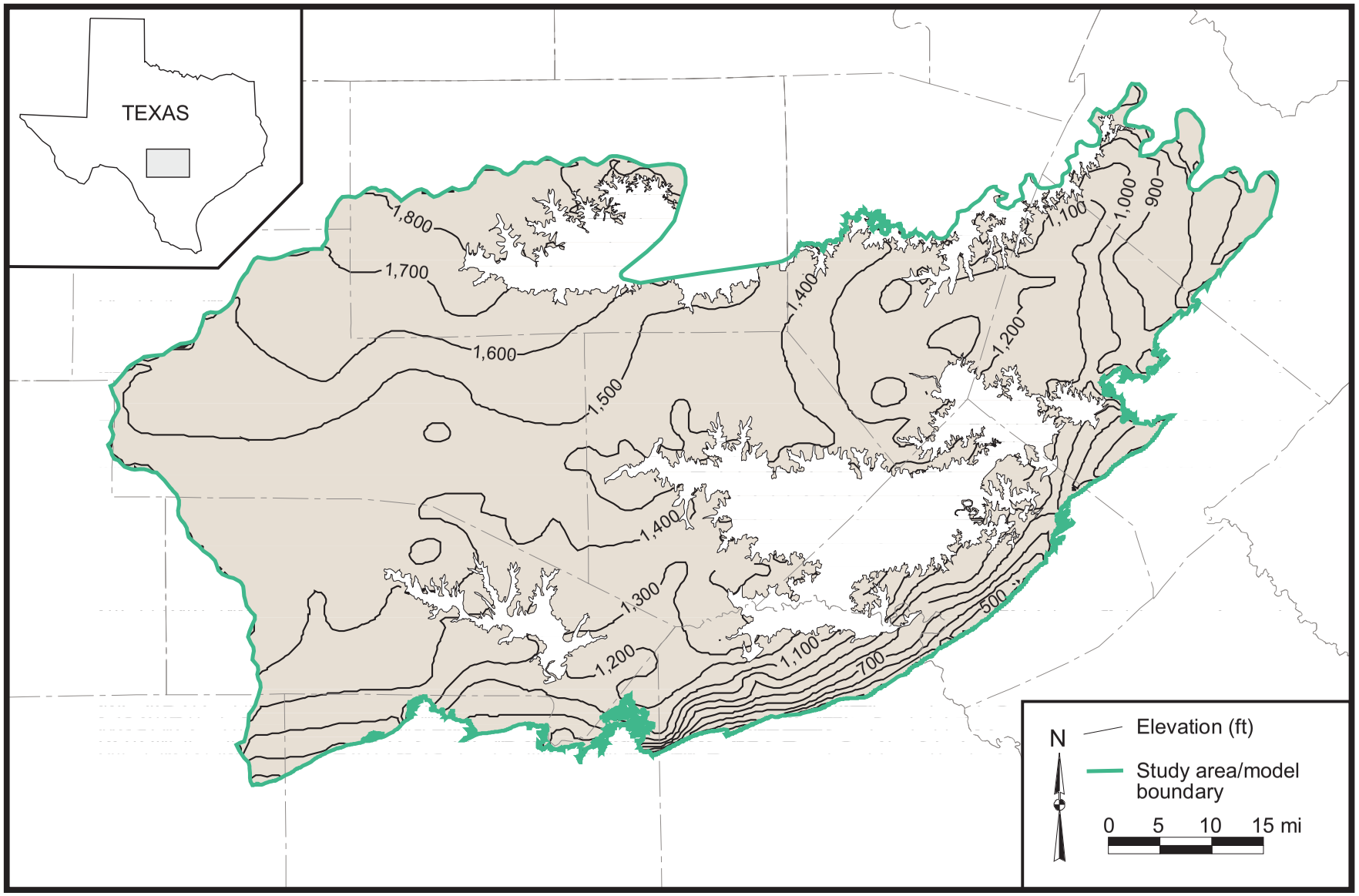

Figure 12. Elevation of the base of the Upper Trinity aquifer. Figure 14 shows the control points.

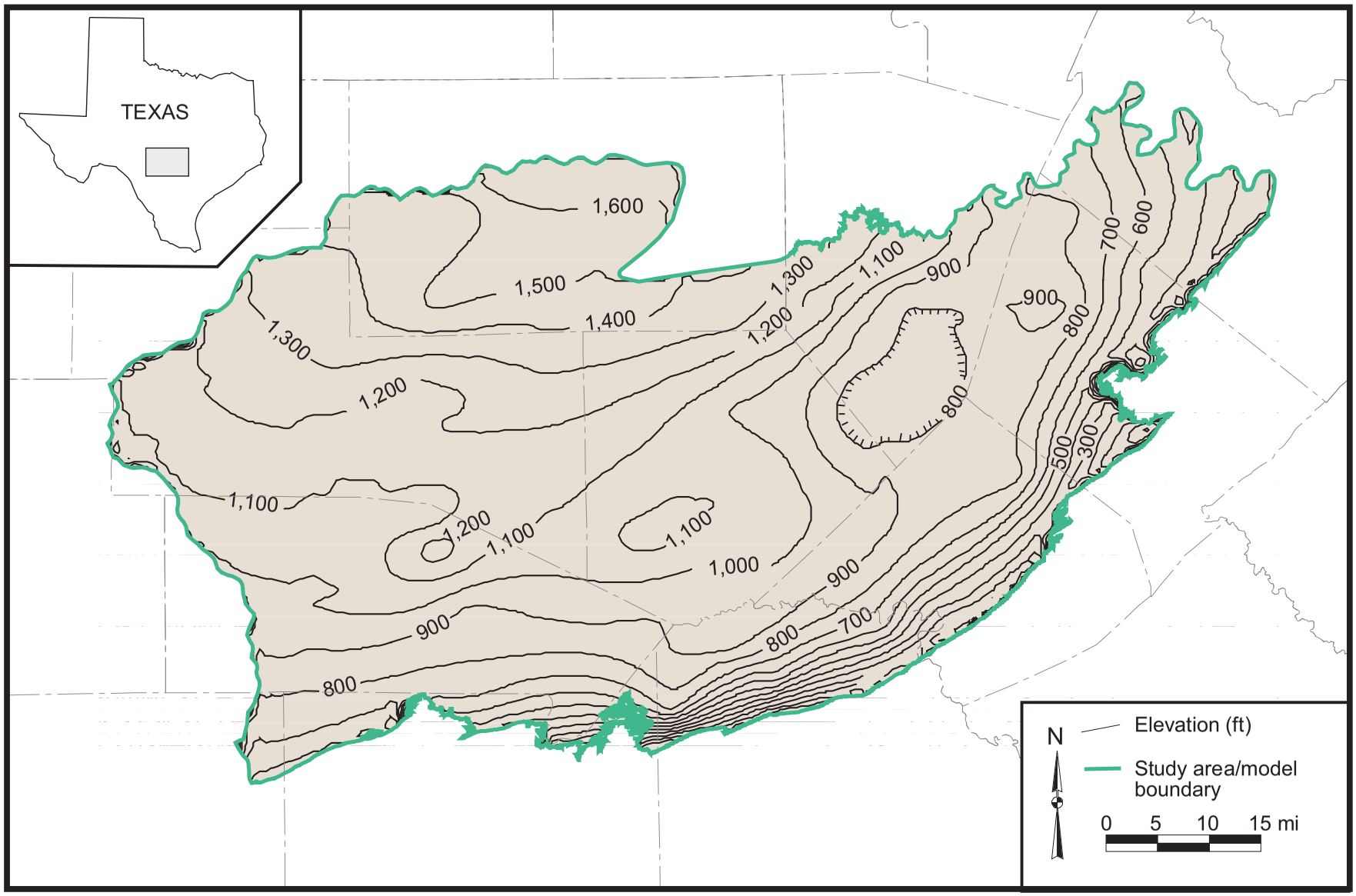

Figure 13. Elevation of the base of the Middle Trinity aquifer. Figure 14 shows the control points.

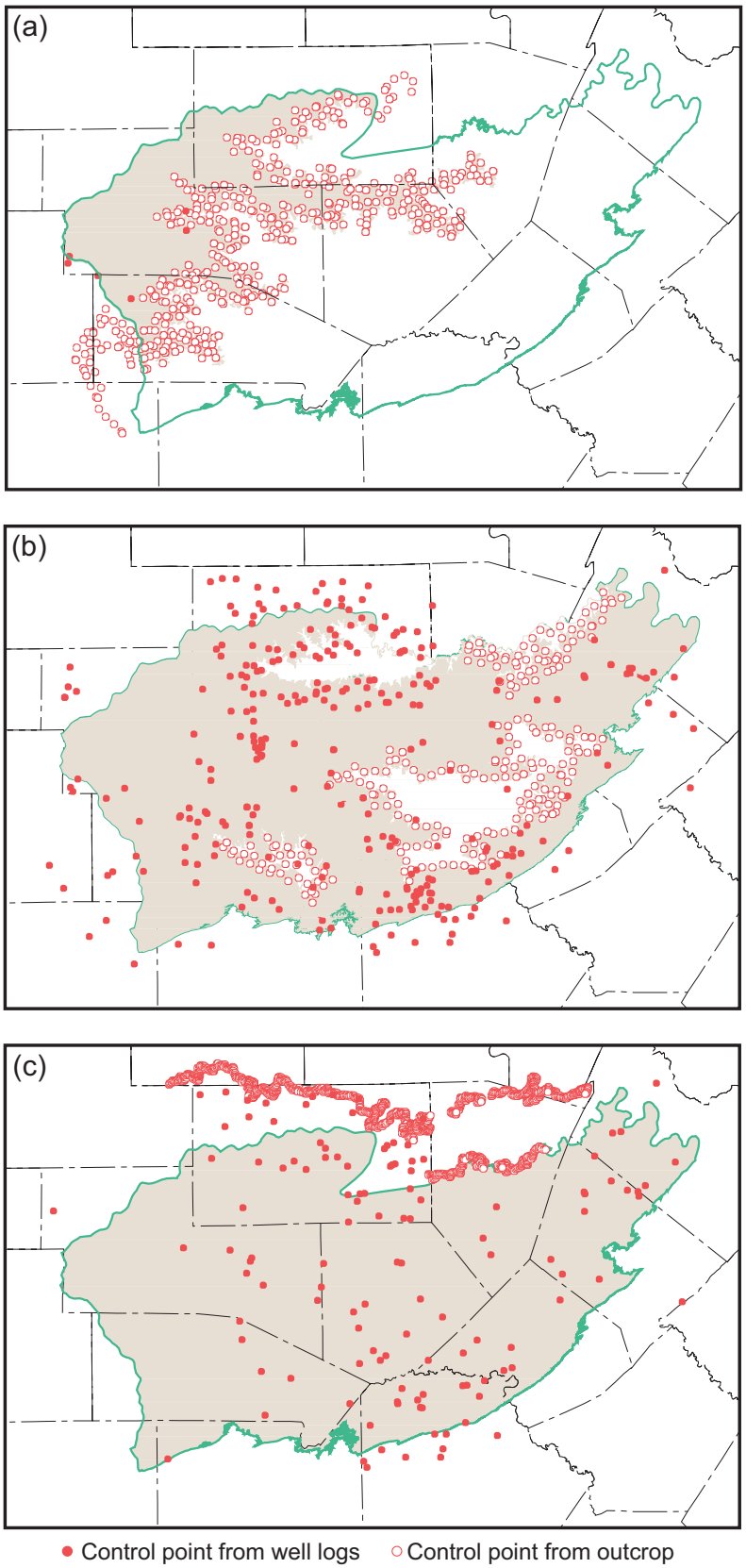

Figure 14. Location of control points for the bottom elevations of (a) the Edwards Group, (b) the Upper Trinity aquifer, and (c) the Middle Trinity aquifer.

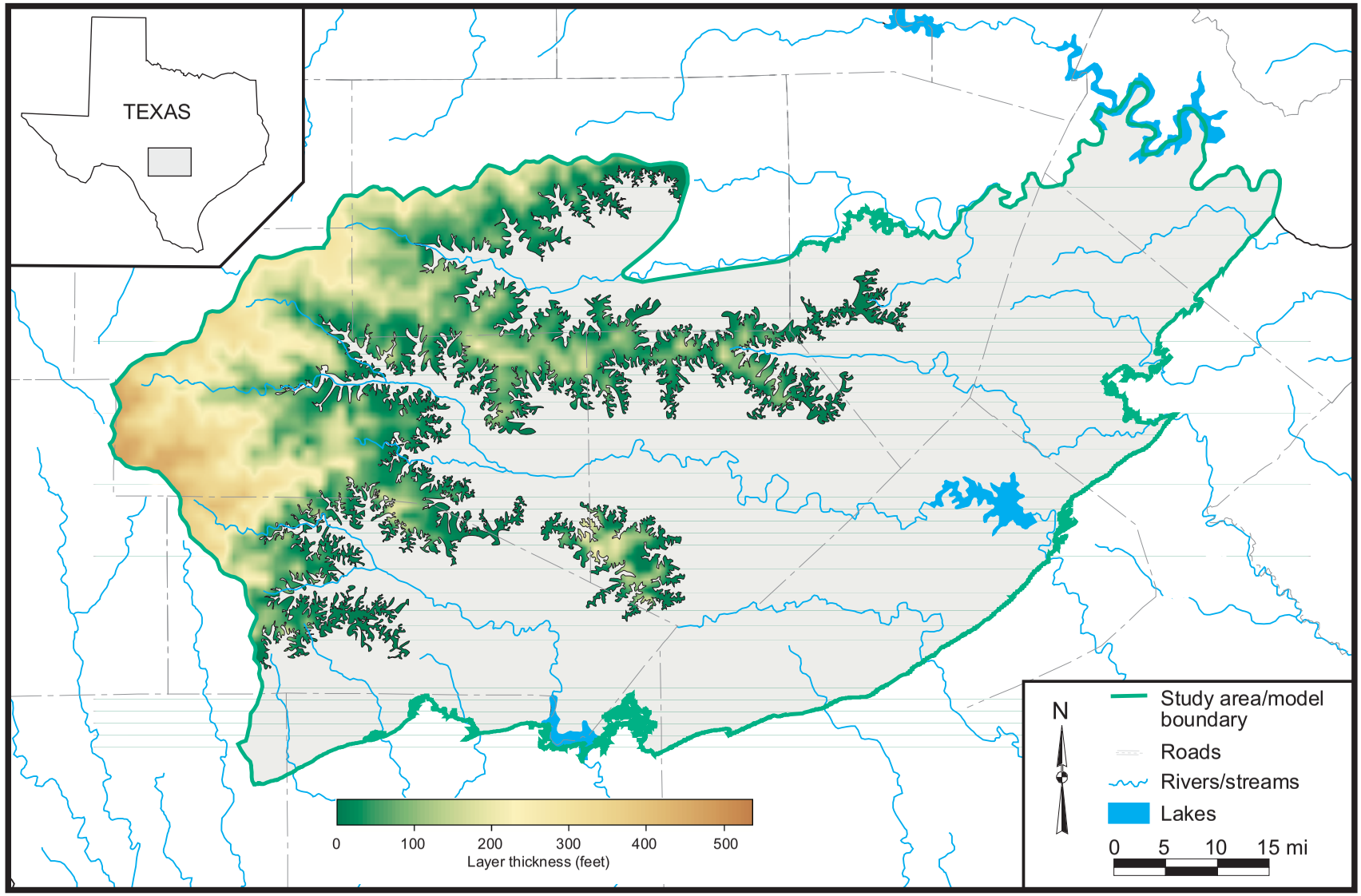

Figure 15. Approximate thickness of the Edwards Group in the plateau area.

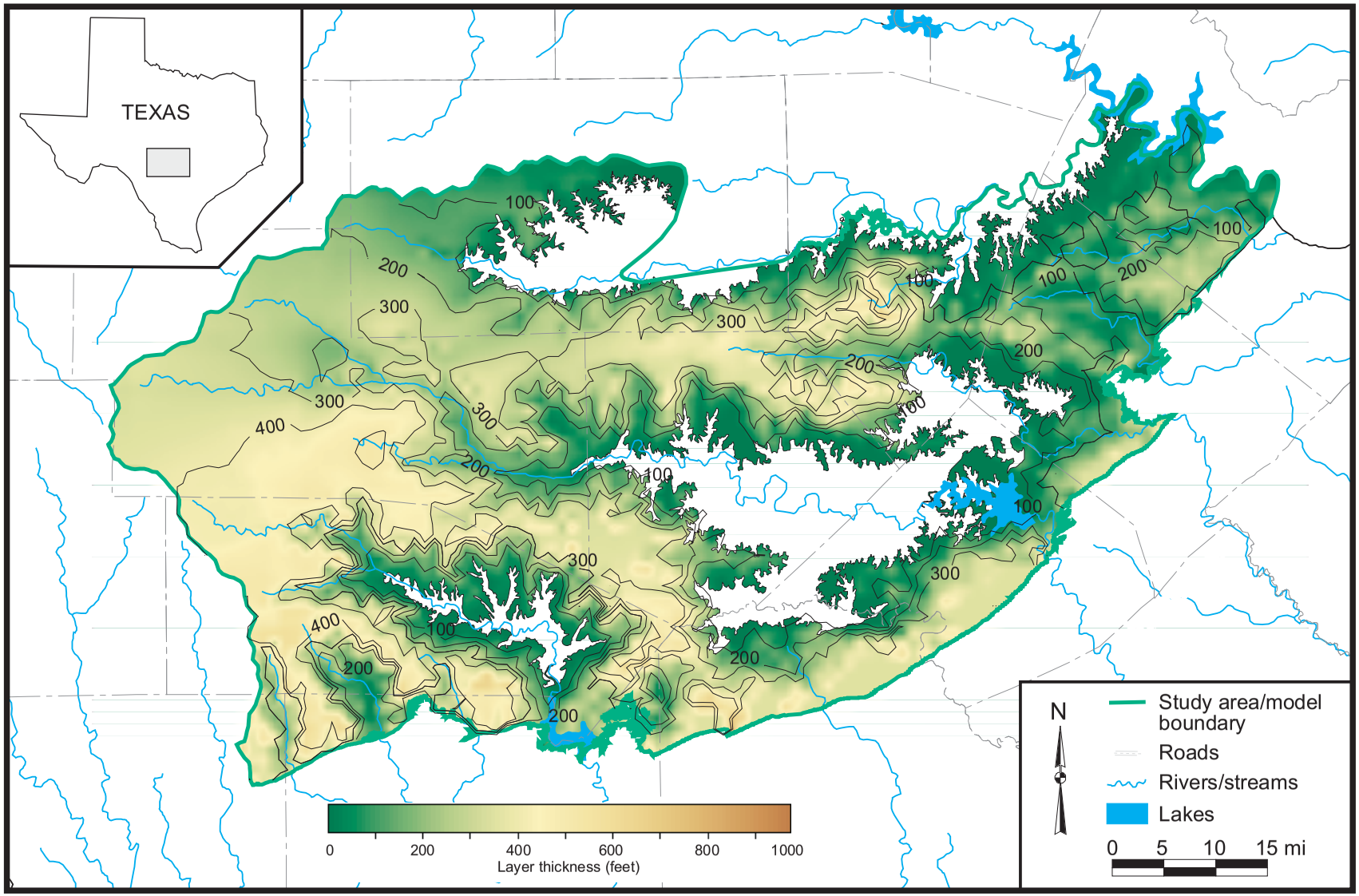

Figure 16. Approximate thickness of the Upper Trinity aquifer.

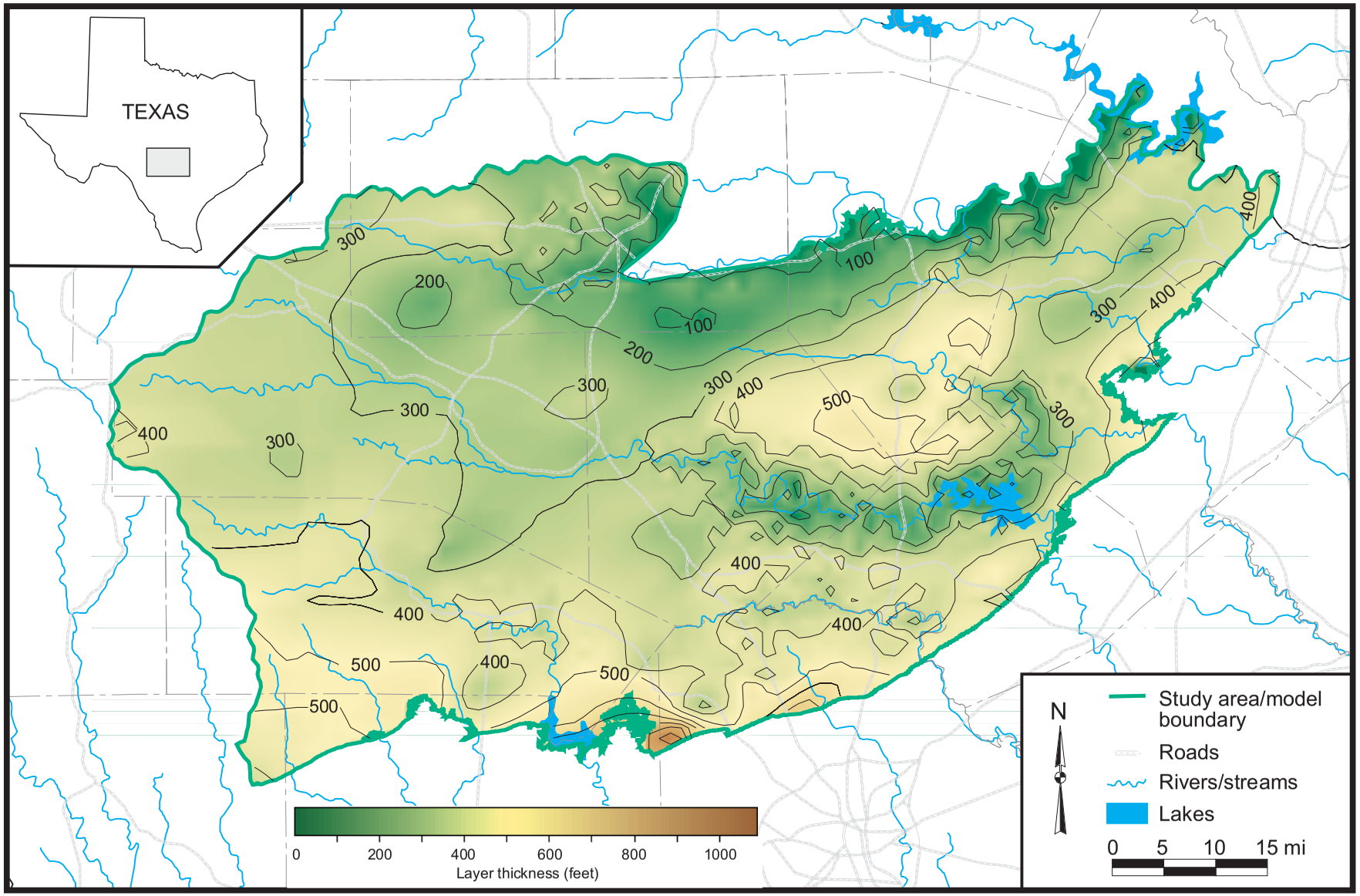

Figure 17. Approximate thickness of the Middle Trinity aquifer.

Water Levels and Regional Groundwater Flow

We compiled water-level measurements and developed generalized water-level maps for the Upper and Middle Trinity aquifers and the Edwards Group in the plateau area for 1975. To increase the number of measurement points, we expanded our time interval to lie between 1965 and 1985. If a well had multiple water-level measurements, the measurement closest to the winter of 1975 was chosen for contouring.

Water levels in the aquifers generally follow topography with higher water-level elevations coinciding with higher land-surface elevations and lower water-level elevations coinciding with lower land-surface elevations (figs. 18, 19, and 20). Kuniansky and Holligan (1994) also noted that water levels in this area are a subdued representation of surface topography due to recharge in the uplands and discharge in the lowlands. Water-level maps indicate that water levels are influenced by the location of rivers and springs. For example, the water-level maps show that groundwater in the aquifer flows toward most of the rivers in the study area (figs. 18, 19, and 20). In the case of the Edwards Group, water also flows east toward the escarpment where there are numerous springs at the geologic contact between the Edwards Group and the Upper Member of the Glen Rose Limestone (fig. 18). Barker and Ardis (1996) also noted that water-level elevations and the direction of groundwater flow in the Trinity aquifer are largely controlled by the position of springs and streams.

Water flows from higher water-level elevations toward lower water-level elevations. The water-level maps show that regional groundwater flow is from the northwest toward the southeast except where there is local flow to streams and springs and where the flow is from the southwest to the northeast in Comal and Travis counties (figs. 18, 19, and 20). Water-level maps also show that groundwater in the Upper and Middle Trinity aquifers flows out of the study area to the southeast in the direction of the Edwards (BFZ) aquifer (figs. 19 and 20). The 'Discharge' section discusses the estimated amount of groundwater that flows from the Trinity aquifer into the Edwards (BFZ) aquifer.

Water levels, especially in shallow wells (<100-ft deep), can seasonally vary up to 50-ft (Barker and Ardis, 1996) in response to changes in precipitation. Some wells show relatively small changes in water level over time (e.g. figs. 21a, 22b, 23c, 23d) while others show large fluctuations (e.g. figs. 21c, 21d). Wells with detailed measurements show seasonal fluctuations (e.g. figs. 21c, 22a, 22d). Some wells also show an overall decrease in water level over time (e.g. figs. 22a, 22c) while one shows a rise (fig. 22b).

Over the past twenty years, water levels have generally declined in the Middle Trinity aquifer in Kerr, Kendall, Bandera, and Bexar counties and risen, at least locally, in central Gillespie County (fig. 24). In other parts of the study area, water levels show seasonal fluctuations but have remained fairly constant since 1980. The area with the most significant water-level decline is near the city of Kerrville in Kerr County. The largest water-level drop is approximately 70 feet observed in well 69-08-201. Fifty feet of water-level decline was observed in well 56-63-916, a public water-supply well operated by Kerrville South Water. Well 56-61-601 supplies water to Camp Waldemar and showed a water-level decline of about 35 feet since 1980. Well 68-08-102, which is located near the city of Wimberley (Hays County), shows a water-level decline of approximately 40 feet since 1980. In Gillespie County, wells 57-41-403 and 57-41-903 near the city of Fredericksburg show water-level increases, perhaps due to decreases in nearby pumping. There is only one well (68-19-806) located in northern Bexar County with a continuous water-level record since 1990. The water levels in this well show a decline of approximately 20 feet since 1990. Note that this figure does not accurately portray local changes in water levels and only reflects changes in wells with historical information.

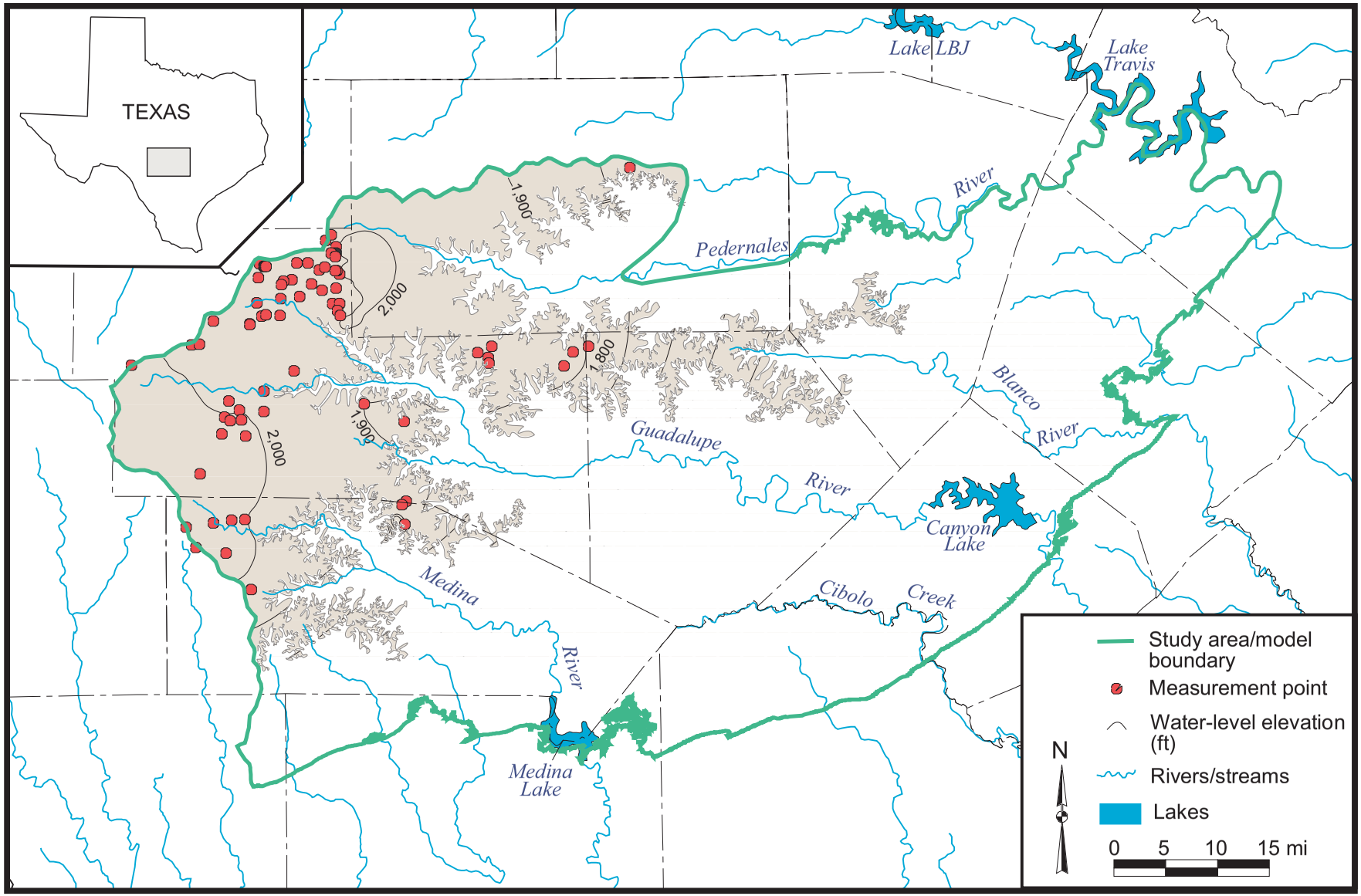

Figure 18. Water-level elevations in the Edwards Group in the plateau area (includes water-level measurements from 1965 to 1985).

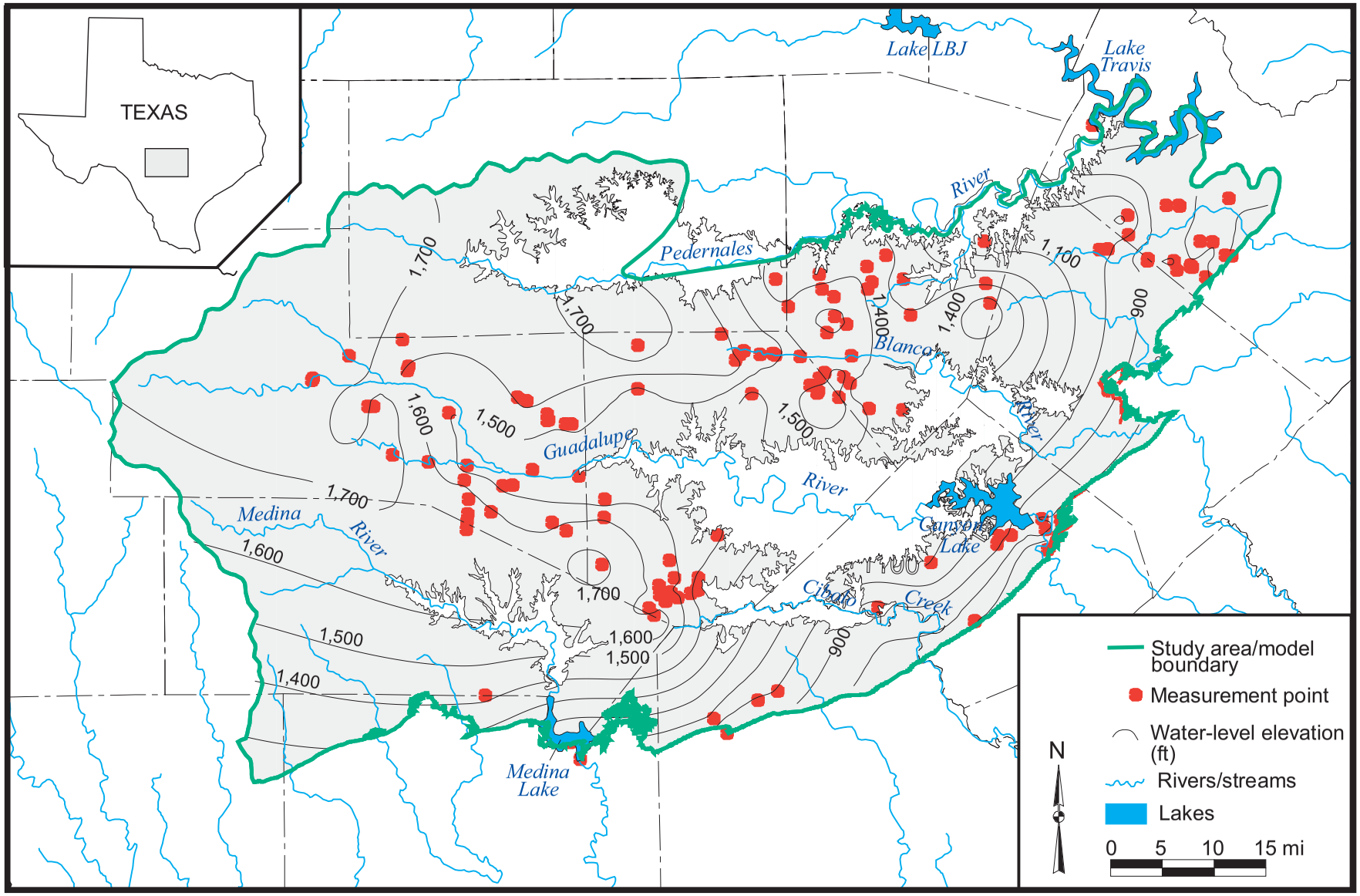

Figure 19. Water-level elevations in the Upper Trinity aquifer (includes water-level measurements from 1965 to 1985).

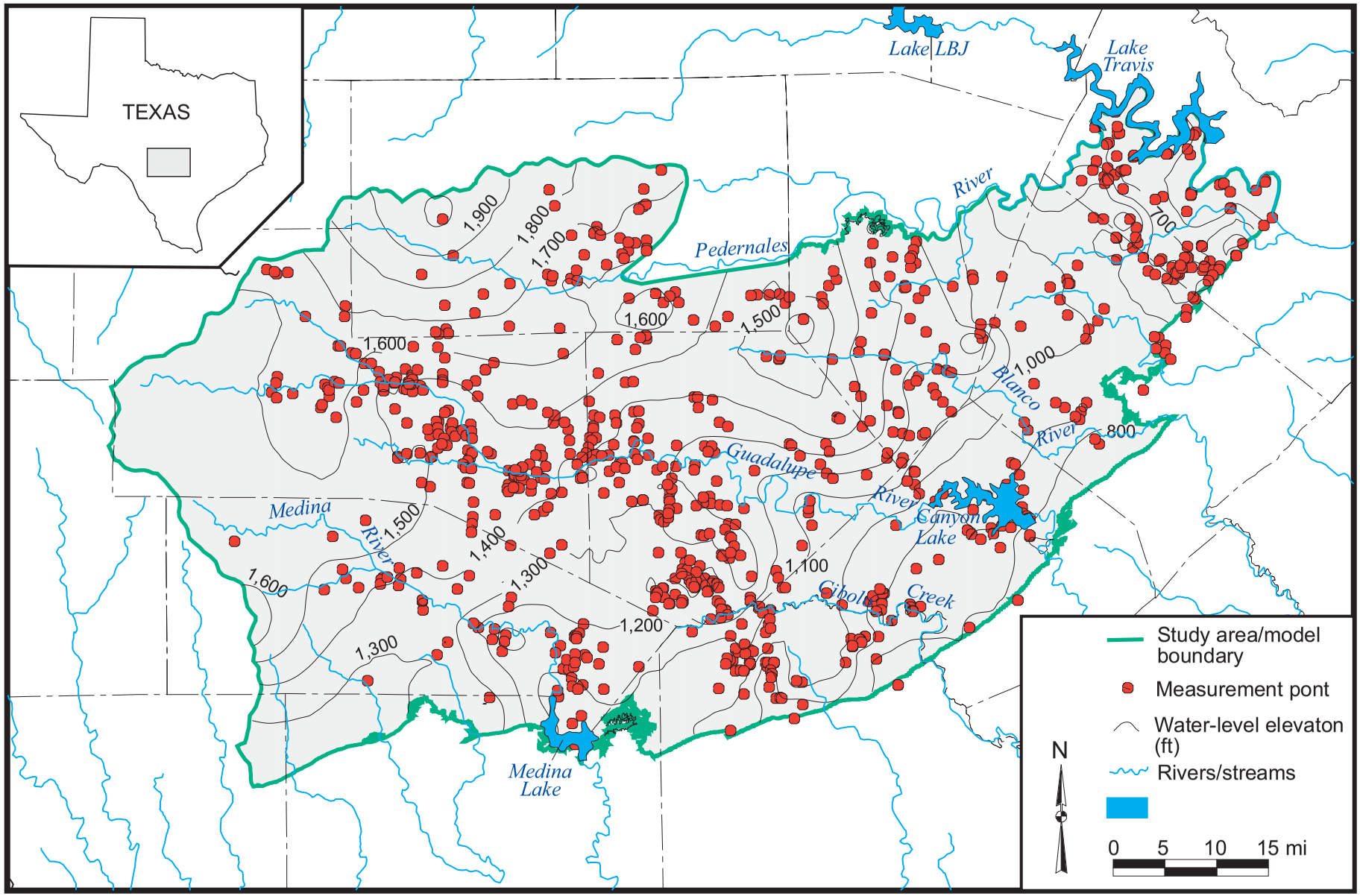

Figure 20. Water-level elevations in the Middle Trinity aquifer (includes water-level measurements from 1965 to 1985).

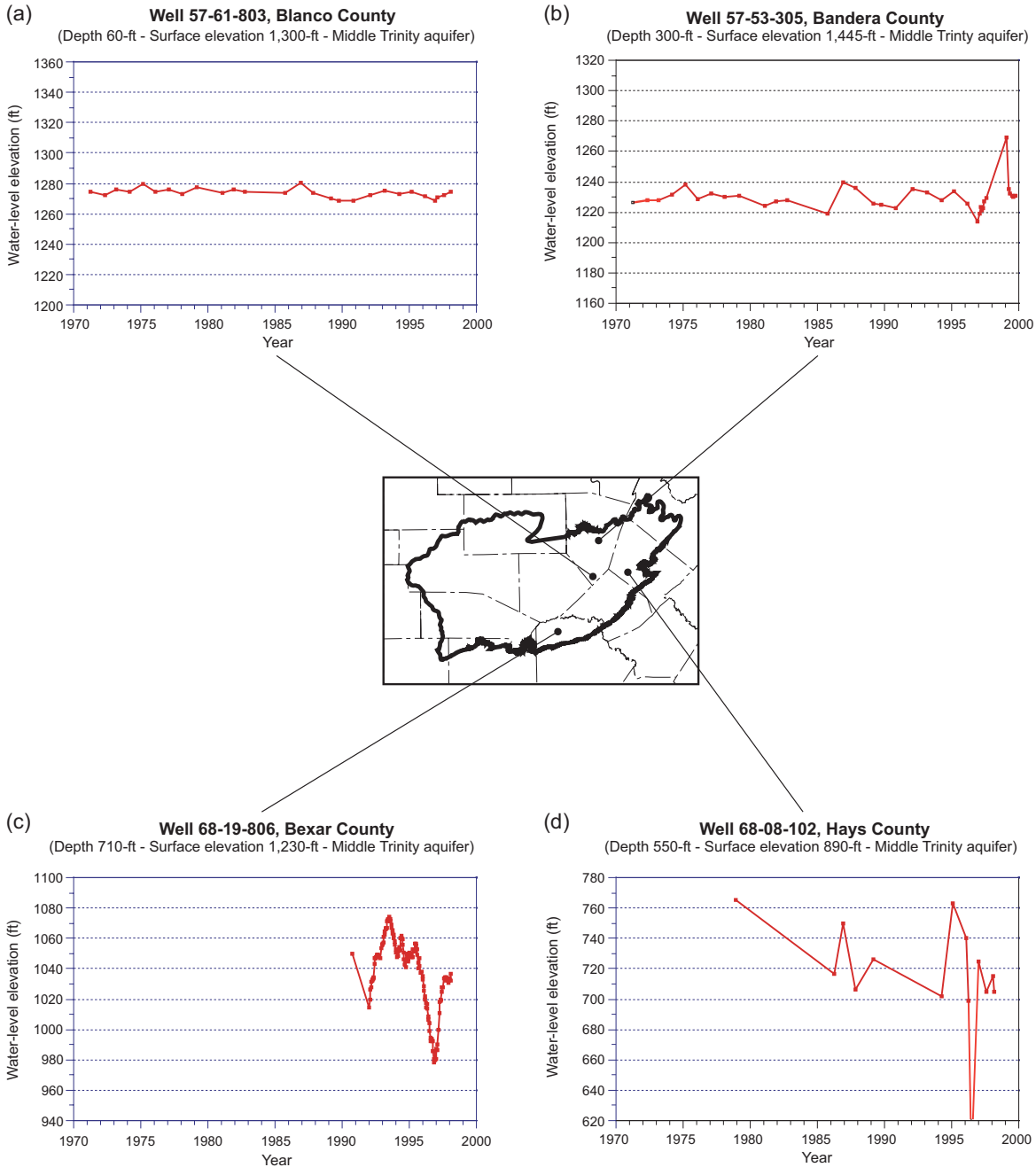

Figure 21. Hydrographs for wells (a) 57-61-803, (b) 57-33-305, (c) 68-19-806, and (d) 68-08-102.

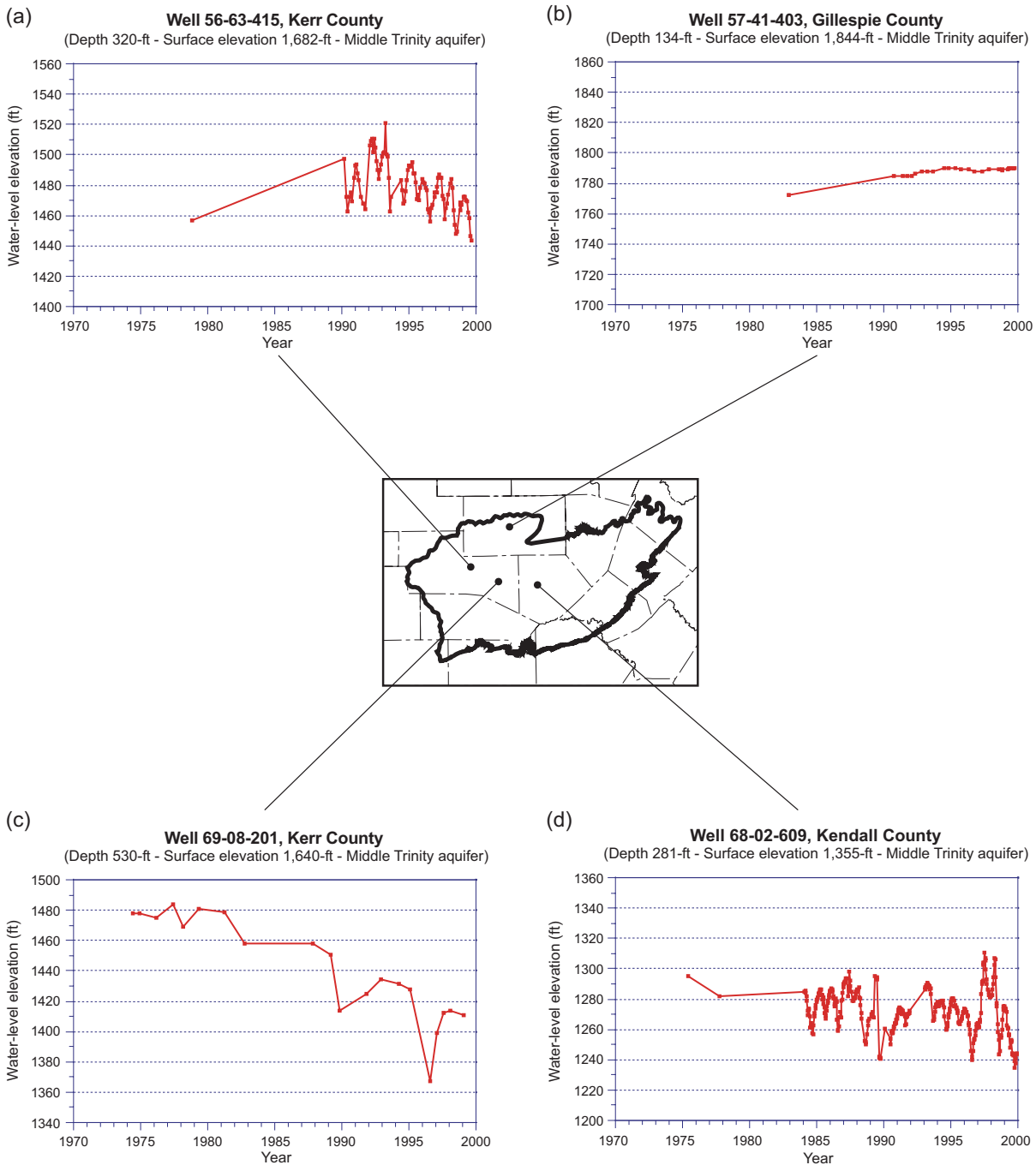

Figure 22. Hydrographs for wells (a) 56-63-415, (b) 57-41-403, (c) 68-08-201, and (d) 68-02-609.

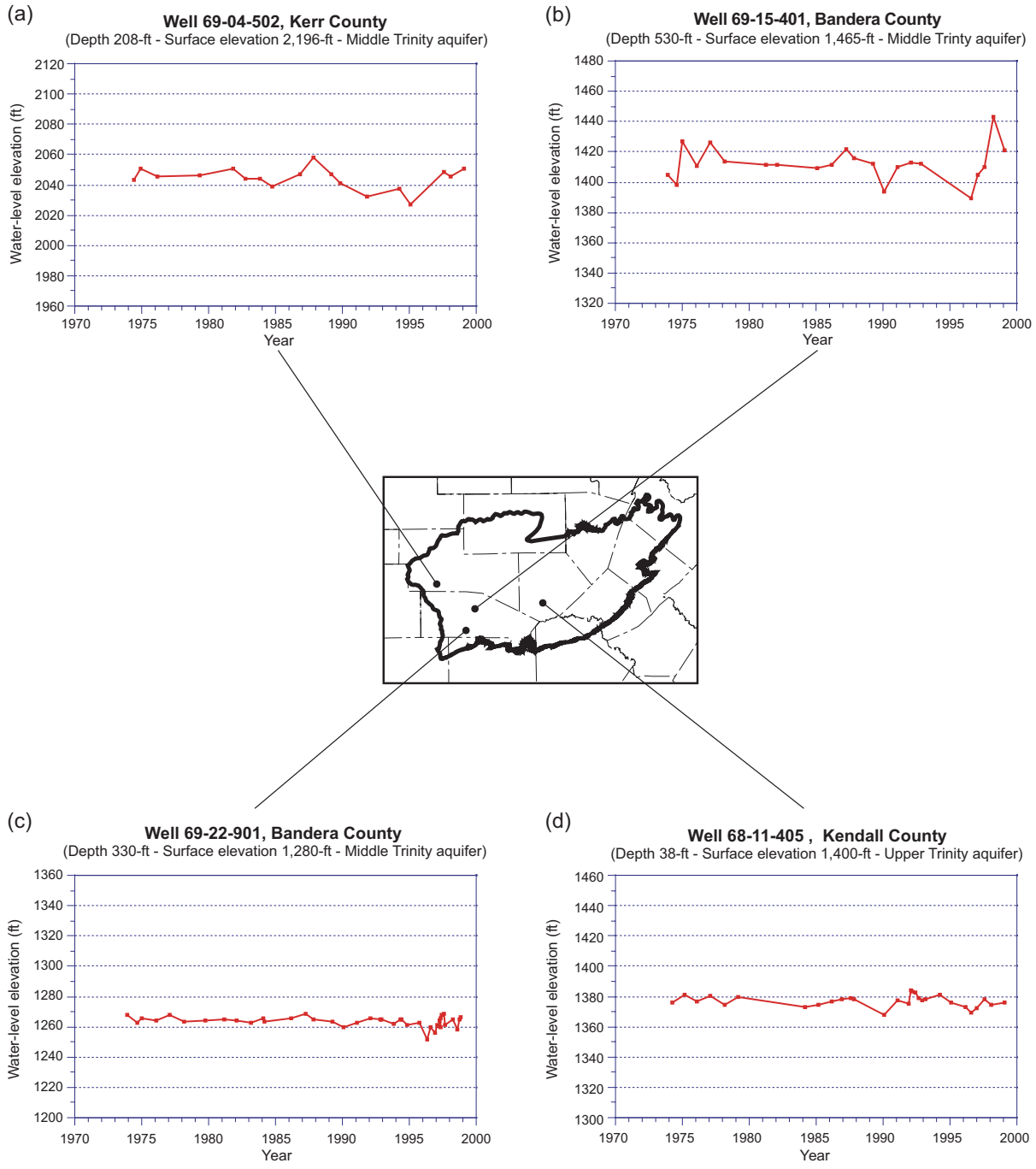

Figure 23. Hydrographs for wells (a) 69-04-502, (b) 69-15-401, (c) 69-22-901, and (d) 68-11-405.

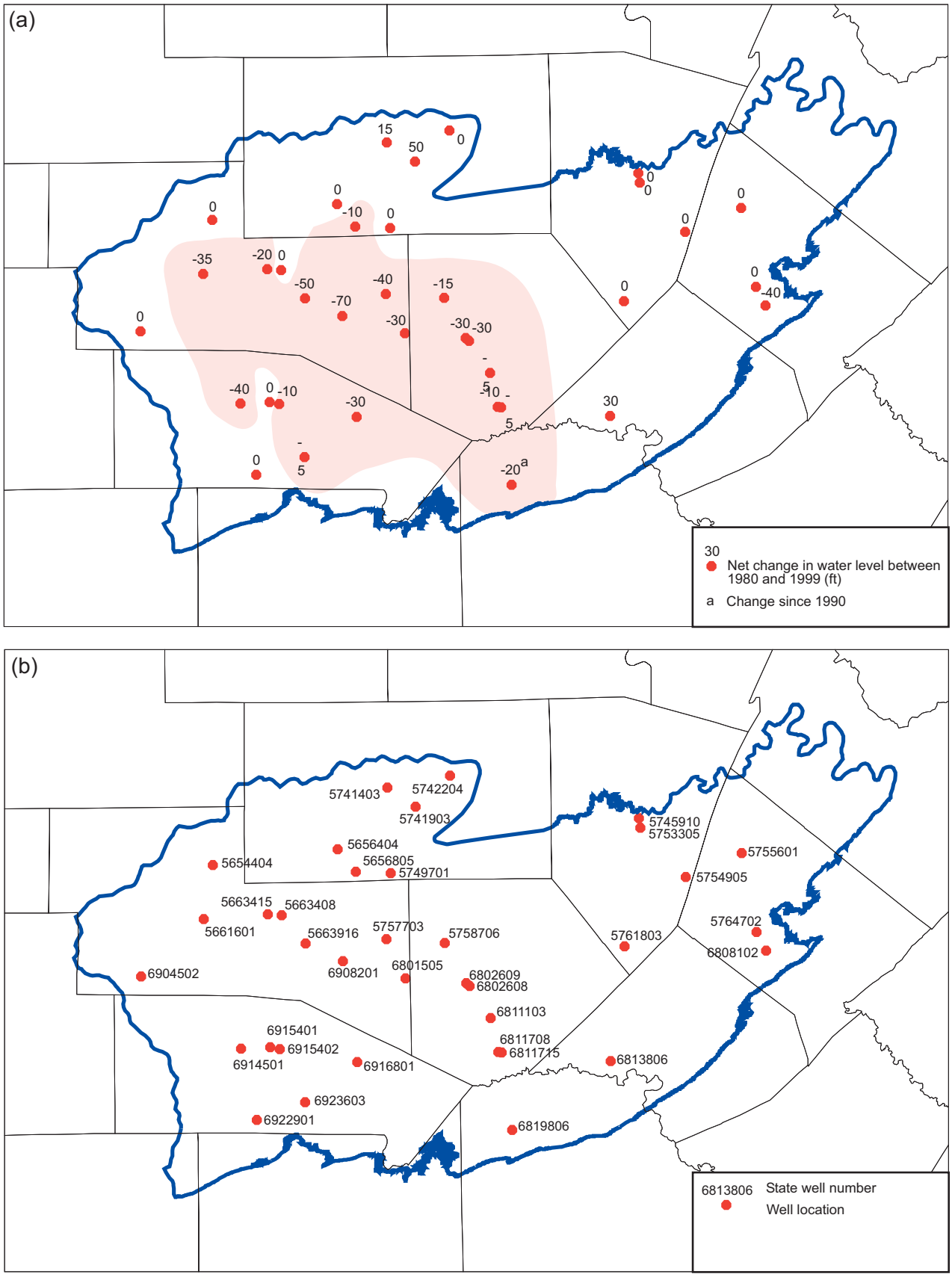

Figure 24. (a) Net change in water level in the Middle Trinity aquifer between 1980 and 1999. (b) State well number for the analyzed wells.

Recharge

The primary sources of recharge to the Trinity aquifer in the Hill Country area are from rainfall on the outcrop, seepage losses through headwater creeks, and perhaps lakes during high stage levels. The outcrops in the study area are composed of the Upper Member of the Glen Rose Limestone, the Lower Member of the Glen Rose Limestone, Hensel Sand, and Edwards Group and receive all of the direct recharge. The Cow Creek Limestone and Lower Trinity aquifer sediments are recharged by vertical leakage from overlying strata (Ashworth, 1983). Interbeds of relatively low permeability marl sediments within the Upper Member of the Glen Rose Limestone impede downward percolation of interstream recharge and provide for baseflow and springflow to the mostly gaining perennial streams that drain the Hill Country (Barker and Ardis, 1996; Ashworth, 1983). Recharge in the Edwards Group limestones of the northwestern portion of the study area occurs as infiltration of rainfall and losing streams. Much of this water later emerges as springs and seeps along the geologic contact of the Edwards Group with the Upper Member of the Glen Rose Limestone.

Sinkholes and caverns in the Glen Rose Limestone of southern Kendall, northern Bexar, and western Comal counties may transmit large quantities of water to the Trinity aquifer. Some caverns, such as Honey Creek Cave, promote groundwater piracy between and within the Cibolo Creek and Guadalupe River drainage basins (Elliot and Veni, 1994). Karst-enhanced recharge is especially significant for the area along Cibolo Creek between Boerne and Bulverde (Ashworth, 1983; Veni, 1994). However, because much of this recharge is quickly transmitted to the Edwards (BFZ) aquifer (Barker and Ardis, 1996; Veni, 1994), it has minimal effects on the Trinity aquifer.

Several investigators have estimated recharge rates for the Trinity aquifer (table 1). Most of them used stream baseflow to estimate recharge. Muller and Price (1979) assumed a recharge rate of 1.5 percent (of mean annual precipitation) for their estimates of groundwater availability. This estimate of recharge is an 'availability recharge' that is meant to minimize impacts of groundwater production to baseflow and groundwater flow to the Edwards (BFZ) aquifer. Based on a study of baseflow gains in the Guadalupe River between the Comfort and Spring Branch gaging stations during a 20-year period between 1940 and 1960, Ashworth (1983) estimated a mean annual effective recharge rate of 4 percent of mean annual rainfall for the Hill Country. Kuniansky (1989) estimated baseflow for 11 drainage basins in our study area for a 28-month period between December 1974 and March 1977 and estimated an annual recharge rate of about 11 percent of mean annual rainfall. However, Kuniansky and Holligan (1994) reduced this recharge rate to seven percent of mean annual rainfall to calibrate a groundwater model that included the Trinity aquifer. They suggested that the numerical model did not include all the local streams accepting discharge from the aquifer.

Bluntzer (1992) calculated long-term mean annual baseflow from the Pedernales, Blanco, Guadalupe, Medina, and Sabinal Rivers and Cibolo and Seco Creeks to be 369,100 acre-ft/yr, which is equivalent to a recharge rate of 6.7 percent of mean annual precipitation (using a long-term mean annual precipitation of 30 in/yr [Riggio and others, 1987]). However, Bluntzer (1992) suggests that a recharge rate of 5 percent is more appropriate to account for human impacts on baseflow such as nearby groundwater pumpage, stream-flow diversions, municipal and irrigation return flows, and retention structures. Bluntzer (1992) also noted that baseflow was highly variable over time.

Our analysis suggests that differences in recharge rates reflect biases in the record of analysis due to variation of precipitation. The higher recharge rate estimated by Kuniansky (1989) is likely due to the higher than normal precipitation between December 1974 and March 1977, her record of analysis. Ashworth's (1983) recharge rate is probably biased toward

Table 1: Estimates of recharge rates expressed as percent of rainfall in the Trinity aquifer in the Hill Country area.

Source	Value
Muller and Price (1979)	1.5%
Ashworth (1983)	4.0%
Kuniansky (1989)	11.0%
Kuniansky and Holligan (1994)	7.0%
Bluntzer (1992, calc.)	6.7%
Bluntzer (1992, est.)	5.0%
Our analysis	6.6%
Our model	4.0%

a lower value because his record of analysis includes the 1950's drought.

To account for differences between the recharge rates, we developed an automated digital hydrograph-separation technique (based on Nathan and McMahon, 1990; Arnold and others, 1995) to estimate baseflow for the drainage basin defined by the Guadalupe River gaging stations between Comfort and Spring Branch. We used the program to estimate baseflow from 1940 to 1990 and adjusted parameters to attain the best fit with Ashworth's (1983) and Kuniansky's (1989) baseflow values for the same stream reach. Using this technique, we estimated a recharge rate of 6.6 percent of mean annual precipitation (note that the recharge rate calibrated for our model is about 4 percent). Note that all baseflow-based estimates of recharge, if accurate, underestimate recharge because they do not consider the component of recharge that follows the regional flow path.

We used Kuniansky's (1989) baseflow study and the mean annual rainfall for 1975 to spatially distribute recharge for the Trinity aquifer. We first generated a map of mean annual rainfall for 1975 using 37 rainfall gaging stations (fig. 25) and spatially distributed rainfall using a TIN surface model in ArcInfo® (fig. 26). We then digitized Kuniansky's (1989) 11 sub-basins from her baseflow study, intersected them with the rainfall distribution (fig. 27), and calculated recharge coefficients on 1-mile centers where the recharge coefficient is defined as the basin-averaged baseflow divided by the rainfall. The recharge coefficient is the percent of precipitation that recharges the aquifer. Because Kuniansky's (1989) baseflow study did not have complete coverage of the Hill Country area (see fig. 26), we extrapolated recharge coefficients to the rest of the study area. We then adjusted the recharge coefficients (multiplied by 0.45) so that the mean recharge would more closely match the mean annual recharge estimates reported by Ashworth (1983), Bluntzer (1992), and our analysis (fig. 28).

Rivers, Streams, Lakes, and Springs

Most of the rivers in the area arise along the eastern margins of the Edwards Plateau and descend with a steep gradient into the Hill Country (fig. 5). Upper reaches of many of these streams are contained within narrow canyons but broaden into flat-bottomed valleys further downstream (Barker and Ardis, 1996). Three major drainage basins, including the San Antonio, Guadalupe, and Colorado Rivers, traverse the study area and funnel flow towards the southeast.

Most of the rivers in the study area gain water from the Trinity aquifer (Ashworth, 1983) and are hydraulically connected to the regional flow system (Kuniansky, 1990). Groundwater seeps into streams and springs along the tops of impermeable bedding where cut by the rugged topography of the Hill Country (Barker and Ardis, 1996). Much of the water in shallow parts of the Trinity aquifer discharge to deeply entrenched, perennial streams that drain the area instead of flowing to deeper portions of the aquifer (Ashworth, 1983, p. 47). Many springs issue from the Edwards Group along the plateau in the western part of the study area (Ashworth, 1983, p. 33).

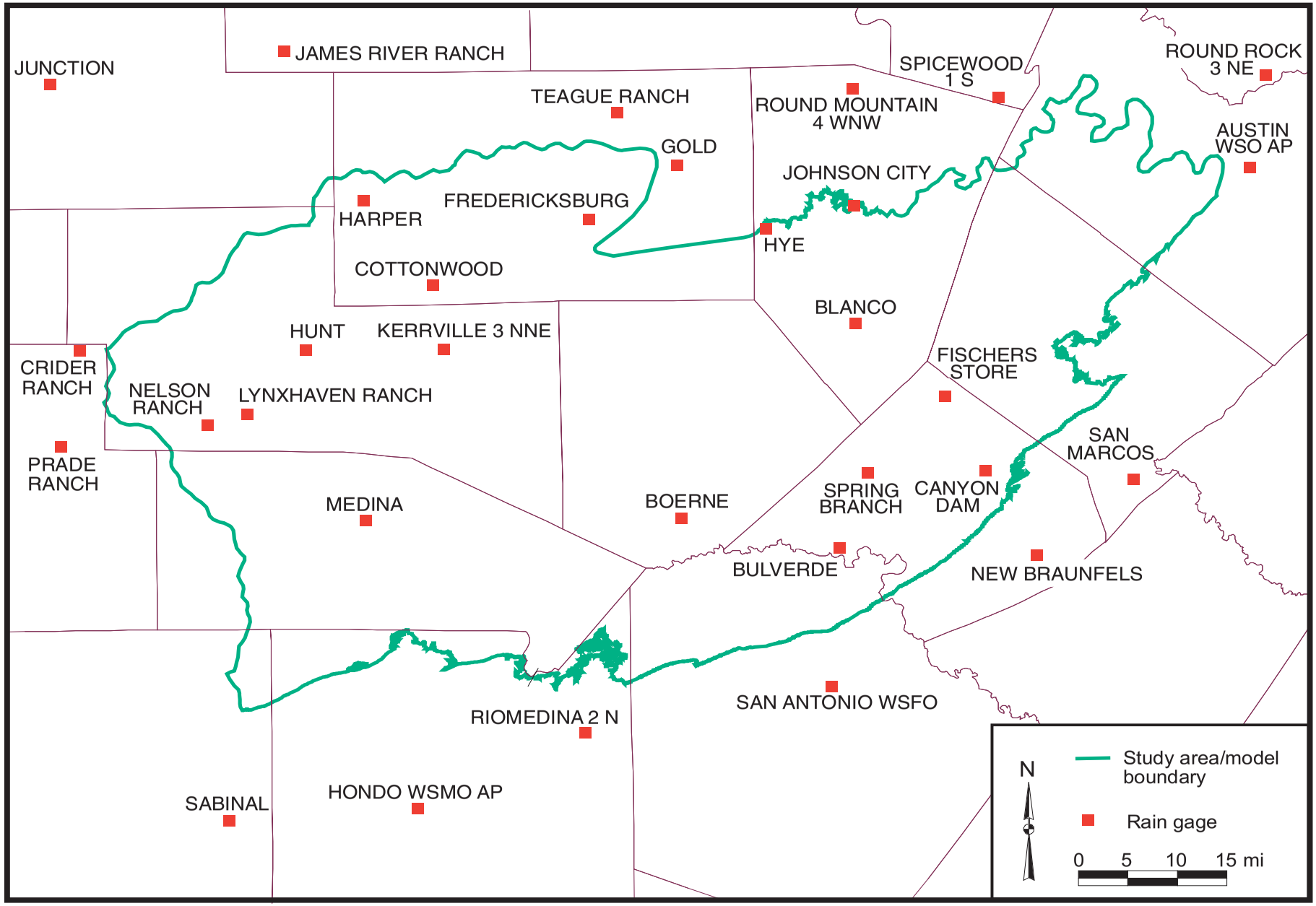

Figure 25. Location of National Weather Service rain gages in the Hill Country area.

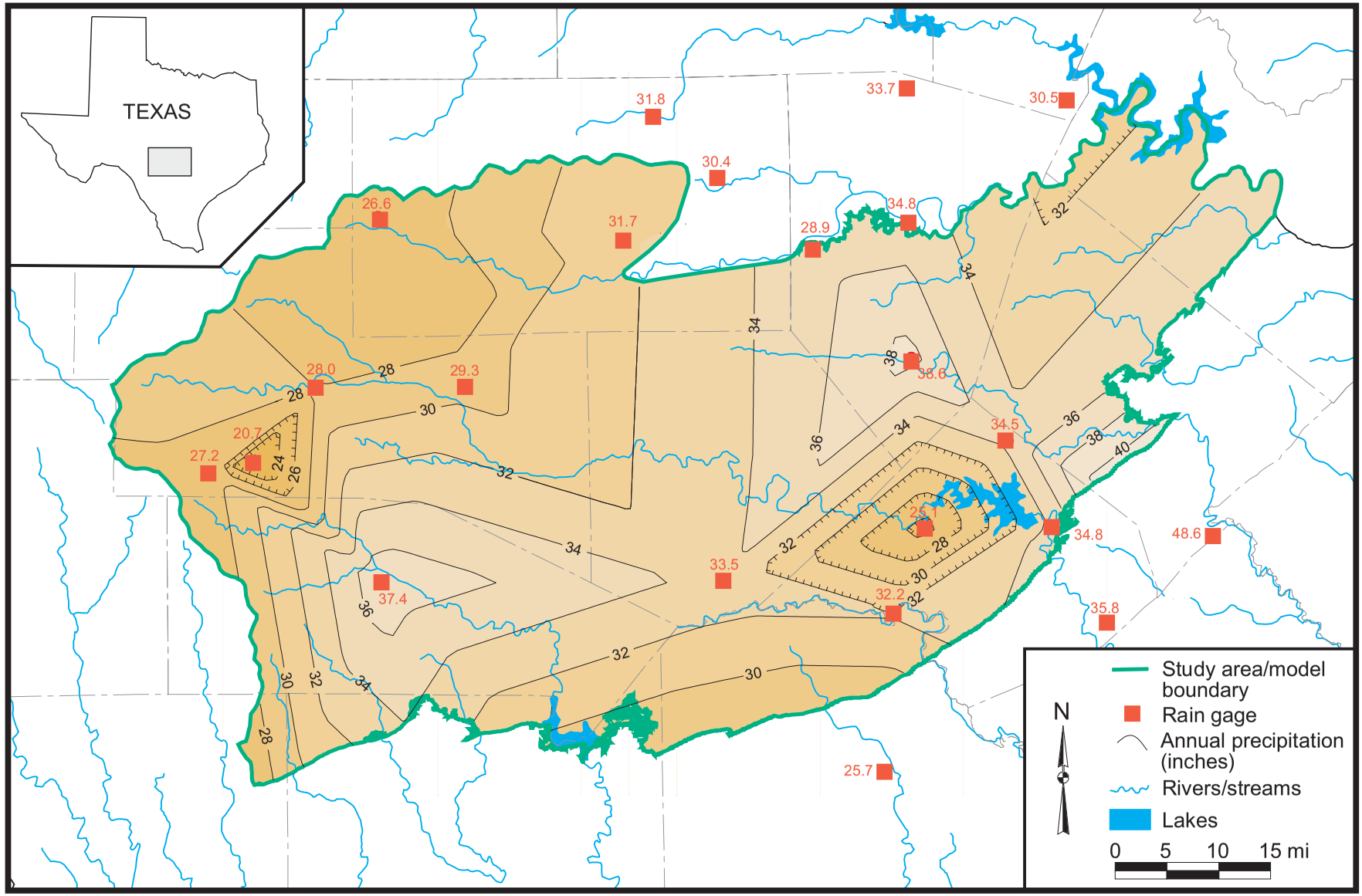

Figure 26. Rainfall distribution for 1975.

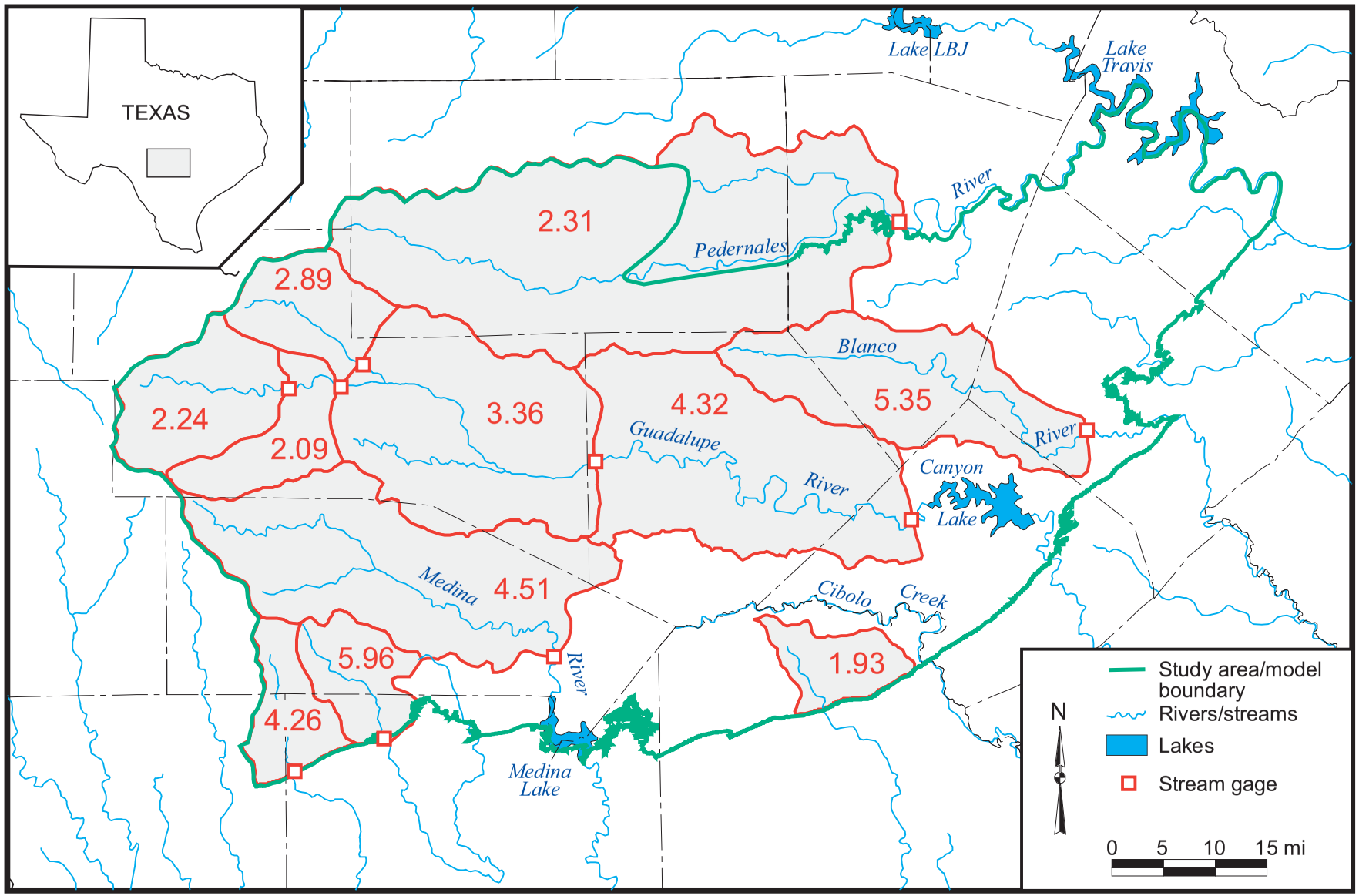

Figure 27. Basin-averaged baseflow (in/yr) for analyzed areas in the study area for the time between December 1974 and March 1977 (after Kuniansky, 1989).

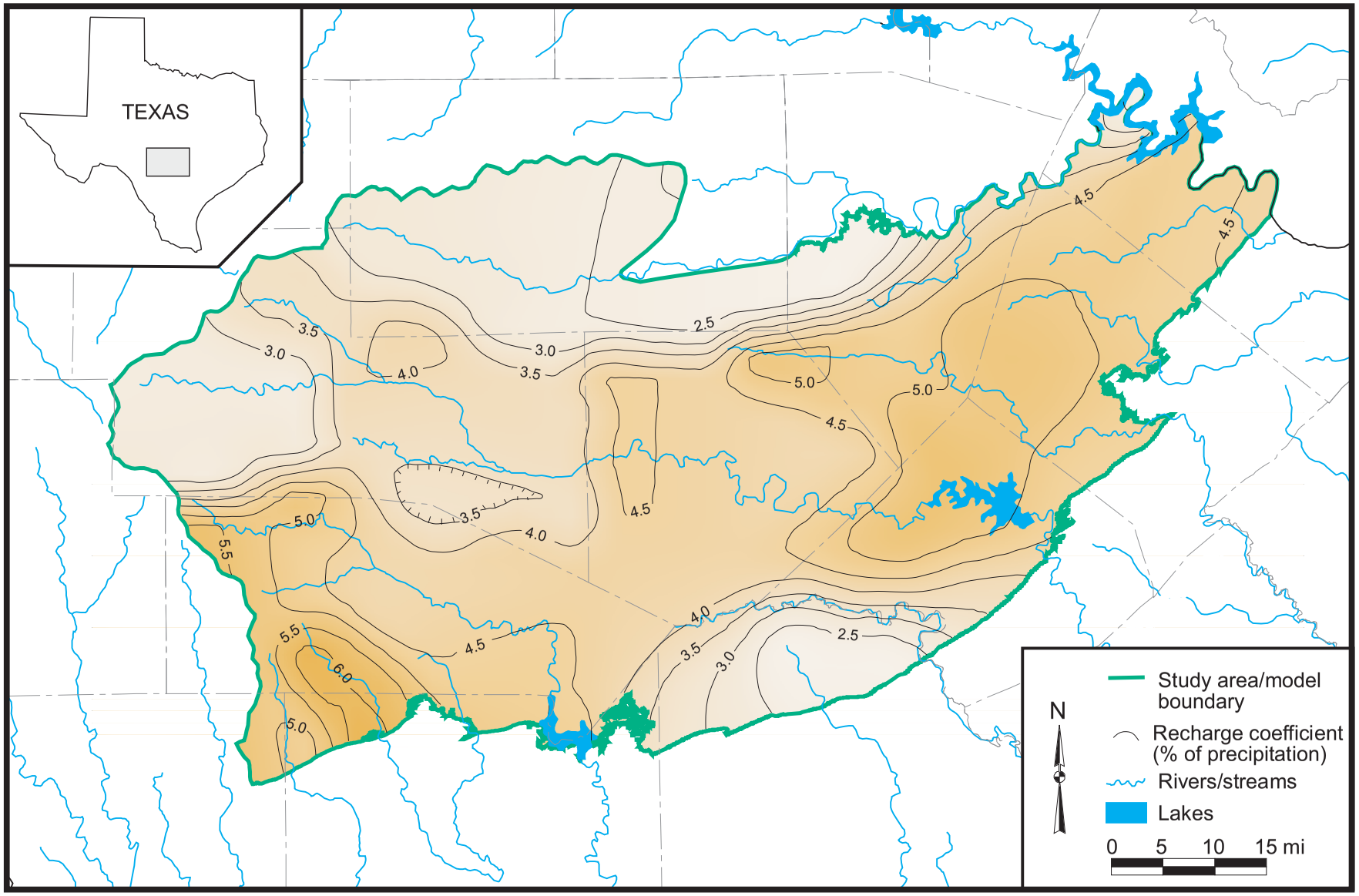

Figure 28. Recharge coefficients (percent of rainfall that recharges the aquifer) for the Trinity aquifer in the Hill Country area.

While most of the rivers are perennial (figs. 29, 30, 31, 32, 33, 34), Cibolo Creek loses flow between Boerne and Bulverde where it flows over the Lower Member of the Glen Rose Limestone (Ashworth, 1983, p. 47) (fig. 34). The upper reaches of Cibolo Creek (upstream of Boerne) where it overlies the Upper Member of the Glen Rose Limestone, are gaining water (Guyton and Associates, 1958, 1970; Espey, Huston, and Associates, 1982; Stein and Klemt, 1995; our field observations in fall 1999 and summer 2000). Lower reaches of most of the streams lose significant quantities of flow where they cross the recharge zone of the Edwards (BFZ) aquifer (Barker and others, 1994). Most perennial rivers have had brief episodes of no flow during droughts (figs. 30, 31, 32).

The study area includes four major lakes: (1) Lake Travis, (2) Lake Austin, (3) Canyon Lake, and (4) Medina Lake (fig. 1). Canyon Lake and Lake Travis have maintained approximately constant levels (+/- 20-ft) although Lake Travis had large declines during the drought of the 1950s and again in the mid-1960s (fig. 36). Lake Medina has much more variation in levels and has nearly been dry on a couple occasions (Espey, Huston, and Associates, 1989) (fig. 36).

Numerous springs occur in the study area (fig. 37). Most of these springs issue from topographically low lying areas below the base of the bluffs and source their water from groundwater flowing laterally along the hard, more-resistant tops of Glen Rose Limestone interbeds. Other springs drain the edges of the Edwards-Trinity plateau and contribute significant flow to the headwaters of the major rivers in the area. Many of the spring discharge areas have marsh purslane, cattail, ferns, and cypress trees all indicative of constant supply of water (Brune, 1981). Springs that occur in the Edwards Group generally have higher discharge rates than those occurring in the Lower and Upper Members of the Glen Rose Limestone and the Cow Creek Formation (table 2) presumably due to the cavernous nature of the Edwards Group.

Hydraulic Properties

Although the Trinity aquifer is recognized by the State as a major aquifer (Ashworth and Hopkins, 1995), its yields can be comparatively lower than other aquifers. For example, average yields in the Trinity aquifer in the Hill Country are about 250 times lower than average yields in the Edwards (BFZ) aquifer immediately to the south. Yields in the aquifer can vary considerably over a short distance because many of the formations that make up the Trinity aquifer are limestone and yields may be controlled by the location of fractures and dissolution features.

Ashworth (1983, p. 48) reports average transmissivities of about 1,300 ft^2/day and 230 ft^2/day for the Lower and Middle Trinity aquifers, respectively, and that substantially lower transmissivities are expected for the Upper Trinity aquifer. Kuniansky and Holligan (1994) determined that transmissivity for the Trinity aquifer in the Hill Country region ranged from 100 to 58,000 ft^2/day. Stein and Klemt (1995) summarized 53 aquifer tests in the Glen Rose Limestone along the Edwards (BFZ) aquifer and found a median transmissivity of about 220 ft^2/day. The Glen Rose Limestone can be unusually permeable in outcrop and shallow subcrop in northern Bexar County and southwestern Comal County near Cibolo Creek (Kastning, 1986; Veni, 1994). Barker and Ardis (1996, fig. 18) developed a map of transmissivity for the Trinity aquifer in the Hill Country area based on aquifer tests, geologic observation, and computer modeling. They determined that transmissivity is generally less than 5,000 ft^2/day but increases from 5,000 to 50,000 ft^2/day along the boundary between Comal and Bexar counties and through Kendall and the eastern part of Kerr County. The quarztose clastic facies of the updip Hensel Sand include some of the most permeable sediments in the Trinity aquifer (Barker and Ardis, 1996). Ardis and Barker (1993) and Barker and Ardis (1996) surmised that the variations in transmissivity in the Hill Country are probably due more to variations in

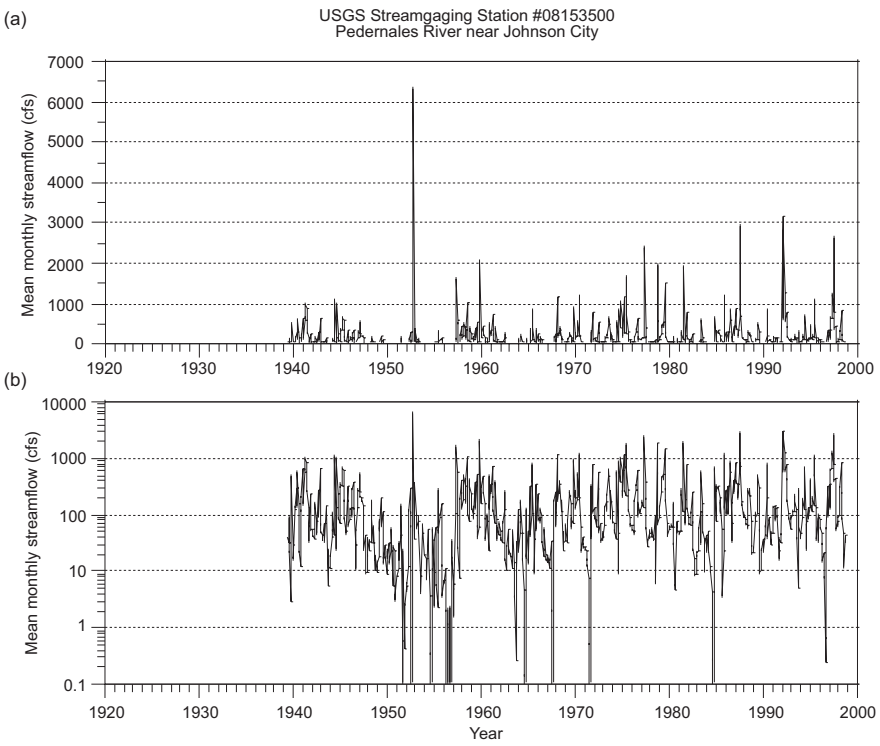

Figure 29. Mean monthly streamflow for USGS gaging station #08153500 on the Pedernales River near Johnson City for (a) linear and (b) logarithmic scales. Figure 35 shows the location of the stream gage.

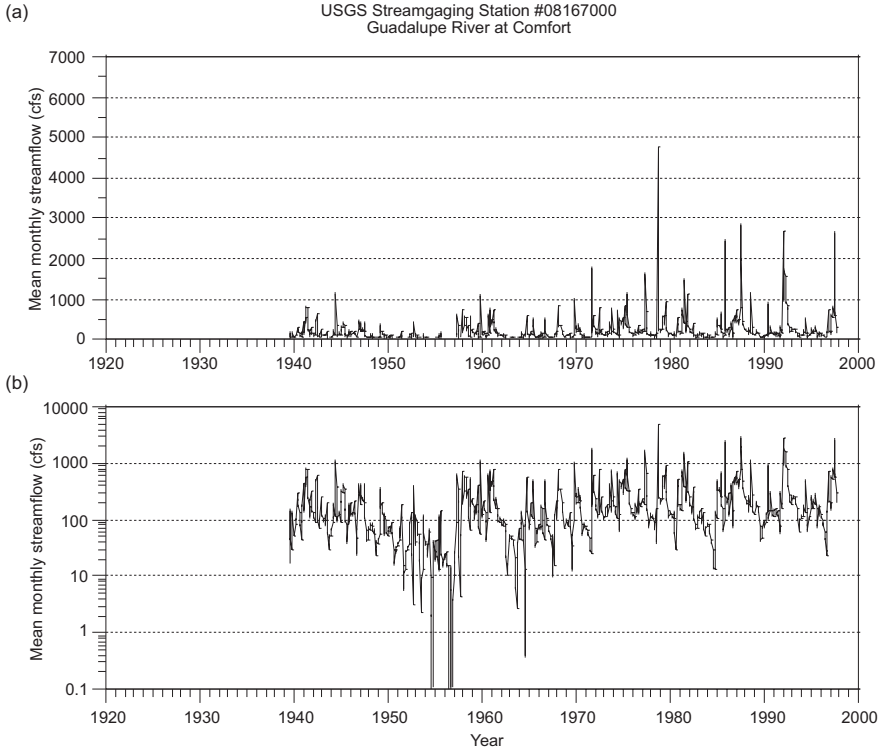

Figure 30. Mean monthly streamflow for USGS gaging station #08167000 on the Guadalupe River near Comfort for (a) linear and (b) logarithmic scales. Figure 35 shows the location of the stream gage.

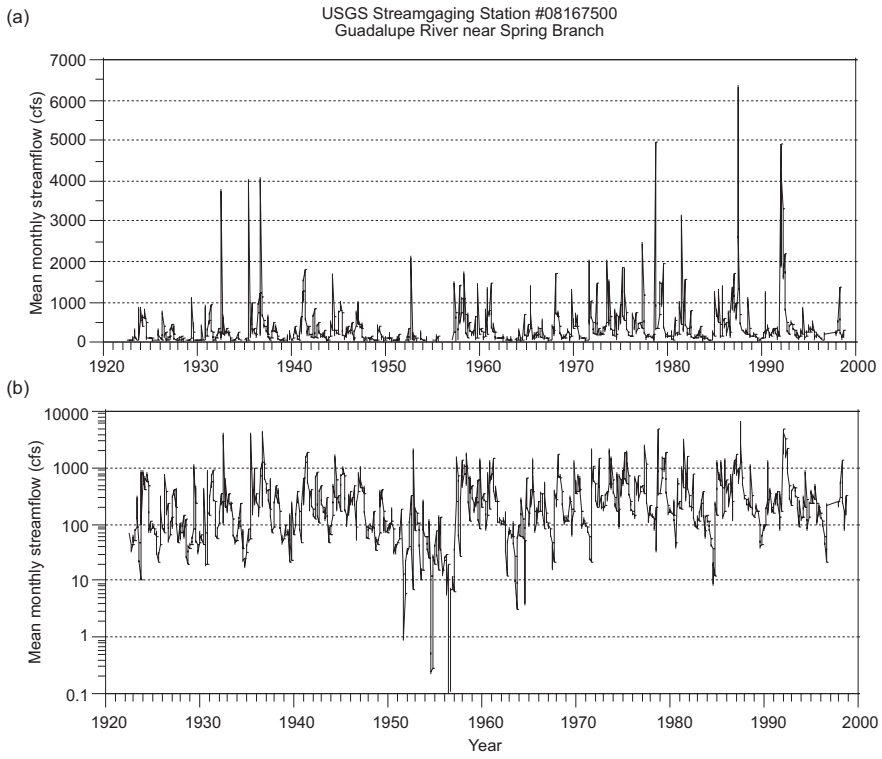

Figure 31. Mean monthly streamflow for USGS gaging station #08167500 on the Guadalupe River near Spring Branch for (a) linear and (b) logarithmic scales. Figure 35 shows the location of the stream gage.

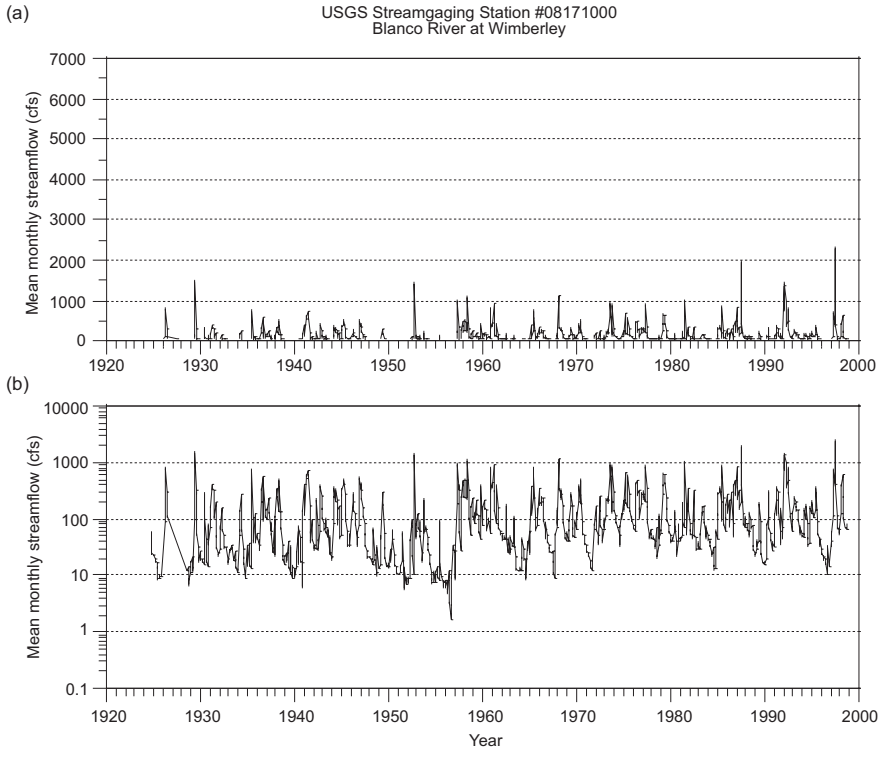

Figure 32. Mean monthly streamflow for USGS gaging station #08171000 on the Blanco River at Wimberley for (a) linear and (b) logarithmic scales. Figure 35 shows the location of the stream gage.

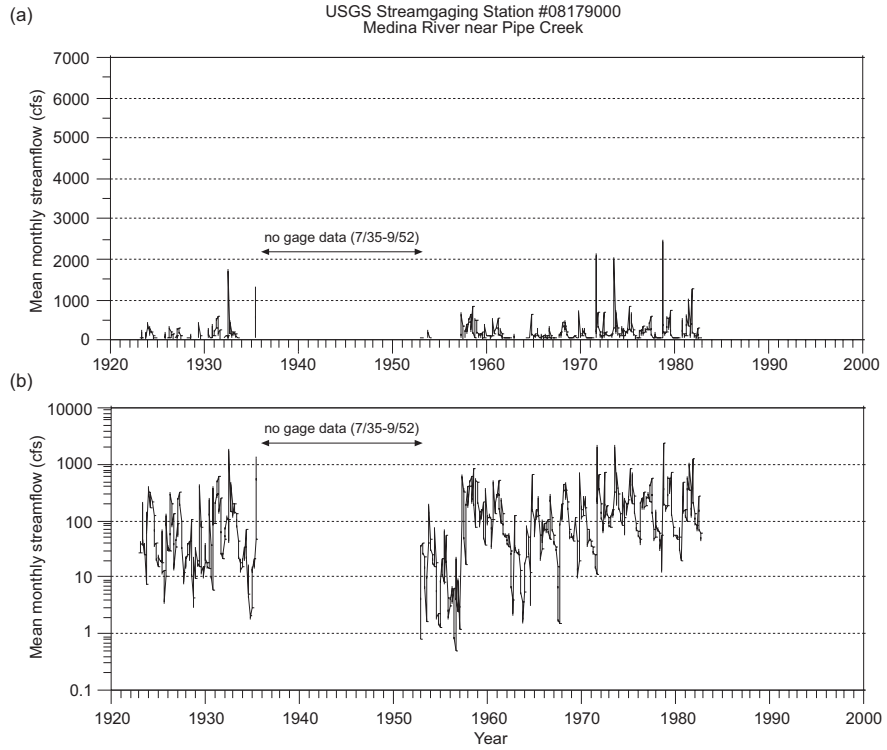

Figure 33. Mean monthly streamflow for USGS gaging station #08179000 on the Blanco River at Wimberley for (a) linear and (b) logarithmic scales. Figure 35 shows the location of the stream gage.

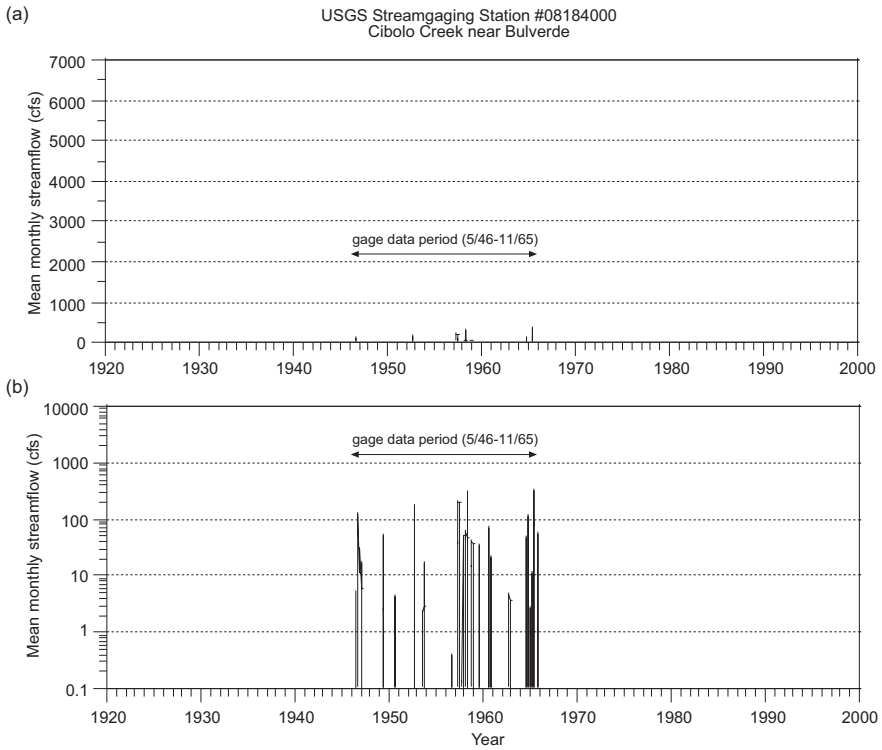

Figure 34. Mean monthly streamflow for USGS gaging station #08184000 on Cibolo Creek near Bulverde for (a) linear and (b) logarithmic scales. Figure 35 shows the location of the stream gage

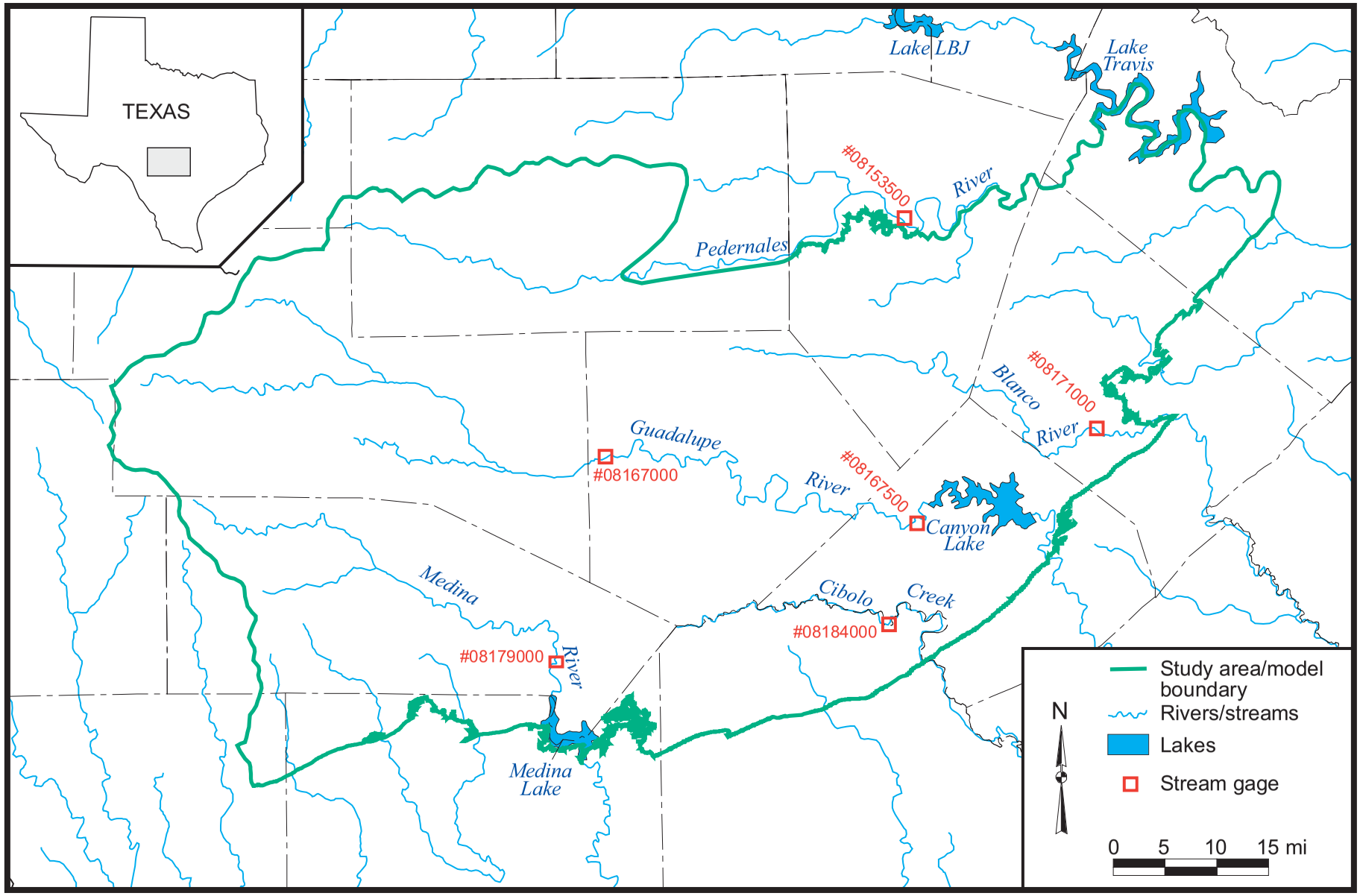

Figure 35. Location of stream gages for the stream-flow hydrographs shown in figures 29, 30, 31, 32, 33, and 34.

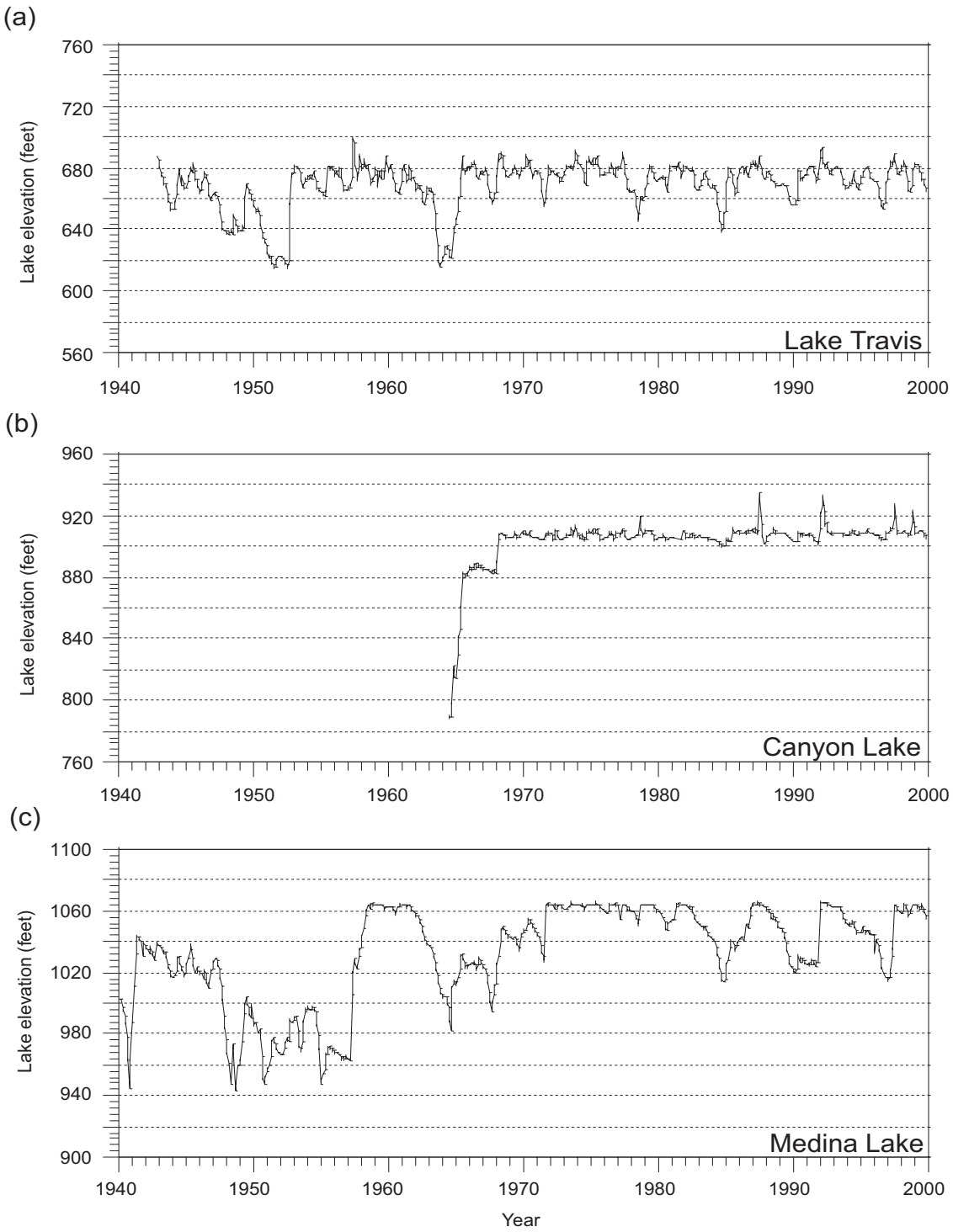

Figure 36. Lake-level elevations in (a) Lake Travis, (b) Canyon Lake, and (c) Medina Lake. Lake levels for Lake Travis are from the Lower Colorado River Authority. Lake levels for Canyon Lake are from the U.S. Army Corps of Engineers, Fort Worth District. Lake levels for Medina Lake between January 1940 and December 1986 are from Espey, Huston, and Associates (1989). Lake levels for Medina Lake between January 1987 and September 1994 and between October 1997 and September 1999 are from the U.S. Geological Survey, Texas District. We calculated lakes levels between October 1994 and September 1997 by relating lake volumes from a TWDB database to lake level using the rating curve by Espey, Huston, and Associates (1989).

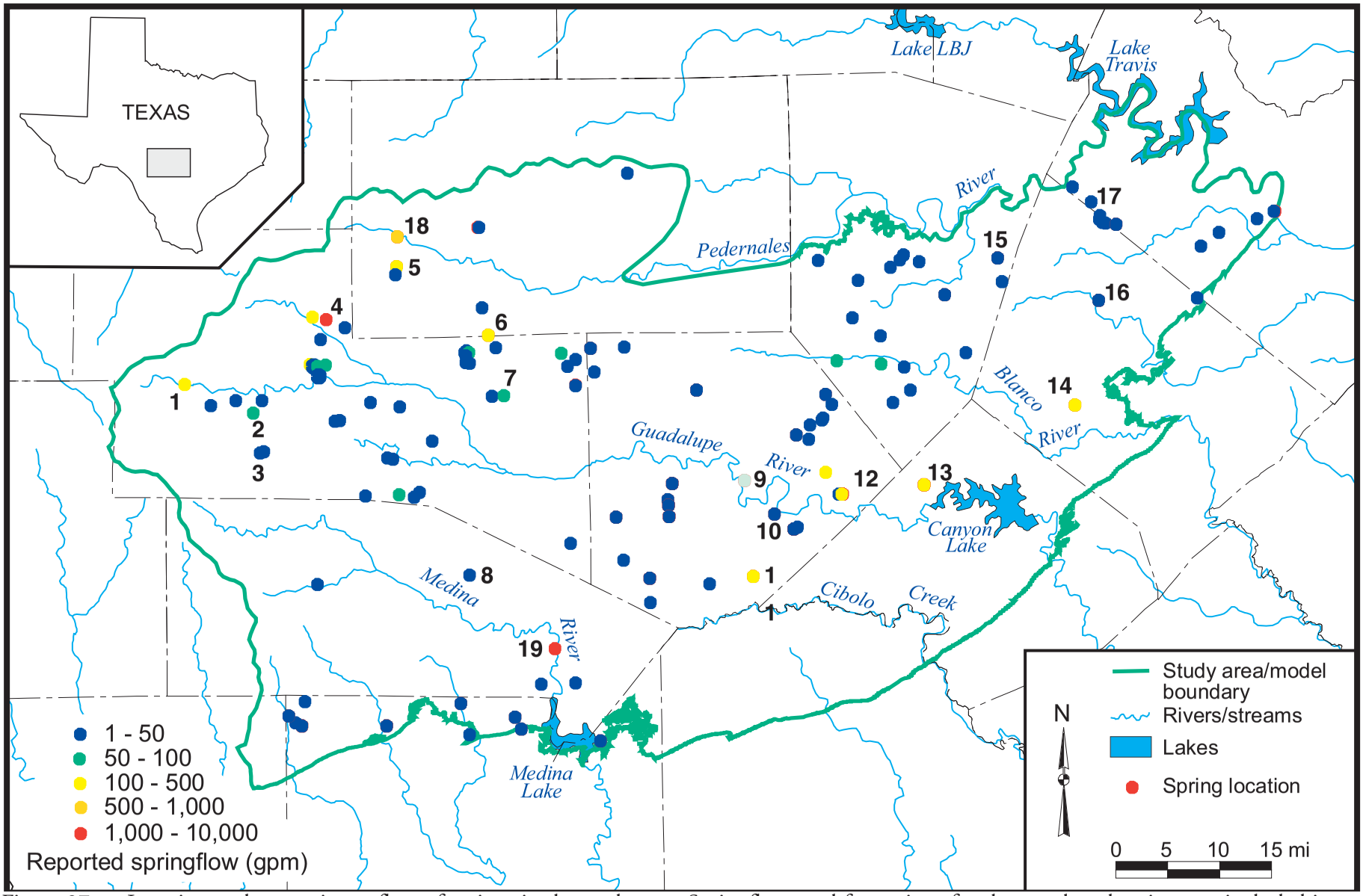

Figure 37. Location and approximate flow of springs in the study area. Springflows and formations for the numbered springs are included in Table 2.

Table 2: Estimated flow for selected springs issuing from the Edwards and Trinity aquifers of the Hill Country.

Springs	Est. flow (gpm)	Formation	Remarks
1	150	EDRDA	Measured on 4/13/67
2	100	EDRDA	Measured on 4/12/67, reported flow never ceased
3	100	EDRDA	
4	2,500	EDRDA	Measured on 3/31/66, reported flow never ceased
5	310	EDRDA	Measured on 3/11/70
6	480	EDRDA	Measured on 3/11/70, owner's trough spring
7	100	EDRDA	Measured on 6/15/66, never ceased flowing
8	20	GLRSU	Measured on 7/13/76
9	75	GLRSL	Measured on 7/10/75, ceased flowing in 1956
10	50	GLRSL	Measured on 1/17/40
11	150	GLRSL	Measured on 7/17/75, owners well #9
12	300	GLRSL	
13	300	CCRK	Measured on 7/11/75
14	500	CCRK	Measured on 8/31/76, estimated flow 1,070 gpm, Jan. 1955
15	25	GLRSL	Measured on 1/1/66
16	50	GLRSU	Measured on 12/30/88, Bassett springs
17	50	GLRSU	Measured on 5/25/73
18	9,000	EDRDA	Measured on 12/20/60
19	5,000	GLRSL	Measured on 8/20/91, springs discharge into Medina River

EDRDA = Edwards Group and associated limestone
GLRSL = Lower Member of the Glen Rose Limestone
GLRSU = Upper Member of the Glen Rose Limestone
CCRK = Cow Creek Limestone

aquifer thickness than to tectonic or diagenetic character. However, Barker and Ardis (1996) note that the evolution of stable minerals has diminished permeability in most downgradient, subcropping strata and that the leaching of carbonate constituents has enhanced permeability in some of the outcrop.

Based on 15 aquifer tests, Hammond (1984) determined that hydraulic conductivity ranges from 0.1 to 10 ft/day in the Lower Member of the Glen Rose Formation. Barker and Ardis (1996) thought that hydraulic conductivity probably averages about 10 ft/day in the aquifer. No one has investigated vertical hydraulic conductivities, although vertical hydraulic conductivities are likely to be much lower than horizontal hydraulic conductivities, especially in the Upper Member of the Glen Rose Limestone. Barker and Ardis (1996) note that recharging water moves laterally more easily atop dense interbeds than vertically through them. Guyton and Associates (1993, p. 21) estimated that the vertical hydraulic conductivity of the Hammett Shale, Bexar Shale, and the marls of the Upper Member of the Glen Rose Limestone was about 0.0001 to 0.003 ft/day. In their model that included the Trinity aquifer, Kuniansky and Holligan (1994, p. 31)

considered part of the Trinity aquifer along the Edwards (BFZ) aquifer to have anisotropic properties: greater hydraulic conductivity in the direction of faulting than perpendicular to the direction of faulting.

Walker (1979, p. 73) found an average storativity of 0.074 for four aquifer tests in the basal Cretaceous sands in the area. Ashworth (1983, p. 48) estimates that the confined storativity ranges between 10^{-5} and 10^{-3} (a specific storage of about 10^{-6} per ft) and that the unconfined storativity (specific yield) ranges between 0.1 and 0.3. Based on two aquifer tests, Hammond (1984) determined a storativity of 3×10^{-5} for the Lower Member of the Glen Rose Limestone. Although we could not locate values for the Edwards Group in the plateau area, the specific yield for the Edwards Group in the Edwards (BFZ) aquifer is 0.03 (Maclay and Small, 1986, p. 68-69).

To estimate hydraulic properties for our study area and expand upon previous studies, we (1) compiled available information on aquifer properties or tests from published reports and well records, (2) conducted and analyzed detailed aquifer tests in the study area, (3) used specific-capacity information to estimate transmissivity, and (4) summarized the results of our analysis using statistics.

We compiled aquifer tests from Meyers (1969), Hammond (1984), W. E. Simpson Company Inc. and W. F. Guyton Associates, Inc. (1993), LBJ - Guyton Associates (1995), and Bradley and others (1997). In addition, we conducted 35 aquifer tests in the study area and analyzed the results using standard techniques (such as Theis, 1935; Cooper and Jacob, 1946; Kruseman and de Ridder, 1994). We also compiled information on 297 specific-capacity (well-performance) tests from the TWDB water-well database and used an analytical technique (Theis, 1963) to estimate transmissivity. Twenty-one of these tests were from the Upper Trinity aquifer, 260 were from the Middle Trinity aquifer, and 16 were from the Lower Trinity aquifer (fig. 38).

Based on results from the data compilation, aquifer testing, and specific-capacity analysis, we found that hydraulic conductivity for all the tests in the Trinity aquifer appear to be lognormally distributed (fig. 39a) with a geometric mean of 1.3 ft/day and a standard deviation that spans from 0.18 to 9.7 ft/day (table 3). (A lognormal distribution means that the logarithms of the values are normally distributed, and a geometric mean is the antilogarithm of the mean of the logarithms of the values.) Our study resulted in 15 measurements of hydraulic conductivity in the Upper Trinity aquifer (Upper Member of the Glen Rose Limestone) with a geometric mean of 0.54 ft/day (table 3). These fifteen measurements do not appear to be log-normally distributed (fig. 39b). However, there may not be enough measurements to adequately define the distribution of hydraulic conductivity in the Upper Trinity aquifer. Geometric mean hydraulic conductivity values for the Lower Member of the Glen Rose Limestone, the Cow Creek Limestone, and the Hensel Sand are 1.9, 2.0, and 4.1 ft/day, respectively (table 3). Hydraulic conductivity appears to be log-normally distributed in these units (figs. 39 c, d, e). We were not able to locate any aquifer tests for the Edwards Group in the plateau area.

Using semivariograms (see Clark, 1979; McCuen and Snyder, 1986), we showed that hydraulic conductivity in the Lower Member of the Glen Rose Limestone and the Hensel Sand is spatially correlated (fig. 40). Spatial correlation infers that points that are closer together are more similar to each other than points that are further apart. There was not enough data to assess the spatial correlation of hydraulic conductivity for the Edwards Group in the plateau area, the Upper Member of the Glen Rose Limestone, and the Cow Creek Limestone. The experimental semivariogram for log hydraulic conductivity in the Lower Member of the Glen Rose Limestone showed strong spatial correlation. Fitting a spherical theoretical semivariogram to the experimental semivariogram for

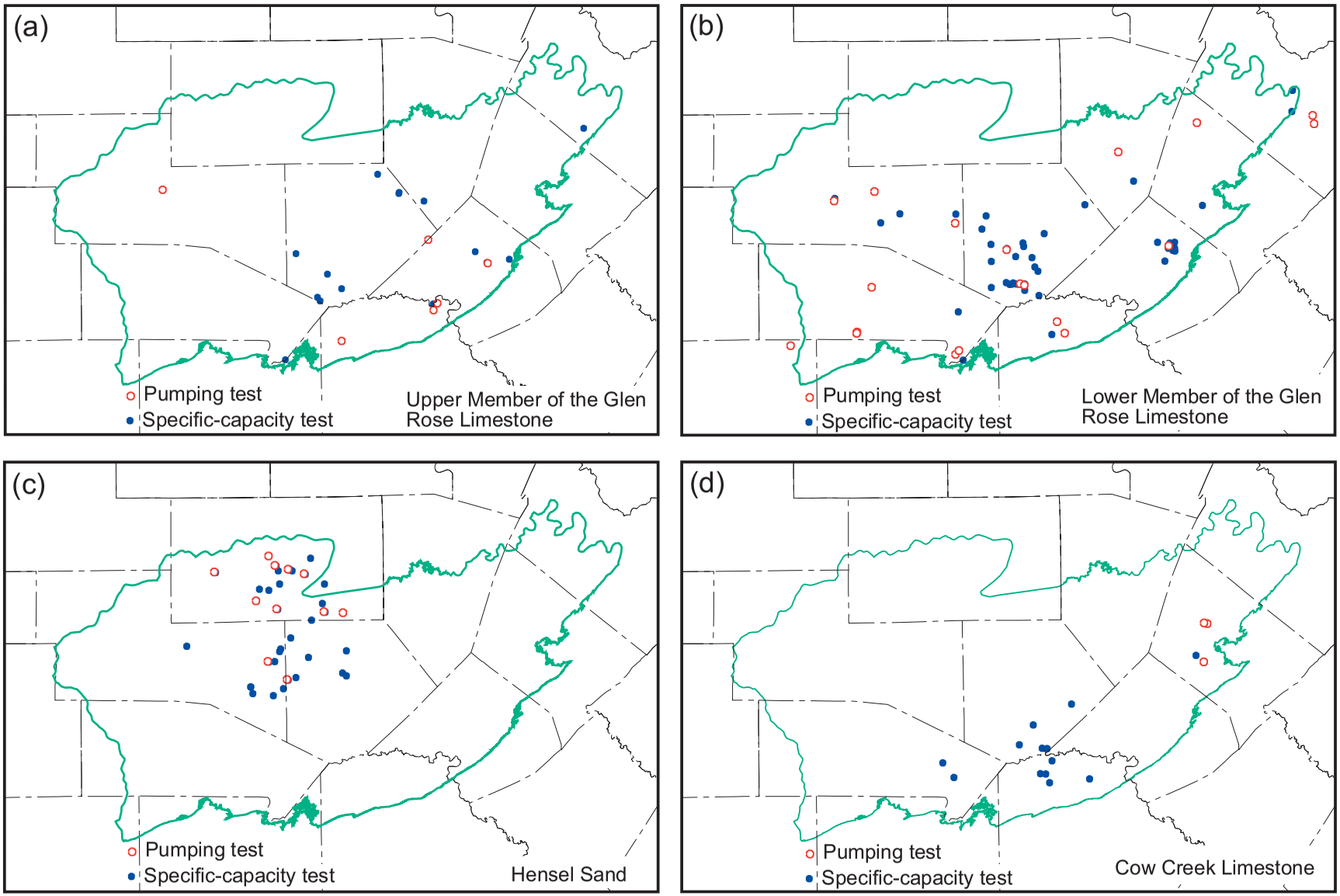

Figure 38. Location of pumping and specific-capacity tests for tests of the (a) Upper Member of the Glen Rose Limestone, (b) Lower Member of the Glen Rose Limestone, (c) Hensel Sand, and (d) Cow Creek Limestone.

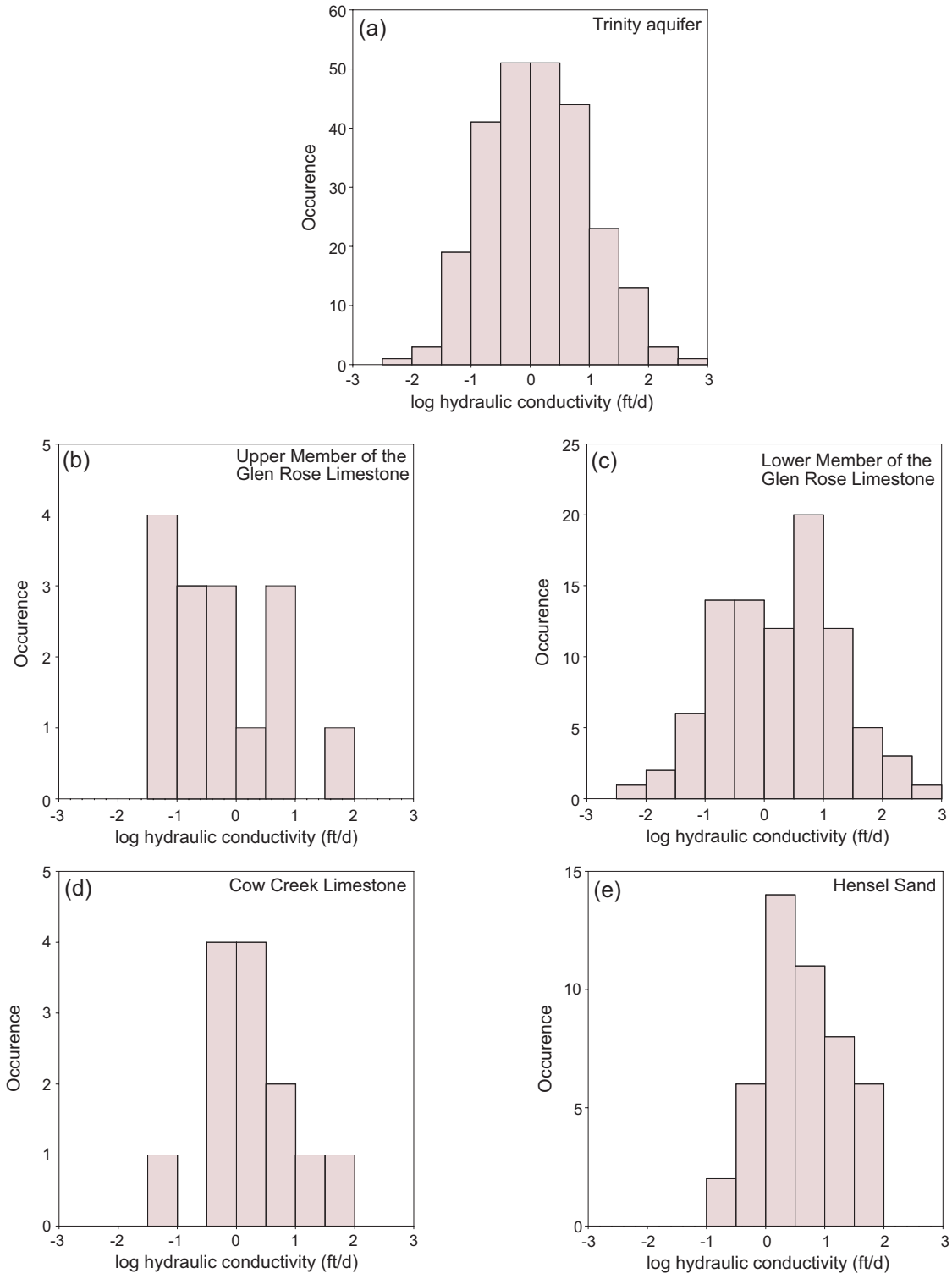

Figure 39. Histograms of measured hydraulic conductivity for (a) all tests and tests from the (b) Upper Member of the Glen Rose Limestone, (c) Lower Member of the Glen Rose Limestone, (d) Cow Creek Limestone, and (e) Hensel Sand.

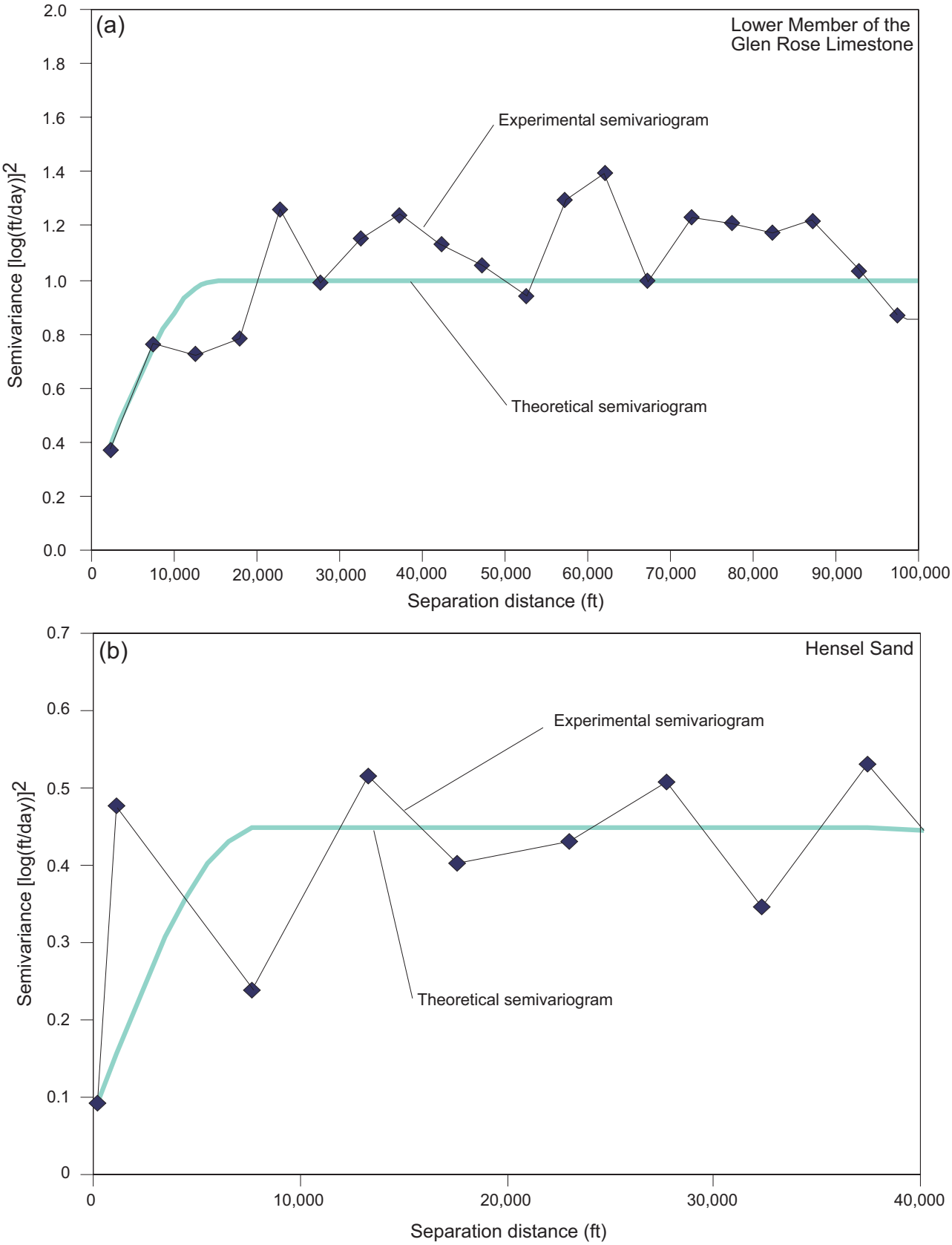

Figure 40. Experimental and theoretical semivariograms for the (a) Lower Member of the Glen Rose Limestone and (b) Hensel Sand.

the Lower Member of the Glen Rose Limestone resulted in a nugget of 0.2 [log(ft/day)]^2, a sill of 1.0 [log(ft/day)]^2, and a range of 15,000 ft (fig. 40a). The range suggests that hydraulic conductivity is spatially correlated within 15,000 ft in the Lower Member of the Glen Rose Limestone.

The experimental semivariogram for hydraulic conductivity in the Hensel Sand did not show spatial correlation as strong as for the Lower Member of the Glen Rose Limestone (fig. 40b). However, fitting a spherical theoretical semivariogram to the experimental semivariogram for the Hensel Sand resulted in a nugget of 0.08 [log(ft/day)]^2, a sill of 0.45 [log(ft/day)]^2, and a range of 8,000 ft (fig. 40b).

We used ordinary kriging and the semivariograms to spatially distribute hydraulic conductivity in the Lower Member of the Glen Rose Limestone and the Hensel Sand (figs. 41 and 42). These maps have several localized areas of high or low values of hydraulic conductivity. This is due to local variations in the number of data points available for interpolation (see fig. 38). In areas with no control points, the kriging algorithm results in the geometric mean hydraulic conductivity as the best estimate of

Table 3: Statistical summary of hydraulic conductivity values for the Trinity aquifer in the Hill Country area.

	K_{CC}	K_H	K_{LGR}	K_{MT}	K_{UGR}	K_H+ K_{CC}	K_{LGR}+ K_{CC}	K_{LGR}+ K_H	all
n	13	47	90	24	15	10	8	44	251
p_{25}	1.2	3.2	2.0	0.38	0.49	0.95	0.22	0.77	1.2
p_{50}	0.86	1.5	0.28	0.19	0.09	0.58	0.16	0.17	0.28
p_{75}	5.5	14.	9.1	1.2	2.0	1.3	0.65	1.6	5.1
$\overline{x}_g$	2.0	4.1	1.9	0.39	0.54	1.0	0.34	0.63	1.3
$\overline{x}_g - s$	0.33	0.88	0.19	0.11	0.06	0.36	0.10	0.14	0.18
$\overline{x}_g + s$	12.	19.	19.	1.4	4.6	2.8	1.1	2.8	9.7
s^2	0.59	0.45	0.99	0.32	0.86	0.20	0.27	0.43	0.75

K_{CC} - Cow Creek Limestone
K_H - Hensel Sand
K_{LGR} - Lower Member of the Glen Rose Limestone
K_{MT} - Middle Trinity aquifer
K_{UGR} - Upper Member of the Glen Rose Limestone
all - All formations pooled together
n - number of data points
p_{25} - 25th percentile (median) (ft/d)
p_{50} - 50th percentile (median) (ft/d)
p_{75} - 75th percentile (median) (ft/d)
$\overline{x}_g$ - geometric mean (ft/d)
$\overline{x}_g - s$ - geometric mean minus a standard deviation (ft/d)
$\overline{x}_g + s$ - geometric mean plus a standard deviation (ft/d)
s^2 - variance (log[ft/d])^2

Standard deviations are calculated from the log-normal distribution.

hydraulic conductivity. Because we did not have geologic information to help guide the distribution of hydraulic properties, we felt that the geometric mean resulted in the best estimate. For the Hensel Sand, control points are heavily biased toward the northwestern part of the study area (fig. 38c). Therefore, hydraulic conductivity for the rest of the study area may be biased toward values in that area.

To develop a map of hydraulic conductivity for the Middle Trinity aquifer, we used the spatial distribution of hydraulic conductivity in each unit of the Middle Trinity aquifer (Cow Creek Limestone, Hensel Sand, and Lower Member of the Glen Rose Limestone) and the relative thickness of each unit. For the Lower Member of the Glen Rose Limestone and Hensel Sand, we used the maps of hydraulic conductivity developed using kriging (figs. 41 and 42, respectively). Because there was not enough information for kriging hydraulic conductivity in the Cow Creek Limestone, we used a constant value of 2.0 ft/day, the geometric mean of the available measurements (table 3). To define the relative thickness for each of the units in the study area, we first developed structure maps of the approximate elevation of the contacts between (1) the Cow Creek Limestone and the Hensel Sand and (2) the Hensel Sand and the Lower Member of the Glen Rose Limestone. Using these structure maps and the structure maps for the bottom of the Cow Creek Limestone and the bottom of the Upper Member of the Glen Rose Limestone, we calculated the thickness of the Cow Creek Limestone, Hensel Sand, and Lower Member of the Glen Rose Limestone for the study area. The sum of each of these thicknesses equaled the thickness of the Middle Trinity aquifer.

To estimate the hydraulic conductivity of the Middle Trinity aquifer at any given point, we weighted the hydraulic conductivity of each layer by the relative thickness of each respective layer at that point. In mathematical terms, we estimated the hydraulic conductivity of the Middle Trinity aquifer at any given spatial location, $K(x, y)_{MTa}$, by:

$$K(x, y)_{MTa} = \frac{b_{cc}}{b_{MTa}} \bar{K}_{cc} + \frac{b_h}{b_{MTa}} K_h + \frac{b_{lgr}}{b_{MTa}} K_{lgr} \qquad (1)$$

where b_{MTa} is the thickness of the Middle Trinity aquifer at point (x, y); b_{cc} is the thickness of the Cow Creek Limestone at point (x, y); $\bar{K}_{cc}$ is the geometric mean hydraulic conductivity of the Cow Creek Limestone; b_h is the thickness of the Hensel Sand at point (x, y); K_h is the hydraulic conductivity of the Hensel Sand at point (x, y); b_{lgr} is the thickness of the Lower Member of the Glen Rose Limestone at point (x, y); and K_{lgr} is the hydraulic conductivity of the Lower Member of the Glen Rose Limestone at point (x, y). The resulting distribution of hydraulic conductivity in the Middle Trinity aquifer (fig. 43) shows (1) higher hydraulic conductivity in the Gillespie County area due to the higher hydraulic conductivity of the Hensel Sand and the greater relative thickness of the Hensel Sand and (2) a dampening of the variations in hydraulic conductivity seen in the maps for the Hensel Sand and Lower Member of the Glen Rose Limestone caused by the weighting described above. The mean hydraulic conductivity for the resulting distribution of hydraulic conductivity in the Middle Trinity aquifer is 2.6 ft/day.

Storativity values were calculated from ten multiple-well pumping tests in and near the Hill Country area (fig. 44). Storativity values show a range of several orders of magnitude. The value of storativity, determined from four pumping tests for the entire section of the Middle Trinity aquifer, range from 4.9×10^{-5} to 7.0×10^{-4}. Two pumping tests in Gillespie County showed large variation in storativity value for the Hensel sand - 1.4×10^{-4} and 8.0×10^{-4}. Two pumping tests in Travis County showed storativity values of 7.0×10^{-4} and 2.2×10^{-5} for the Cow Creek Limestone. A

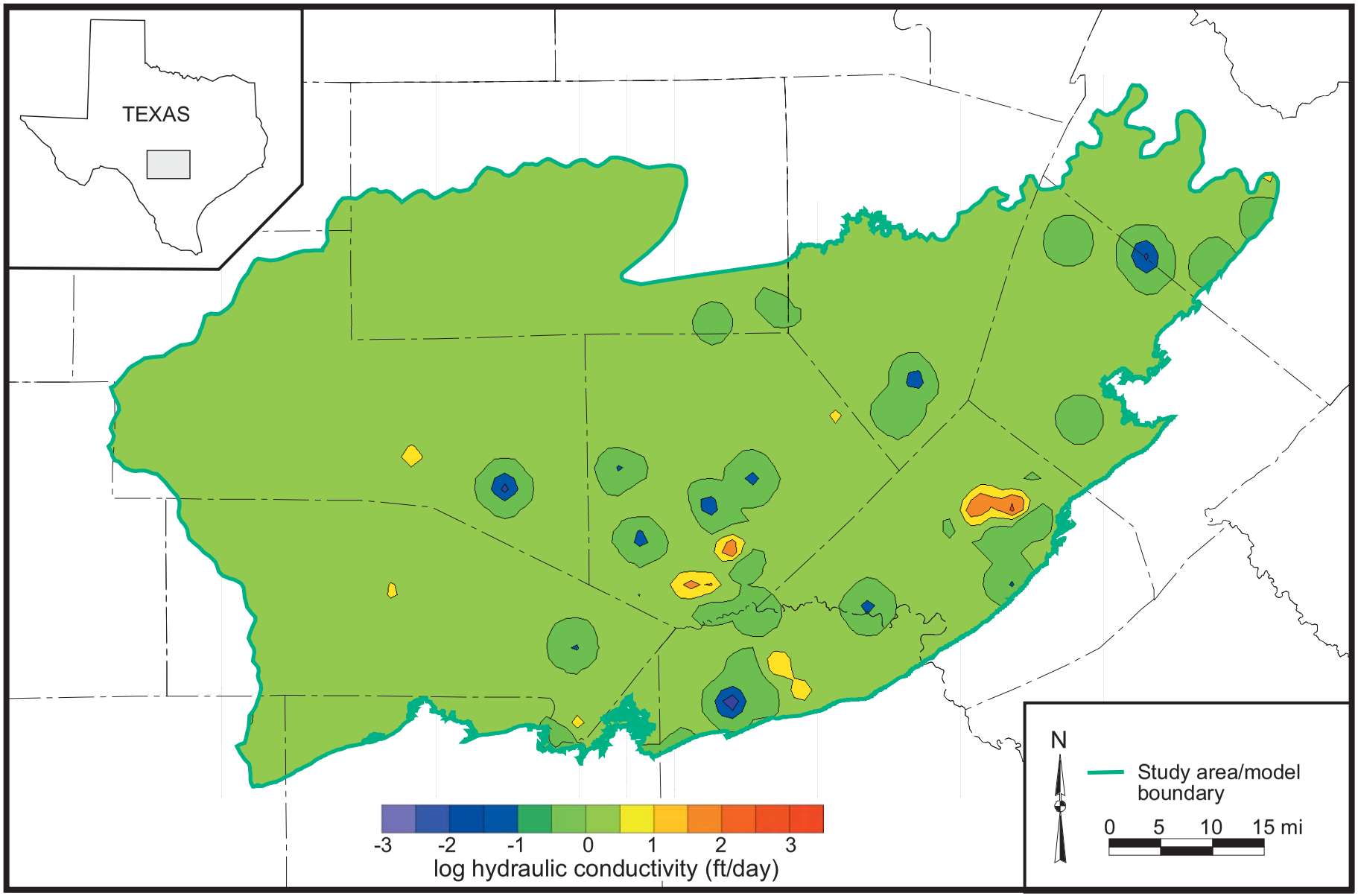

Figure 41. Kriged distribution of hydraulic conductivity in the Lower Member of the Glen Rose Limestone.

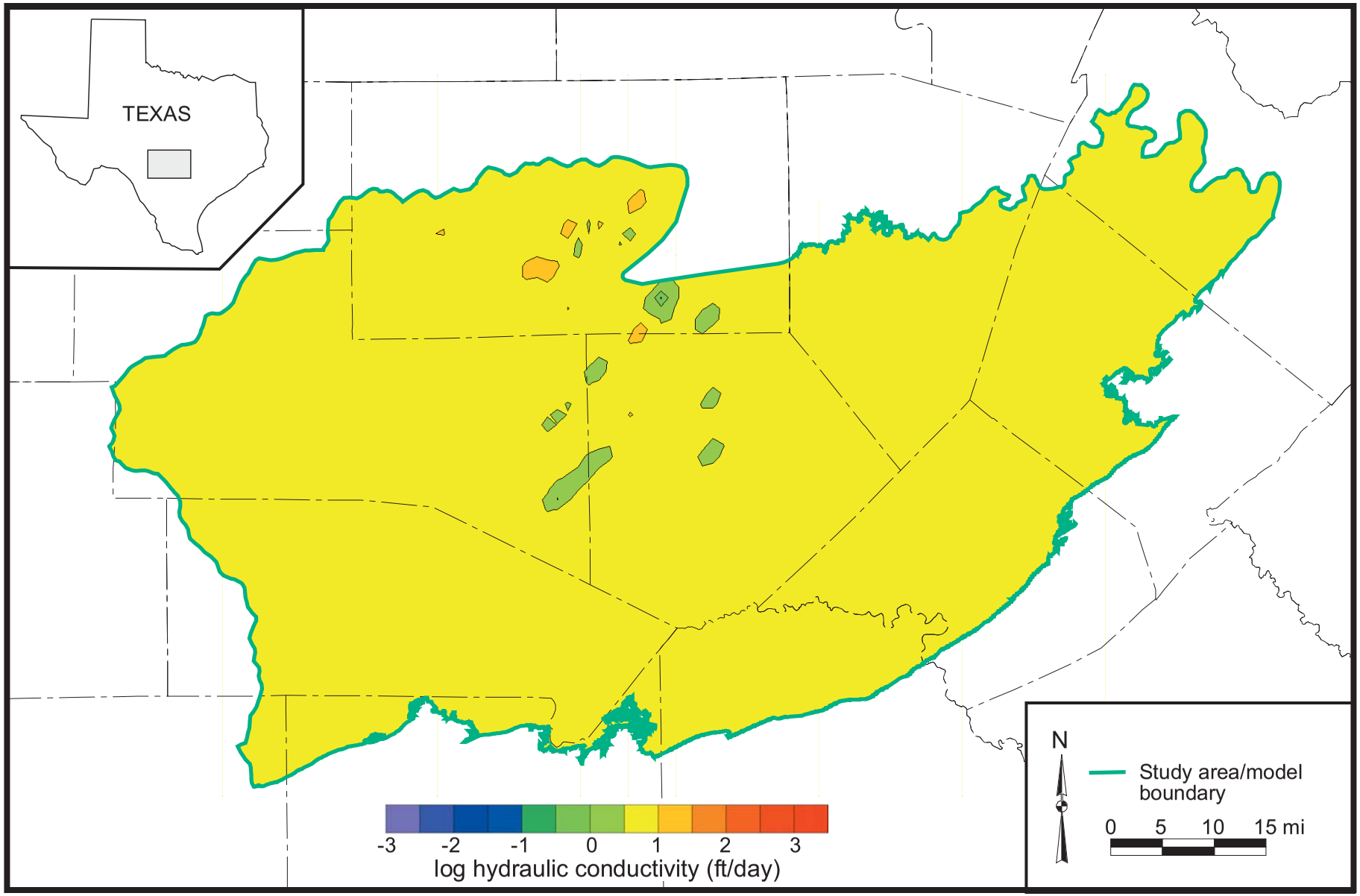

Figure 42. Kriged distribution of hydraulic conductivity in the Hensel Sand.

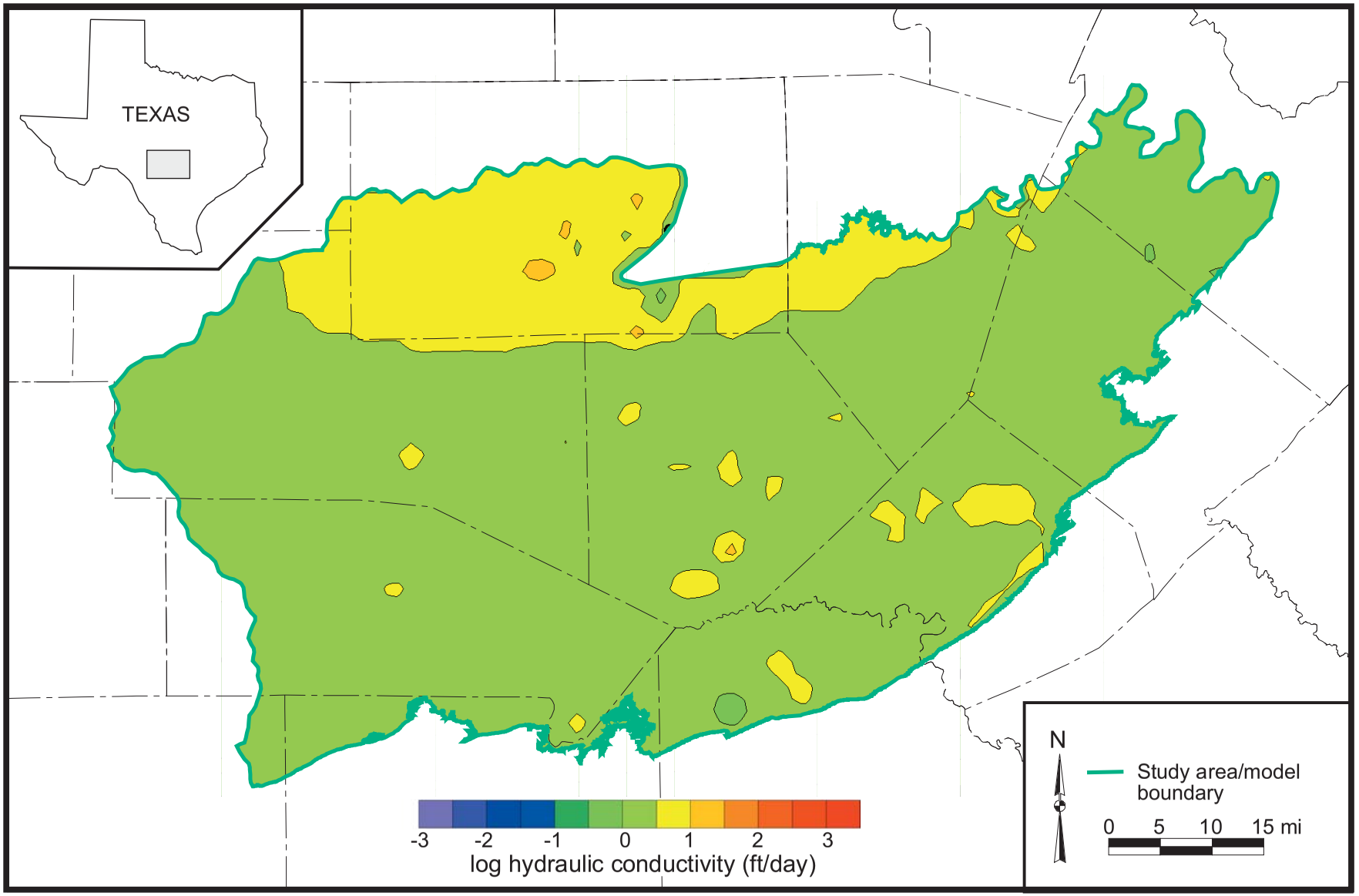

Figure 43. Distribution of hydraulic conductivity in the Middle Trinity aquifer based on measured values of hydraulic conductivity. This is the distribution of hydraulic conductivity before calibration of the model.

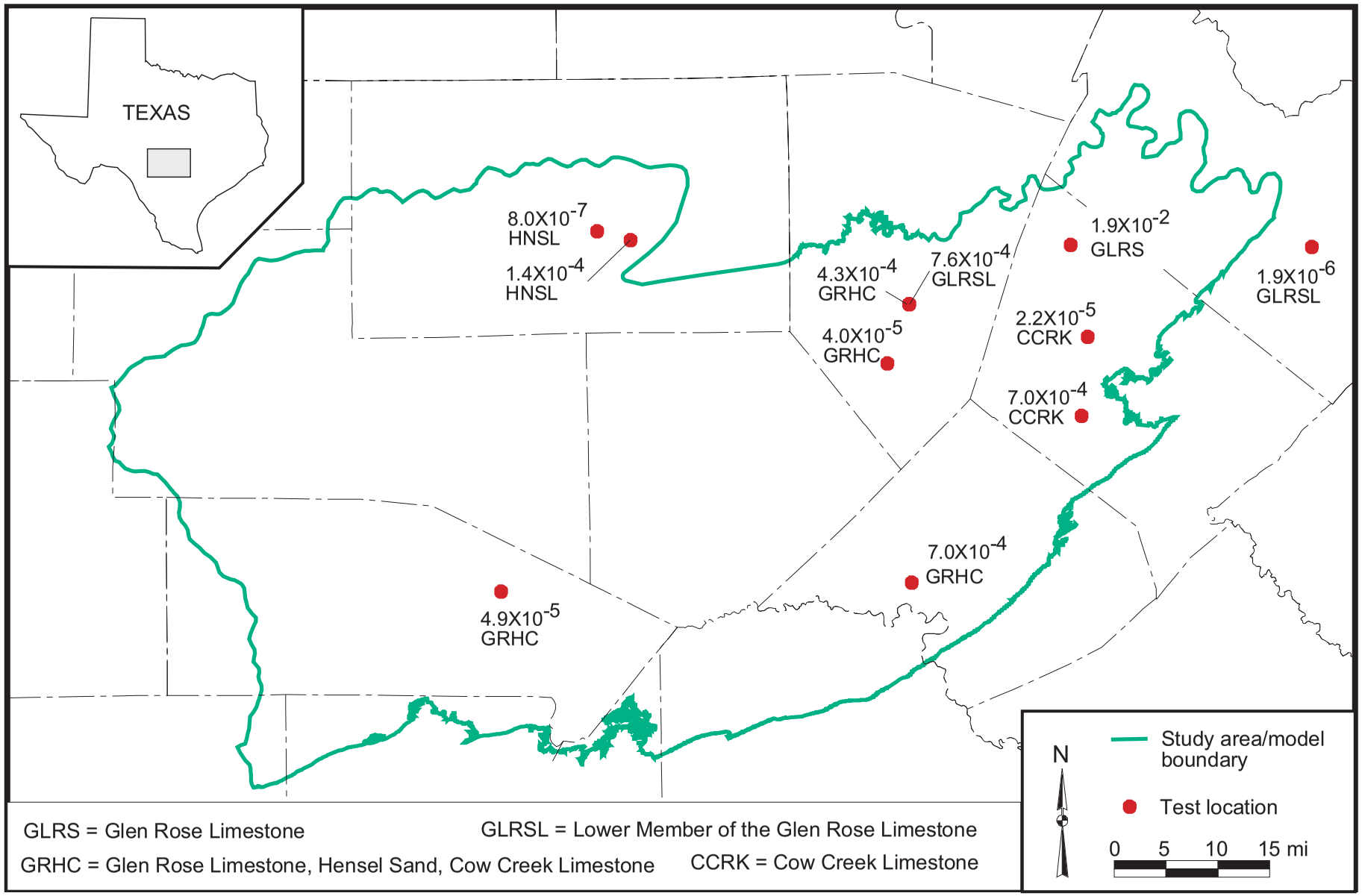

Figure 44. Locations, formations, and values of storativity values in the Trinity aquifer in the Hill Country area based on aquifer tests.

pumping test performed in northwestern Travis County indicated a storativity value of 1.9×10^{-2}. This test well was completed partly in the Upper Member of the Glen Rose Limestone and partly in the Lower Member of the Glen Rose Limestone. The high storativity value represents the unconfined nature of the Upper Member of the Glen Rose Limestone at that location.

Discharge

Discharge from the Upper and Middle Trinity aquifer in the Hill Country area is, from greatest to lowest, through (1) discharge to streams and springs (Ashworth, 1983, p. 48), (2) lateral subsurface flow and diffuse upward leakage to the Edwards (BFZ) aquifer (Veni, 1994), (3) pumping of the aquifer, and (4) vertical leakage to the Lower Trinity aquifer. Kuniansky (1989) estimates that baseflow (flow from the aquifer to rivers) accounts for 25 to 90 percent of total streamflow from December, 1974, to March, 1977. Kuniansky and Holligan's (1994, fig. 14) calibrated model shows streams gaining 408,000 acre-ft/yr. The volume of baseflow varies from year-to-year depending on precipitation.

The volume of water that moves laterally from the Trinity aquifer into the Edwards (BFZ) aquifer is not known, partially because of the difficulty in estimating the amount of flow. A number of studies have shown, either through hydraulic or chemical analyses, that groundwater likely flows from the Trinity aquifer into the Edwards (BFZ) aquifer (see Long, 1962; Klemt and others, 1979; Walker, 1979; Senger and Kreitler, 1984; Slade and others, 1985; Maclay and Land, 1988; Waterreus, 1992; Veni, 1994, 1995). Most of the studies have focused on the movement of groundwater from the Glen Rose Limestone into the Edwards aquifer. However, water levels (fig. 20) suggest that groundwater from the Trinity aquifer discharges to the south and east in the direction of the Edwards (BFZ) aquifer. Part of this groundwater moves into the Edwards through faults, and part continues to flow in the Trinity aquifer beneath the Edwards (BFZ). It is likely that the groundwater that continues to flow in the Trinity aquifer eventually discharges upward to the Edwards (BFZ) aquifer. Kuniansky and Holligan's (1994) model directs all of the flow from the Trinity aquifer into the Edwards (BFZ) aquifer. The Glen Rose Limestone in the Cibolo Creek area has been argued to be a part of the Edwards (BFZ) aquifer due to the hydraulic response and continuity of the formations (George, 1947; Pearson and others, 1975; Veni 1994, 1995).

A few studies have estimated the volume of flow from the Trinity aquifer into the Edwards (BFZ) aquifer. Lowry (1955) attributed a five percent error between measured inflows and outflows in the Edwards (BFZ) aquifer to cross-formational flow from the Glen Rose Limestone. Woodruff and Abbott (1986), citing a personal communication with Bob Klemt, report that recharge from cross-formational flow accounts for six percent of total recharge (about 41,000 acre-ft/yr on average) to the Edwards (BFZ) aquifer. Kuniansky and Holligan's (1994) model suggests about 360,000 acre-ft/yr flows from the Trinity aquifer to the Edwards (BFZ) aquifer. However, this value, about 53 percent of average annual recharge to the Edwards (BFZ) aquifer, is probably too high. LBG-Guyton Associates (1995) estimated cross-formational flow from the Glen Rose Limestone to the Edwards (BFZ) aquifer in the San Antonio area, excluding recharge from Cibolo Creek, to be about two percent of total recharge to the aquifer. None of the numerical groundwater flow models of the Edwards (BFZ) aquifer (see Klemt and others, 1979; Maclay and Land, 1988; Slade and others, 1985; Wanakule and Anaya, 1993; Barrett and Charbeneau, 1996) include cross-formational flow from the Trinity aquifer.

Groundwater also discharges from the aquifer through pumping of water wells. Lurry and Pavlicek (1991), Barker and Ardis (1996,

p. 47), Kuniansky and Holligan (1994, fig 14) estimate pumping from the Trinity aquifer in the Hill Country area (including the Lower Trinity aquifer) to be between 10,000 and 15,000 acre-ft/yr in the 1970s. Based on information in Bluntzer (1992), about 14,000 acre-ft/yr was produced from the Trinity aquifer (including the Lower Trinity aquifer) and Edwards-Trinity Plateau aquifer in our study area in 1985. Guyton and Associates (1993) estimated that about 6,350 acre-ft was pumped from the Trinity aquifer in Bexar County in 1990 with 85 percent of production from the Middle Trinity aquifer.

For our study, we estimated pumping for 1975, 1996, and 1997 based on the Water Use Survey (WUS) database at the TWDB and predicted dry-demand pumping through 2050 based on the current (1997) distribution of pumping according to the WUS and the predicted demands reported by Regional Water Planning Groups.

The primary categories for water use in the WUS database are (1) municipal, (2) manufacturing, (3) power, (4) mining, (5) unreported domestic, (6) livestock and (7) irrigation. For our analysis, we combined manufacturing, power and mining into one 'industrial use' category. Municipal and industrial water uses are based on reported values from the users. We associated these values with well locations and aquifers by cross referencing the water use to the municipal and industrial well through the Texas Natural Resource Conservation Commission (TNRCC) municipal water-well database, the TWDB water-well database, and through telephone interviews with water users. Industrial use was lumped into municipal usage for predictive pumping through 2050.

The distribution of unreported domestic use for 1975 was based on agricultural and rangeland land-use maps developed by the United States Geologic Survey, digitized by the United States Environmental Protection Agency, and stored by the Texas Natural Resources Information System at the TWDB Web site. The 1996, 1997 and predictive domestic pumpage were evenly distributed over drainage basins in the county, excluding municipal areas, for each of the counties in the model area. We vertically distributed pumping into the different aquifers according to the percentage of domestic wells completed in the respective aquifers.

The distribution of livestock use was based on land-use maps. Areas that were classified as rangeland were used for the distribution of livestock pumpage. We vertically distributed pumping into the different aquifers according to the percentage of livestock wells completed in the respective aquifers. The distribution of irrigation use for 1975 was based on agricultural land-use maps. The distribution of irrigation use for 1996, 1997, and through 2050 were based on the location of irrigation wells from the WUS database. The distribution of irrigation use among the different aquifers was based on comparing the locations of irrigation wells relative to surface geology and the well completion interval.

As part of Senate Bill 1 water planning (see Hubert, 1999), Regional Water Planning Groups have estimated future water demands under drought of record conditions for 2000, 2010, 2020, 2030, 2040, and 2050. These demands are for combined surface water and groundwater sources. To estimate future groundwater demands, we used the WUS database to define the ratio between groundwater and surface-water use for each usage category and county. We used these ratios and applied them to future water demands to estimate groundwater demand for each usage category in each county.

Based on our analysis, about 10,000 acre-ft/yr of groundwater was produced in the study area in 1975 (table 4, fig. 45). The amount of groundwater produced increased to about 36,000 acre-ft/yr by 1997 (table 4, fig. 45). We estimate that the drought demand for groundwater will be about 59,000 acre-ft/yr by 2030 and about 73,000 acre-ft/yr by 2050 (table 4, fig. 45).

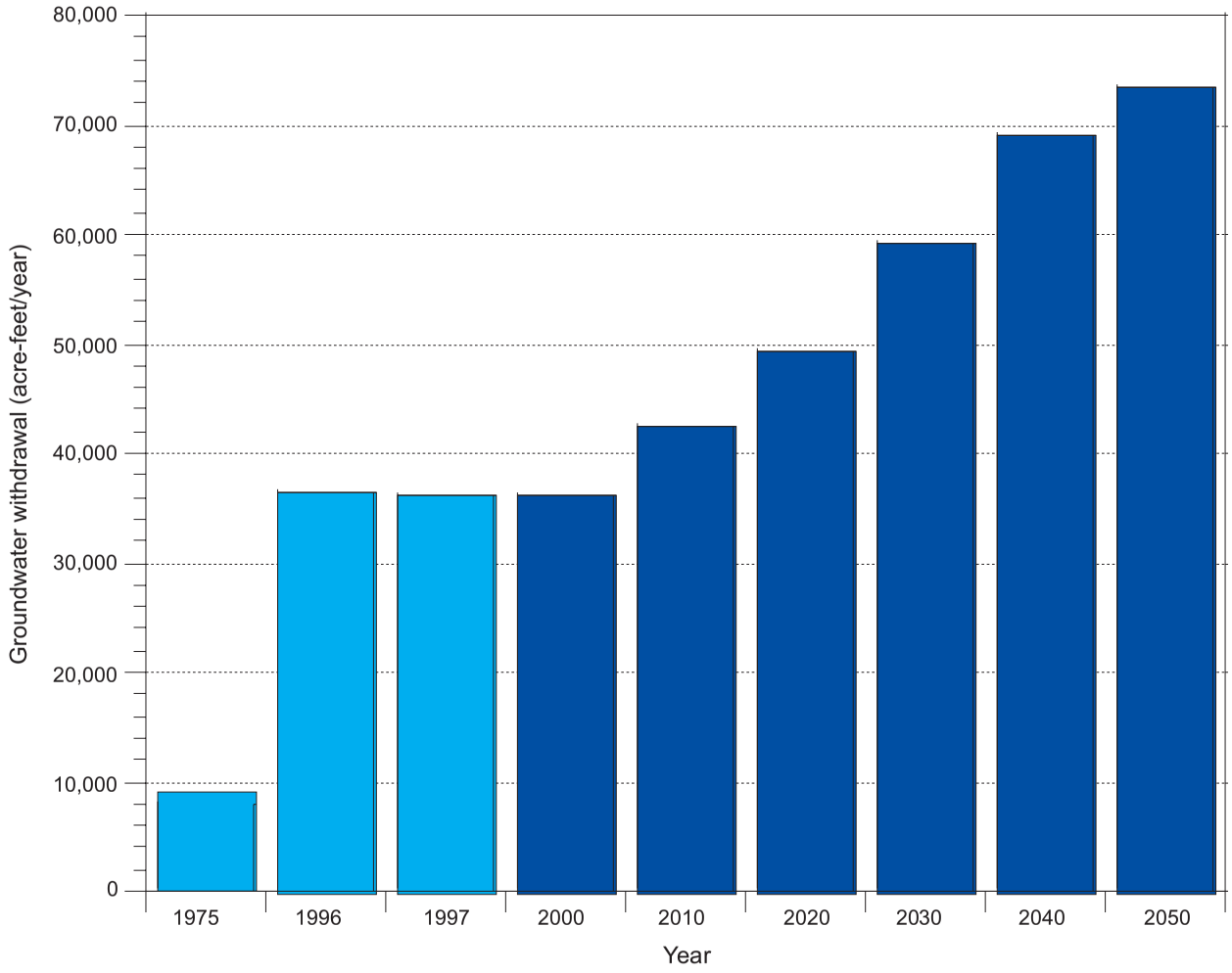

Figure 45. Total groundwater withdrawals from the Edwards Group in the plateau area, the Upper Trinity aquifer, and the Middle Trinity aquifer in the study area. Values for 1975, 1996, and 1997 area based on TWDB water-use survey information and values for 2000, 2010, 2020, 2030, 2040, and 2050 are based on predicted dry demands estimated by the Regional Water Planning Groups in the area.

There are larger withdrawals in counties closer to major metropolitan areas such as Austin and San Antonio (fig. 46, table 4). Over time, the distribution of pumping has changed from isolated areas in 1975 (fig. 47) to areas near the Austin-San Antonio growth corridor (fig. 48). We anticipate that groundwater demands will increase in these areas (fig. 49). Tables 5, 6, 7, and 8 summarize groundwater withdrawals for the Edwards Group in the plateau area, the Upper Trinity aquifer, the Middle Trinity aquifer, and all three aquifers combined.

Conceptual Model of Groundwater Flow in the Aquifer

The conceptual model (fig. 50) is our best understanding of groundwater flow in the aquifer. When precipitation falls on the outcrop areas of the aquifers, much of the water either evapotranspirates or runs off into local streams and eventually discharges through major streams out of the study area. However, some of the precipitation, about four to six percent, infiltrates into and recharges the underlying aquifer. Losing streams also recharge the Edwards Group of the Edwards-Trinity (Plateau) aquifer because the Edwards Group in the plateau area has high permeability and mostly contains stream headwaters. Most of the recharge in the Edwards Group in the plateau area discharges along the edge of the plateau through springs, seeps, lower reaches of streams, and evapotranspiration. A small amount of the flow from the Edwards Group in the plateau area moves downward into the Upper and Middle Trinity aquifer.

Most of the precipitation that recharges the Upper and Middle Trinity aquifer discharges to local and major streams contributing baseflow to these surface-water features. An exception is Cibolo Creek, where karstification of the Lower Member of the Glen Rose Limestone changes the creek from a gaining to a losing stream between Boerne and Bulverde. Most of the remaining recharge in the aquifer discharges either through production from the aquifer or moves laterally into the Edwards (BFZ) aquifer to the south. Groundwater can perch on low permeability interbeds in the Upper Trinity aquifer and flow laterally out of springs. However, some water percolates through the Upper Trinity aquifer into the Middle Trinity

Table 4: Rate of groundwater withdrawal (acre-feet per year) from the Edwards Group and the Upper and Middle Trinity aquifers for county areas within the study area.

	1975	1996	1997	2000	2010	2020	2030	2040	2050
Bandera	482	1,887	2,169	3,095	4,703	4,598	5,019	5,519	6,070
Bexar	1,711	8,257	7,836	7,464	7,534	9,815	12,530	14,665	11,437
Blanco	202	499	507	549	616	687	752	780	771
Comal	510	4,347	4,545	5,246	6,250	7,837	10,229	12,828	15,655
Gillespie	1,151	3,264	2,718	2,011	2,023	2,052	2,076	2,179	2,239
Hays	703	4,495	4,608	4,661	6,486	7,569	9,029	10,727	11,680
Kendall	1,795	4,227	4,410	4,358	5,582	6,864	8,832	10,980	13,157
Kerr	915	4,310	4,545	5,247	5,671	5,995	6,443	6,957	7,623
Medina	269	290	282	270	279	284	299	308	325
Travis	1,855	4,794	4,399	3,274	3,386	3,688	3,997	4,161	4,392
Uvalde	91	74	60	61	58	56	55	54	52
Total	**9,683**	**36,446**	**36,079**	**36,236**	**42,587**	**49,447**	**59,260**	**69,158**	**73,402**

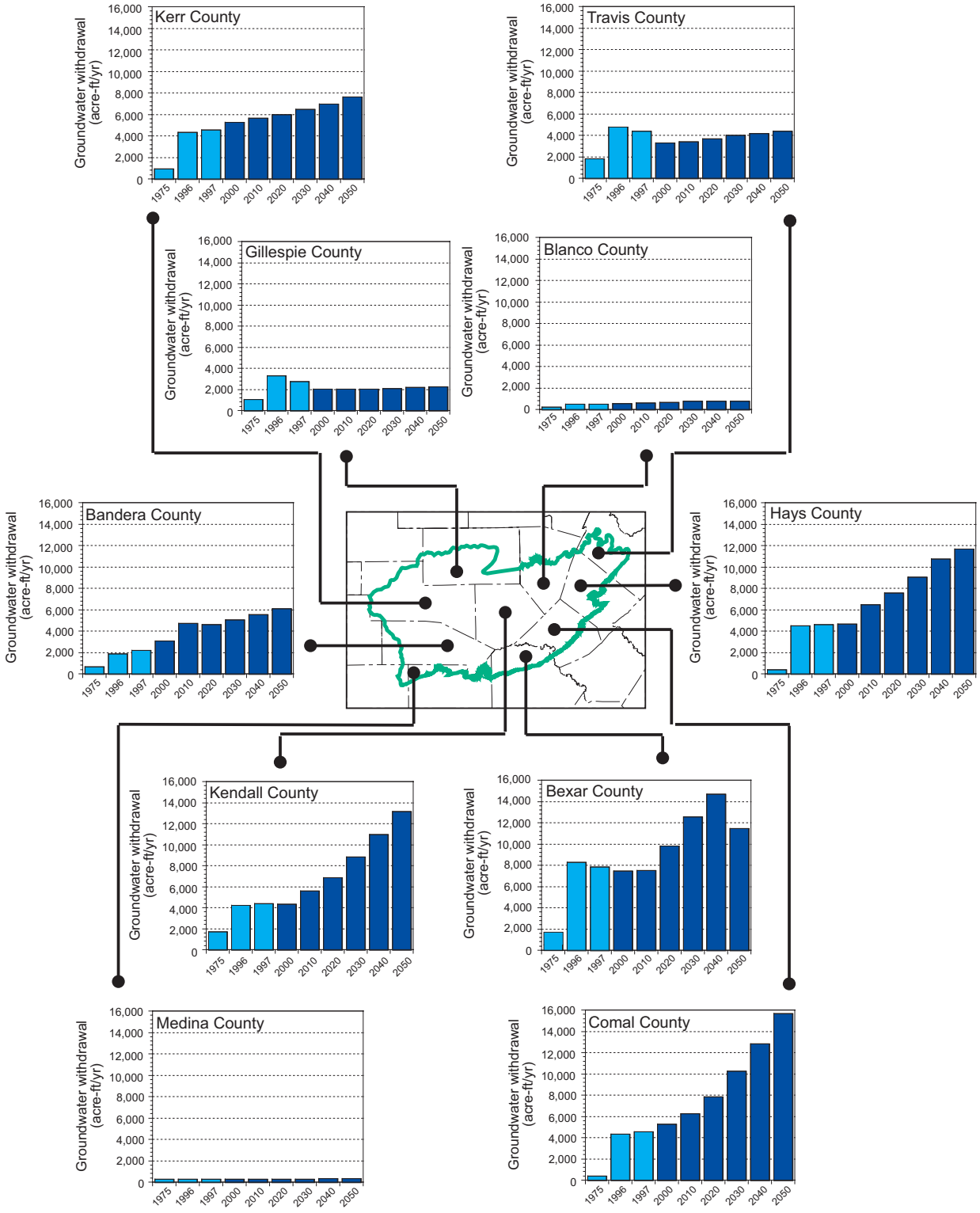

Figure 46. Total groundwater withdrawals from the Edwards Group in the plateau area, the Upper Trinity aquifer, and the Middle Trinity aquifer for parts of each of the counties within the study area. Values for 1975, 1996, and 1997 area based on TWDB water use survey information and values for 2000, 2010, 2020, 2030, 2040, and 2050 are based on predicted dry demands estimated by the Regional Water Planning Groups in the area.

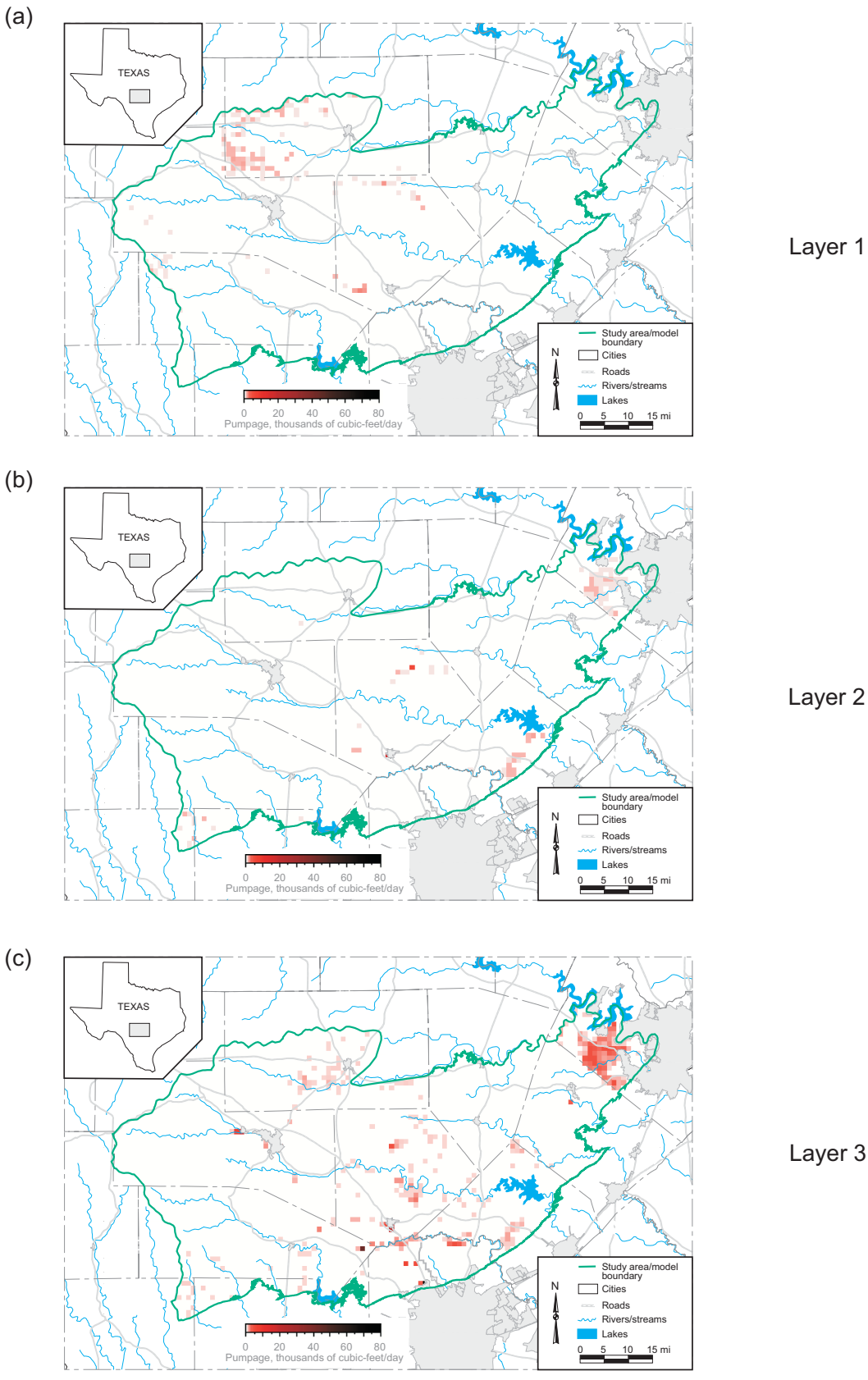

Figure 47. Spatial distribution of pumping in the (a) Edwards Group in the plateau area, (b) the Upper Trinity aquifer, and (c) the Middle Trinity aquifer for 1975.

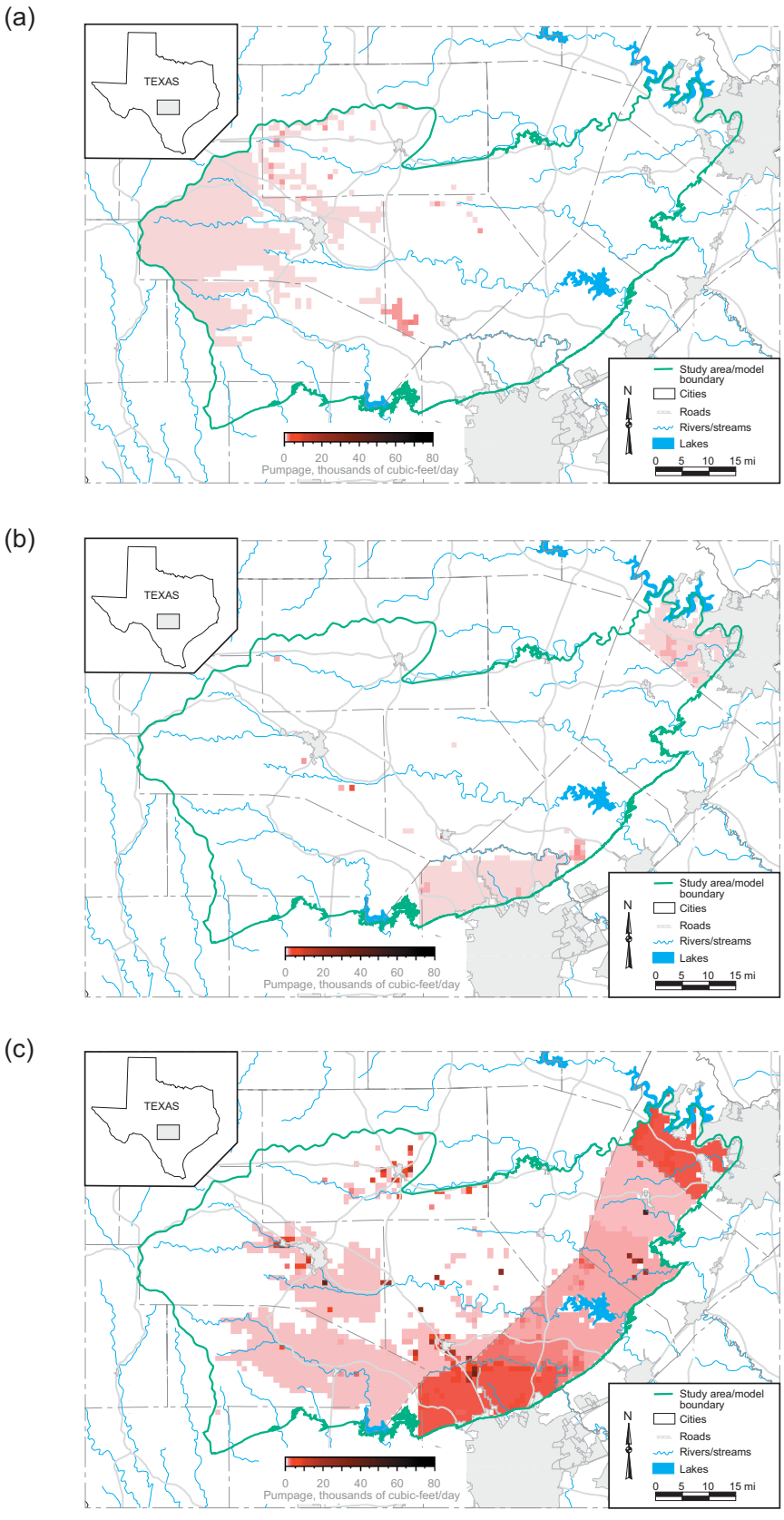

Figure 48. Spatial distribution of pumping in the (a) Edwards Group in the plateau area, (b) the Upper Trinity aquifer, and (c) the Middle Trinity aquifer for 1997.

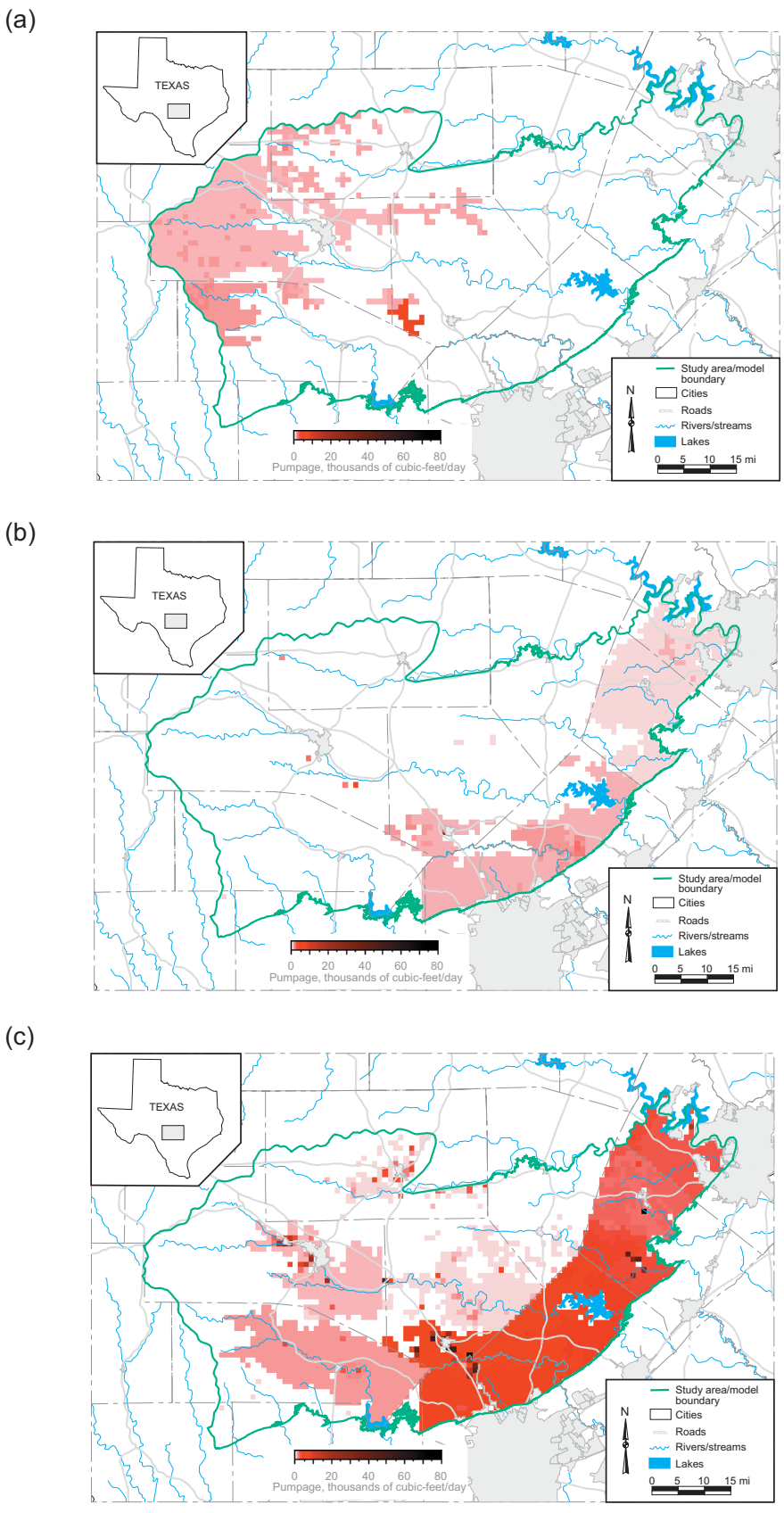

Figure 49. Spatial distribution of pumping in the (a) Edwards Group in the plateau area, (b) the Upper Trinity aquifer, and (c) the Middle Trinity aquifer for 2050.

Table 5: Rate of groundwater withdrawal (acre-feet per year) from the Edwards Group in the Plateau area for county areas within the study area.

	1975	1996	1997	2000	2010	2020	2030	2040	2050
Municipal and Industrial									
Bandera	0	0	0	0	0	0	0	0	0
Bexar	0	0	0	0	0	0	0	0	0
Blanco	0	0	0	0	0	0	0	0	0
Comal	0	0	0	0	0	0	0	0	0
Gillespie	2	10	11	13	14	14	15	17	19
Hays	0	0	0	0	0	0	0	0	0
Kendall	0	0	0	0	0	0	0	0	0
Kerr	0	0	0	0	0	0	0	0	0
Medina	0	0	0	0	0	0	0	0	0
Travis	0	0	0	0	0	0	0	0	0
Uvalde	0	0	0	0	0	0	0	0	0
Domestic									
Bandera	72	394	468	690	1084	1058	1161	1283	1417
Bexar	0	0	0	0	0	0	0	0	0
Blanco	0	0	0	0	0	0	0	0	0
Comal	0	0	0	0	0	0	0	0	0
Gillespie	56	343	356	405	414	432	445	495	525
Hays	0	0	0	0	0	0	0	0	0
Kendall	39	239	240	241	326	533	750	981	1,183
Kerr	165	1,848	2,027	2,564	2,798	2,942	3,151	3,421	3,782
Medina	0	0	0	0	0	0	0	0	0
Travis	0	0	0	0	0	0	0	0	0
Uvalde	0	0	0	0	0	0	0	0	0
Stock									
Bandera	90	56	52	63	63	63	63	63	63
Bexar	0	0	0	0	0	0	0	0	0
Blanco	0	0	0	0	0	0	0	0	0
Comal	0	0	0	0	0	0	0	0	0
Gillespie	661	461	300	327	327	327	327	327	327
Hays	0	0	0	0	0	0	0	0	0
Kendall	150	70	69	95	95	95	95	95	95
Kerr	300	239	244	287	287	287	287	287	287
Medina	0	0	0	0	0	0	0	0	0
Travis	0	0	0	0	0	0	0	0	0
Uvalde	0	0	0	0	0	0	0	0	0
Irrigation									
Bandera	0	0	0	0	0	0	0	0	0
Bexar	0	0	0	0	0	0	0	0	0
Blanco	0	0	0	0	0	0	0	0	0
Comal	0	0	0	0	0	0	0	0	0
Gillespie	0	0	0	0	0	0	0	0	0
Hays	0	0	0	0	0	0	0	0	0
Kendall	0	0	0	0	0	0	0	0	0
Kerr	0	0	0	0	0	0	0	0	0
Medina	0	0	0	0	0	0	0	0	0
Travis	0	0	0	0	0	0	0	0	0
Uvalde	0	0	0	0	0	0	0	0	0

Table 6: Rate of groundwater withdrawal (acre-feet per year) from the Upper Trinity aquifer for county areas within the study area.

	1975	1996	1997	2000	2010	2020	2030	2040	2050
Municipal and Industrial									
Bandera	0	0	0	0	0	0	0	0	0
Bexar	0	0	0	0	0	0	0	0	0
Blanco	0	0	0	0	0	0	0	0	0
Comal	3	0	3	3	3	3	3	3	3
Gillespie	0	7	8	9	10	11	11	13	14
Hays	0	0	0	0	0	0	0	0	0
Kendall	40	50	73	92	120	118	143	174	215
Kerr	0	45	49	52	56	63	70	77	85
Medina	0	0	0	0	0	0	0	0	0
Travis	0	0	0	0	0	0	0	0	0
Uvalde	0	0	0	0	0	0	0	0	0
Domestic									
Bandera	30	154	183	270	425	415	455	503	555
Bexar	53	1,002	978	908	915	1,257	1,641	1,944	1,475
Blanco	7	42	43	44	51	59	66	69	68
Comal	16	346	361	415	498	628	828	1,046	1,283
Gillespie	5	24	26	29	30	31	32	36	38
Hays	58	389	401	440	574	704	868	1,059	1,155
Kendall	126	156	157	161	223	368	520	680	820
Kerr	9	123	133	169	184	194	207	225	249
Medina	1	39	38	36	37	38	40	42	44
Travis	246	571	523	377	389	425	461	479	506
Uvalde	0	4	4	3	3	3	3	2	2
Stock									
Bandera	86	53	50	60	60	60	60	60	60
Bexar	14	30	29	24	24	24	24	24	24
Blanco	47	28	29	39	39	39	39	39	39
Comal	104	71	71	83	83	83	83	83	83
Gillespie	66	46	30	33	33	33	33	33	33
Hays	23	15	13	14	14	14	14	14	14
Kendall	133	62	61	84	84	84	84	84	84
Kerr	19	15	15	18	18	18	18	18	18
Medina	123	14	13	15	15	15	15	15	15
Travis	20	75	75	81	81	81	81	81	81
Uvalde	42	22	16	18	18	18	18	18	18
Irrigation									
Bandera	0	0	0	0	0	0	0	0	0
Bexar	0	0	0	0	0	0	0	0	0
Blanco	0	0	0	0	0	0	0	0	0
Comal	0	0	0	0	0	0	0	0	0
Gillespie	0	0	0	0	0	0	0	0	0
Hays	0	0	0	0	0	0	0	0	0
Kendall	0	0	0	0	0	0	0	0	0
Kerr	0	0	0	0	0	0	0	0	0
Medina	0	0	0	0	0	0	0	0	0
Travis	0	0	0	0	0	0	0	0	0
Uvalde	0	0	0	0	0	0	0	0	0

Table 7: Rate of groundwater withdrawal (acre-feet per year) from the Middle Trinity for county areas within the study area.

	1975	1996	1997	2000	2010	2020	2030	2040	2050
Municipal and Industrial									
Bandera	20	43	44	51	61	63	68	75	83
Bexar	400	978	988	1,113	1,134	1,047	1,098	1,127	1,154
Blanco	0	0	0	0	0	0	0	0	0
Comal	0	0	0	0	0	0	0	0	0
Gillespie	0	0	0	0	0	0	0	0	0
Hays	243	1,247	1,320	1,036	1,766	1,786	1,900	2,037	2,211
Kendall	635	1,298	1,565	1,978	2,584	2,541	3,073	3,760	4,636
Kerr	353	941	943	982	1,075	1,195	1,344	1,474	1,623
Medina	0	0	0	0	0	0	0	0	0
Travis	67	59	52	75	91	110	133	146	163
Uvalde	0	0	0	0	0	0	0	0	0
Domestic									
Bandera	65	1,060	1,249	1,840	2,891	2,822	3,096	3,421	3,779
Bexar	1,228	6,214	5,808	5,391	5,433	7,461	9,740	11,543	8,757
Blanco	58	363	368	380	441	505	563	589	582
Comal	191	3,761	3,941	4,536	5,458	6,915	9,107	11,489	14,080
Gillespie	99	377	395	451	461	479	495	550	584
Hays	349	2,824	2,856	3,151	4,112	5,045	6,226	7,596	8,279
Kendall	308	1,371	1,267	1,244	1,695	2,680	3,731	4,780	5,706
Kerr	50	697	729	923	1,007	1,059	1,134	1,232	1,362
Medina	7	221	217	203	211	215	228	235	250
Travis	1,496	3,998	3,659	2,642	2,726	2,974	3,224	3,356	3,543
Uvalde	2	24	23	20	17	16	15	14	13
Stock									
Bandera	119	74	69	84	84	84	84	84	84
Bexar	16	33	33	27	27	27	27	27	27
Blanco	89	53	54	74	74	74	74	74	74
Comal	196	168	168	196	196	196	196	196	196
Gillespie	318	225	144	157	157	157	157	157	157
Hays	30	21	18	21	21	21	21	21	21
Kendall	364	167	164	226	226	226	226	226	226
Kerr	20	16	16	19	19	19	19	19	19
Medina	137	16	14	16	16	16	16	16	16
Travis	25	91	91	99	99	99	99	99	99
Uvalde	47	24	17	20	20	20	20	20	20
Irrigation									
Bandera	0	53	53	36	35	33	32	30	29
Bexar	0	0	0	0	0	0	0	0	0
Blanco	0	13	13	12	11	11	10	9	9
Comal	0	1	1	13	12	12	11	11	10
Gillespie	0	1,770	1,447	587	578	569	560	551	543
Hays	0	0	0	0	0	0	0	0	0
Kendall	0	813	813	238	228	218	209	200	192
Kerr	0	386	386	233	225	218	211	204	198
Medina	0	0	0	0	0	0	0	0	0
Travis	0	0	0	0	0	0	0	0	0
Uvalde	0	0	0	0	0	0	0	0	0

Table 8: Rate of groundwater withdrawal (acre-feet per year) from the Edwards Group and the Upper and Middle Trinity aquifers for county areas within the study area.

	1975	1996	1997	2000	2010	2020	2030	2040	2050
Municipal and Industrial									
Bandera	20	43	44	51	61	63	68	75	83
Bexar	400	978	988	1,113	1,134	1,047	1,098	1,127	1,154
Blanco	0	0	0	0	0	0	0	0	0
Comal	3	0	3	3	3	3	3	3	3
Gillespie	2	17	19	22	23	25	26	30	33
Hays	243	1,247	1,320	1,036	1,766	1,786	1,900	2,037	2,211
Kendall	675	1,348	1,638	2,070	2,704	2,659	3,216	3,934	4,850
Kerr	353	986	993	1,034	1,132	1,257	1,414	1,551	1,708
Medina	0	0	0	0	0	0	0	0	0
Travis	67	59	52	75	91	110	133	146	163
Uvalde	0	0	0	0	0	0	0	0	0
Domestic									
Bandera	167	1,608	1,900	2,800	4,399	4,295	4,711	5,206	5,751
Bexar	1,281	7,216	6,786	6,300	6,349	8,717	11,381	13,487	10,231
Blanco	65	406	410	425	492	564	629	657	649
Comal	207	4,107	4,302	4,951	5,955	7,543	9,936	12,535	15,362
Gillespie	104	744	777	885	905	942	973	1,081	1,146
Hays	407	3,212	3,257	3,590	4,686	5,749	7,095	8,655	9,434
Kendall	473	1,767	1,664	1,645	2,244	3,581	5,002	6,441	7,709
Kerr	223	2,668	2,890	3,656	3,990	4,195	4,493	4,878	5,393
Medina	9	259	255	239	249	253	268	277	294
Travis	1,742	4,569	4,182	3,019	3,116	3,399	3,685	3,835	4,050
Uvalde	2	28	27	23	20	19	18	17	15
Stock									
Bandera	295	183	171	207	207	207	207	207	207
Bexar	30	63	62	51	51	51	51	51	51
Blanco	137	81	83	113	113	113	113	113	113
Comal	300	239	239	279	279	279	279	279	279
Gillespie	1,045	733	474	517	517	517	517	517	517
Hays	53	36	31	35	35	35	35	35	35
Kendall	647	300	295	405	405	405	405	405	405
Kerr	339	269	276	324	324	324	324	324	324
Medina	260	30	27	31	31	31	31	31	31
Travis	46	166	165	180	180	180	180	180	180
Uvalde	90	46	33	38	38	38	38	38	38
Irrigation									
Bandera	0	53	53	36	35	33	32	30	29
Bexar	0	0	0	0	0	0	0	0	0
Blanco	0	13	13	12	11	11	10	9	9
Comal	0	1	1	13	12	12	11	11	10
Gillespie	0	1,770	1,447	587	578	569	560	551	543
Hays	0	0	0	0	0	0	0	0	0
Kendall	0	813	813	238	228	218	209	200	192
Kerr	0	386	386	233	225	218	211	204	198
Medina	0	0	0	0	0	0	0	0	0
Travis	0	0	0	0	0	0	0	0	0
Uvalde	0	0	0	0	0	0	0	0	0

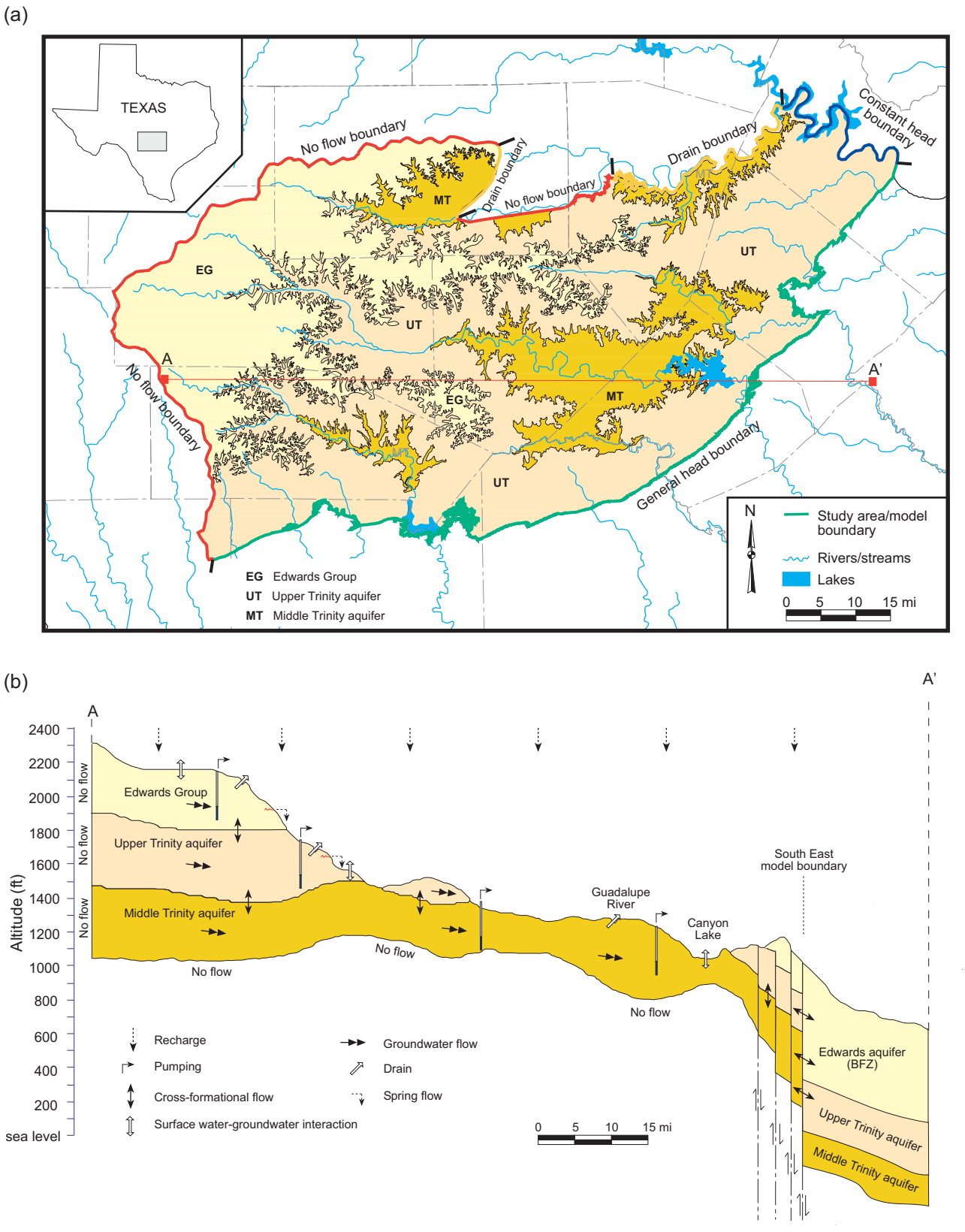

Figure 50. Conceptual model of the aquifer showing (a) the boundary conditions at the outer edge of the model, (b) flows between the layers, and (c) how the conceptual model translates into the numerical model.

(c)

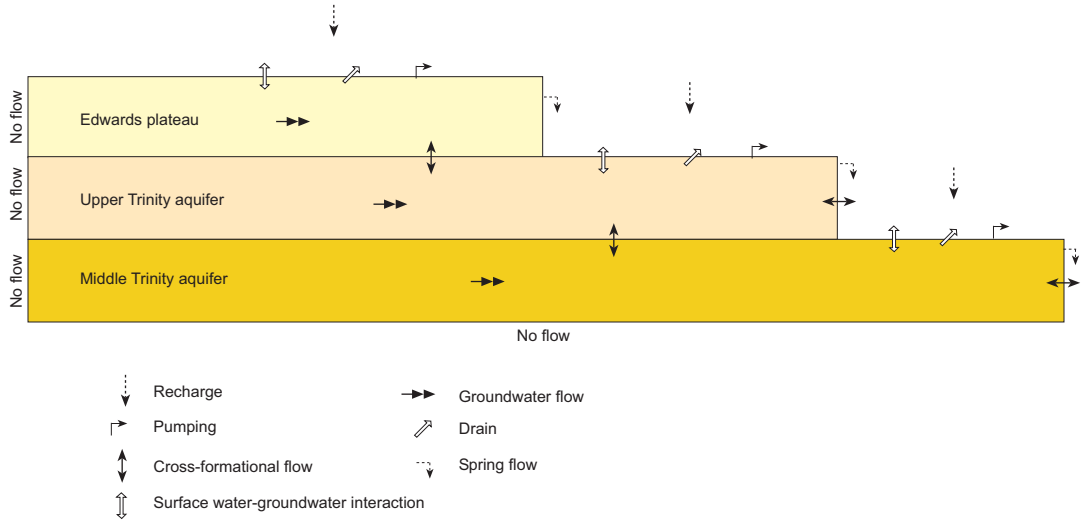

Figure 50. Conceptual model of the aquifer showing (a) the boundary conditions at the outer edge of the model, (b) flows between the layers, and (c) how the conceptual model translates into the numerical model. *(Continued)*

aquifer. In general, groundwater flows from areas of higher topography to areas of lower topography from the west to the east.

In general, the lithology and local fracturing control the permeability of the formations. The Edwards Group in the Plateau area has high vertical and horizontal permeability owing to karstification. The Upper Trinity aquifer generally has lower permeabilities (but can be locally very permeable, especially in outcrop) and, because of shaley interbeds, has a much lower vertical than horizontal permeability. The Middle Trinity aquifer has moderate permeabilities and greater ability to transmit water vertically than the Upper Trinity aquifer. The Middle Trinity aquifer is most permeable in the sandy outcrop area of Gillespie County. Specific yield in the limestones is primarily controlled by fracturing.

Pumping was not very large in 1975 and was dispersed. By 1997, pumping had quadrupled and was more focused along the Austin-San Antonio growth corridor on the eastern and southern sides of the study area. Much of the future increases in pumping will probably occur in this area as Austin, San Antonio, San Marcos, and New Braunfels continue to grow.

Model Design

The design of the model includes the choice of code and processor, the discretization of the aquifer into layers and cells, and the assignment of model parameters. We designed the model to agree as much as possible with our conceptual model of groundwater flow in the aquifer.

Code and Processor

We used MODFLOW-96 (Harbaugh and McDonald, 1996), a widely-used modular finite-difference groundwater flow code written by the USGS, to model groundwater flow in the Trinity aquifer. We chose MODFLOW-96 because it (1) simulates the hydrogeologic processes necessary to model the Trinity aquifer, (2) is well documented (McDonald and Harbaugh, 1988) and widely used (Anderson and Woessner, 1992, p. xvi), (3) has a number of third-party pre- and post-processors available to make the model easy to use, and (4) is available through the public domain. To help us with loading information into the model and observing model results, we used Processing MODFLOW for Windows

(PMWIN) version 5.0.54 (Chiang and Kinzelbach, 1998). Other pre- and post-processors should be able to read the source files for MODFLOW-96. We developed and ran the model on a Dell OptiPlex GX1p with a 450 MHz Pentium II Processor and 128 MB RAM running Windows 98 (4.10.98).

Layers and Grid

The lateral extent of the model corresponds to natural hydrologic boundaries, such as erosional limits, rivers, and the structural boundary with the Edwards (BFZ) aquifer, and hydraulic boundaries to the west that coincide with groundwater divides. According to the hydrostratigraphy and conceptual model, we designed the model to have three layers. Layer 1 consists of the Edwards Group of the Edwards-Trinity Plateau aquifer, Layer 2 consists of the Upper Trinity aquifer, and Layer 3 consists of the Middle Trinity aquifer. We did not include the Lower Trinity aquifer in the model because (1) the Middle and Lower Trinity aquifers are separated by a confining unit (the Hammett Shale) in most of the study area (Ashworth, 1983, p. 27), (2) the Lower Trinity aquifer is not extensively used in most of our study area, and (3) there is not much information on the Lower Trinity aquifer.

We defined the IBOUND by first establishing the lateral extent of the formations in each layer using the geologic map (fig. 8). We assigned a cell as active if the formation covered more than 50 percent of the cell area. We did not include the thin sliver of the Edwards Group in the eastern part of the study area because (1) our structure maps do not accurately represent the complexity of faulting in the area, (2) flow in these rocks is associated with the Edwards (BFZ) aquifer, and (3) the focus of the model is the Middle Trinity aquifer.

Each layer has 69 rows and 115 columns for a total of 23,805 cells in the model. All the cells have uniform lateral dimensions of 1 mile by 1 mile. We chose this cell size to be small enough to reflect the density of input data and the desired output detail and large enough for the model to be manageable. The uniform cell size allowed us to use spreadsheets and grid-based contouring programs to easily manipulate input data. Cell thickness depended on the elevation of the contact between the different layers. After we made cells outside of the model area and outside the lateral extent of each layer inactive, the model had a total of 9,262 active cells: 1,112 active cells in layer 1, 3,625 active cells in layer 2, and 4,525 active cells in layer 3 (fig. 51, 52, 53, respectively).

Model Parameters

We distributed model parameters, including (1) elevations of the top and bottom of each layer, (2) horizontal and vertical hydraulic conductivity, (3) specific storage, and (4) specific yield using both Surfer® and ArcInfo®.

We defined top and bottom elevations for each layer from the structure maps and land-surface elevations from digital elevation models downloaded from the USGS. We used ArcInfo® to assign top and bottom elevations. For layer 1 (the Edwards Group in the plateau area), we assigned the top as the land-surface elevation and the bottom according to the structure map of the bottom of the Edwards Group (fig. 11). The top of layer 2 (Upper Trinity aquifer) was assigned according to the structure map (fig. 11) where covered by Layer 1 and the land-surface elevation where exposed. The bottom was defined by the bottom of the Upper Trinity aquifer (fig. 12). The top of layer 3 (Middle Trinity aquifer) was assigned according to the structure map (fig. 12) where covered by Layer 2 and the land-surface elevation where exposed. The bottom of layer 3 was assigned using the elevation of the bottom of the Middle Trinity (fig. 13).

We assigned initial values of hydraulic conductivity in layer 3 using Surfer® according to our geostatistical interpretation (fig. 43). We assigned uniform values of hydraulic conductivity in layers 1 and 2 because of too few data points. We initially assigned vertical hydraulic

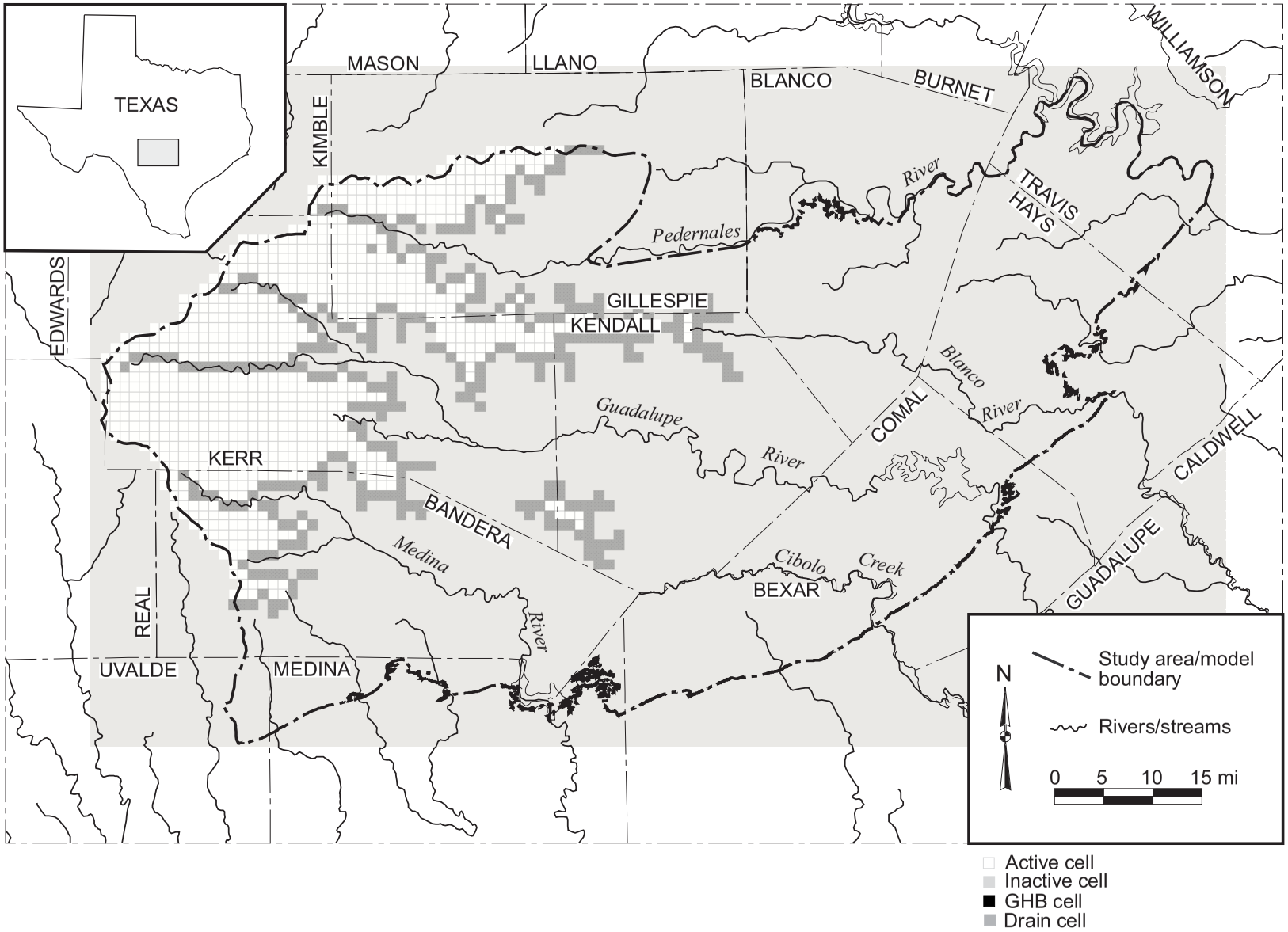

Figure 51. Active cells and boundary assignments in Layer 1 of the model (Edwards Group in the plateau area).

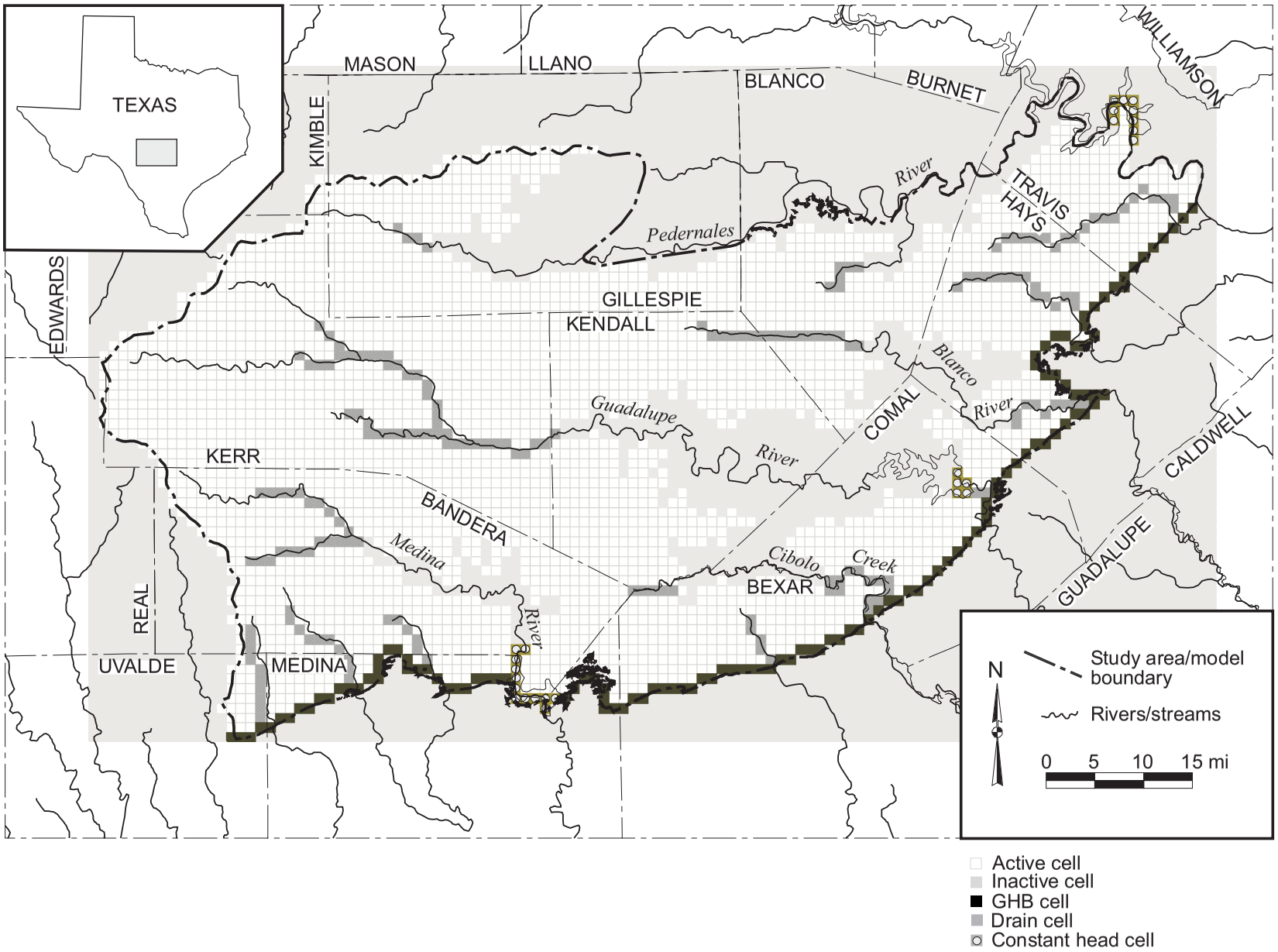

Figure 52. Active cells and boundary assignments in Layer 2 of the model (Upper Trinity aquifer).

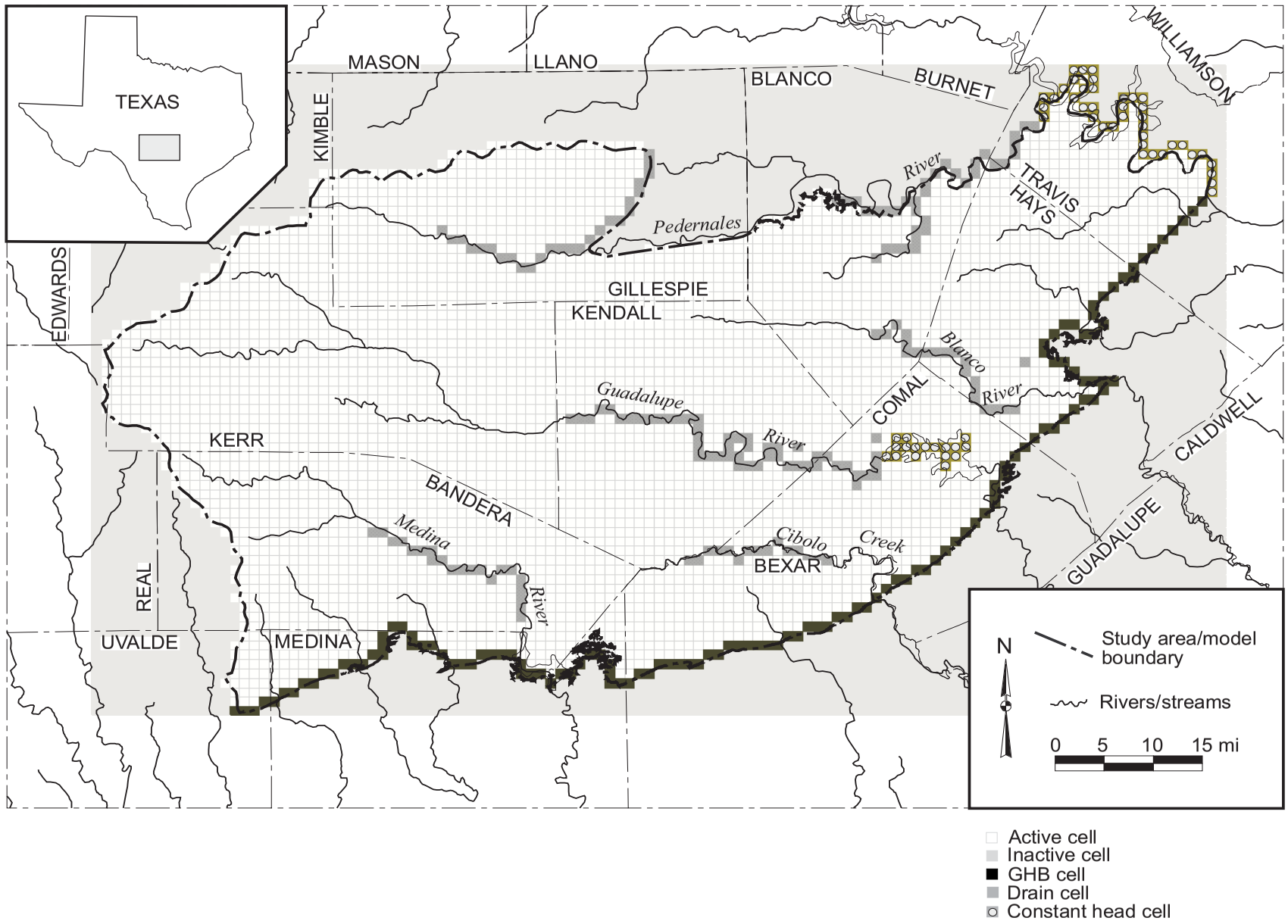

Figure 53. Active cells and boundary assignments in Layer 3 of the model (Middle Trinity aquifer).

conductivity to be 10 times less than the horizontal hydraulic conductivity. Lateral isotropy was assumed in each layer. We assigned uniform values of specific storage and specific yield.

We assigned Layer 1 as unconfined and Layers 2 and 3 as confined/unconfined. We allowed the model to calculate transmissivity and storativity according to saturated thickness. We used units of feet for length and days for time for all input data to the model. To solve the groundwater flow equation, we used the slice successive overrelaxation (SSOR) solver with a convergence criterion of 0.01 ft.

Model Boundaries

We assigned model boundaries for the (1) recharge, (2) pumping, (3) rivers and streams, (4) springs, (5) lakes, (6) outer boundaries, and (7) initial conditions. We assigned initial values of recharge according to our ArcInfo® analysis described in the recharge section of this report (fig. 28 applied to precipitation). We used our interpretation of water levels at the beginning of 1975 (figs. 18, 19, and 20) as initial heads for the steady-state model. We assigned pumping according to our analysis of pumping as discussed in the 'Discharge' section of this report.

We used the Drain Package of MODFLOW to represent rivers and streams in the model (figs. 51, 52 and 53). We used this package to only allow the streams to gain water from the aquifer. The River Package, which is another possible approach for simulating rivers and streams, allows streams to gain and lose water. Sensitivity analysis during initial construction of the model showed that the River Package could allow an unrealistic amount of water to move from the rivers and streams into the aquifer and thus underestimate potential water-level declines due to pumping or drought. The Drain Package requires a drain elevation (the elevation upon which water can flow out of the drain) and a drain conductance (a resistance to flow out of the drain). We defined the drain elevation by intersecting stream-bed location with the digital elevation model in ArcInfo®. We assigned the drain conductance according to the estimated width of the stream, a stream length of 1-mi, an assumed riverbed thickness of 1-ft, and an assumed vertical hydraulic conductivity of 0.1 ft/day. After we calibrated the model, we investigated the sensitivity of simulated water levels to different values of drain conductance. Except for very low values, the conductance term for rivers generally has little effect on water-levels in the model.

We also used drains to represent springflow, seepage from the erosional edge of the Edwards Group in the plateau area, and flow out of the Middle Trinity aquifer in Gillespie County (figs. 51, 52, and 53). For the springs, we assigned the drain elevation as the land-surface elevation at the spring location and an initial conductance based on an assumed one-foot thickness and the geometric mean hydraulic conductivity of the layer. For the erosional edge of the Edwards Group and flow out of the Middle Trinity aquifer in Gillespie County, we assigned a drain elevation 10-ft above the base of Layer 1 and a drain conductance based on a one foot thickness and the geometric mean hydraulic conductivity of the layer. We simulated the influence of Medina, Canyon, Travis, and Austin Lakes using constant-head cells and average lake-level elevations.

To model the movement of water out of the model and through the Balcones Fault Zone, we used the General Head Boundary (GHB) Package of MODFLOW. We placed GHB cells all along the contact with the Edwards (BFZ) aquifer in layers 2 and 3 unless there was a constant-head cell for a lake (figs. 52 and 53). The GHB Package requires values for hydraulic-head and conductance. We assigned the hydraulic head according to the interpreted water-level map (fig. 13 for Layer 3) in the area of the GHB cells. We assigned the GHB conductance according to the hydraulic conductivity and geometry of the cell and an assumed one-foot thickness. Conceptually, the GHB conductance represents the resistance to flow

between a cell in the model and a constant-head source or sink. In this case, we have used the GHB to represent flow out of the study area either into the Edwards (BFZ) aquifer across faults or continuing into the down-dip parts of the Trinity aquifer. For simplicity, we used an arbitrary thickness of unity (1-ft) to define conductance.

We used interpreted water-level maps (fig. 13 for Layer 3) as initial heads for the steady-state model.

Modeling Approach

Our approach for modeling the aquifer included three major steps: (1) calibrating a steady-state model, (2) calibrating a transient model, and (3) using the transient model to make predictions of possible water-level declines over the 50-year planning period. We first developed a steady-state model because steady-state models are often much easier to calibrate than transient models and because results of the steady-state model can easily be used as a starting point in the transient model. We calibrated the steady-state model to reproduce water levels for late 1975. This year was chosen because the aquifer had approximately the same water levels at the beginning and end of the year and pumping from the aquifer was relatively low (Kuniansky and Holligan, 1994). We used the steady-state model to investigate (1) recharge rates, (2) hydraulic properties, (3) boundary conditions, (4) discharge from the Trinity aquifer into the Edwards (BFZ) aquifer, (5) flow budget, and (6) sensitivity of the different model parameters on model results.

Our approach for calibrating the model was to match water levels (for steady-state conditions) and water-level fluctuations (for transient conditions) using the simplest possible conceptual model. The calibration of the model focused on the Middle Trinity aquifer because it had the most water levels to calibrate to and because it is the main water-producing horizon of the modeled intervals. However, we also checked that water levels in Layers 1 and 2 were hydrologically reasonable. We quantified the calibration, or goodness of fit between the

$$RMS = \left[\frac{1}{n} \sum_{i=1}^{n} \left(h_m - h_s \right)_i^2 \right]^{0.5} \qquad (2)$$

simulated and measured water-level values, using the root mean square (RMS) error, where n is the number of calibration points, h_m is the measured hydraulic head at point i, and h_s is the simulated hydraulic head at point i.

Once we completed the steady-state model, we used the framework of the model to develop a transient model for the years 1996 and 1997 using monthly time steps. We chose 1996 and 1997 because they (1) represented the last two years of available water-use data available at the time (and therefore provide a good starting point for predictive simulations) and (2) transition from dry conditions in 1996 to wet conditions in 1997. This transition allowed us to test how well the model could reproduce water-level changes in the aquifer. We calibrated the transient model by adjusting storativity values to minimize the difference between simulated and measured water-level variations.

After the transient model was calibrated, we then used the model to predict how water levels might change over the next 50 years in response to increases in pumping and drought.

Steady-State Model

Once we assembled the input datasets and constructed the framework of the model, we calibrated the steady-state model and assessed the sensitivity of the model to different hydrologic parameters.

Calibration

We calibrated the model to measured water levels in the Middle Trinity aquifer for the winter of 1975-1976 when we expected pumping

to be lowest (fig. 54). These measured water levels are a subset of the measurements used to develop the more detailed water-level map developed for the conceptual model (fig. 20) and represent measurements closer to the winter of 1975-1976.

To calibrate the model, we first adjusted the different model parameters to determine which parameters had the most effect on simulated water levels. Through this initial sensitivity analysis, we determined that the water levels in the Middle Trinity aquifer were most sensitive to the recharge rate and the horizontal hydraulic conductivity of the Middle Trinity aquifer. We also found that the model calibration was not unique. We could calibrate the model as long as the ratio of the recharge rate (expressed as a percent of mean annual precipitation) to the mean hydraulic conductivity of the Middle Trinity aquifer was about 0.6.

If we honored the mean hydraulic conductivity of the Middle Trinity aquifer based on measured values (2.6 ft/day), we could calibrate the model with a recharge rate of about 1.5 percent of mean annual precipitation. If we honored the estimated recharge rate (6.6 percent of mean annual precipitation), we could calibrate the model with a mean hydraulic conductivity of about 13 ft/day for the Middle Trinity aquifer. For the final calibration, we selected a recharge rate of 4 percent of mean annual precipitation and a geometric mean hydraulic conductivity of 7.5 ft/day for the Middle Trinity aquifer (fig. 55). These final calibration values are approximately in the middle of the values discussed above.

The recharge rate in the final calibration is lower than the estimated recharge rate for the aquifer. Because of intracell flow (Anderson and Woessner, 1992, p. 153), recharge in a numerical model can be lower than the actual recharge. This is because some of the water that is recharged within a model cell may discharge locally within the same cell. Therefore, the net recharge within the model cell is lower than the actual recharge in the cell because the model does not consider the local component of recharge (for example, see Feinstein and Anderson, 1987; Stoertz and Bradbury, 1989).

The geometric mean hydraulic conductivity of the Middle Trinity aquifer used to calibrate the model is greater than the measured geometric mean. This may be appropriate because limestone aquifers often exhibit a permeability scale effect. A permeability scale effect is when the geometric mean of the permeability (in our case, hydraulic conductivity) increases with sampling scale (Teutsch and Sauter, 1991; Rovey, 1994; Huntoon, 1995; Halihan and others, 1999). Therefore, the geometric mean permeability of a model cell would be somewhat greater than the geometric mean of the aquifer tests characterizing the model cell. The scale effect is due to larger scales of measurement or sampling larger geologic features (such as fractures, karstification, and/or organized sand structures) that control the permeability of the aquifer. Although the calibrated horizontal hydraulic conductivity for the Middle Trinity aquifer is greater than geometric mean of the measured values, it is well within the statistical distribution of measured values (compare calibrated value to fig. 39).

After fitting the model as best as possible by adjusting mean recharge and geometric mean hydraulic conductivity in the Middle Trinity aquifer, we noticed that the model underestimated water levels in the westernmost part of the model in Bandera, Gillespie, and Kerr counties. We found that lowering the vertical hydraulic conductivity in the Upper Trinity aquifer to 0.00003 ft/day allowed the model to better fit the measured water levels in this area. Unfortunately, we were not able to find measurements of vertical hydraulic conductivity in the Upper Trinity aquifer, although we expect the vertical hydraulic conductivity to be low due to the presence of low-permeability interbeds in the Upper Member of the Glen Rose Limestone (see Ashworth, 1983; Barker and Ardis, 1996).

During calibration, we found that the stability of the model was very sensitive to the structure in Gillespie County where the Trinity

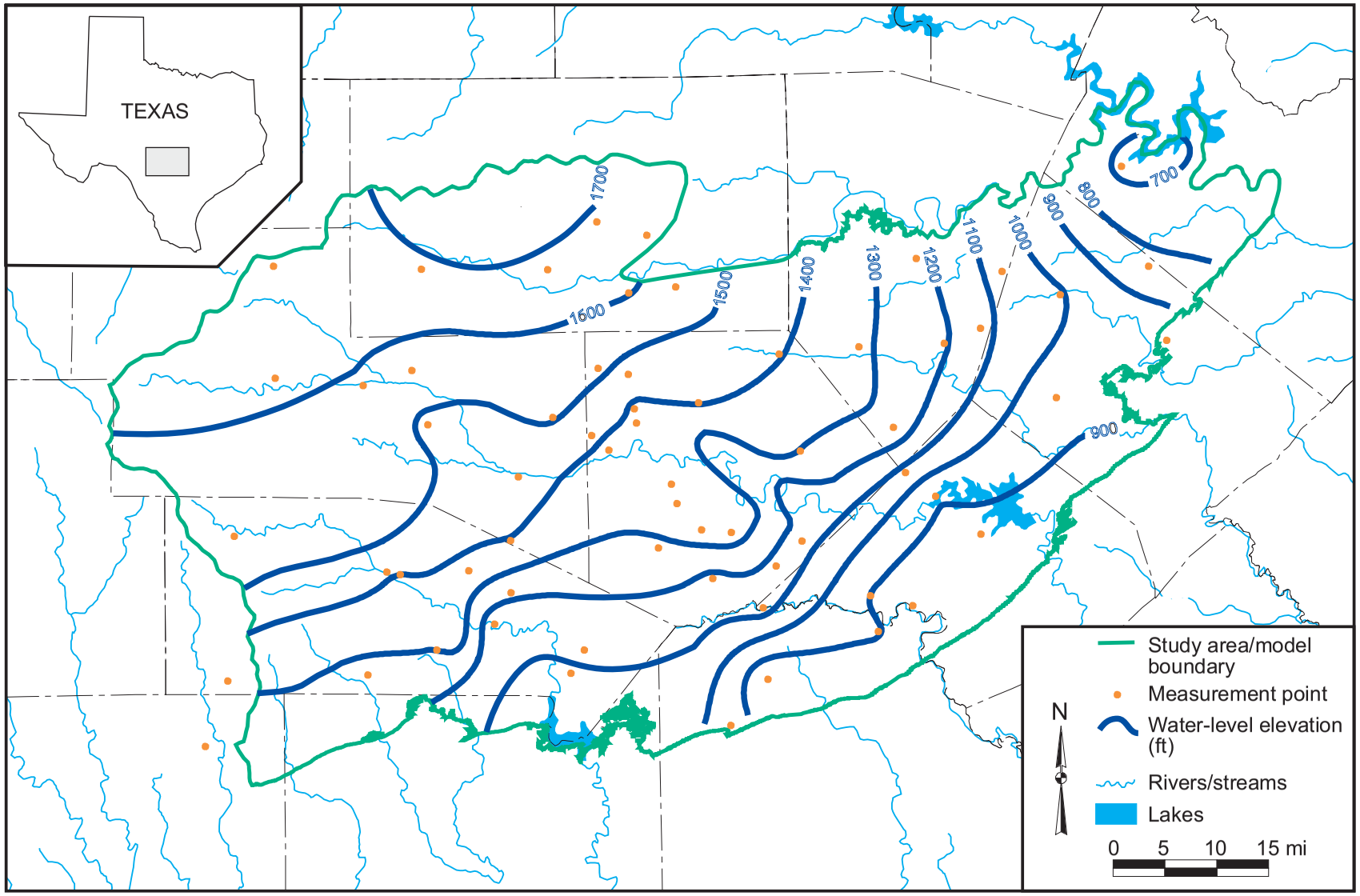

Figure 54. Water level elevations in the Middle Trinity aquifer for fall, 1975.

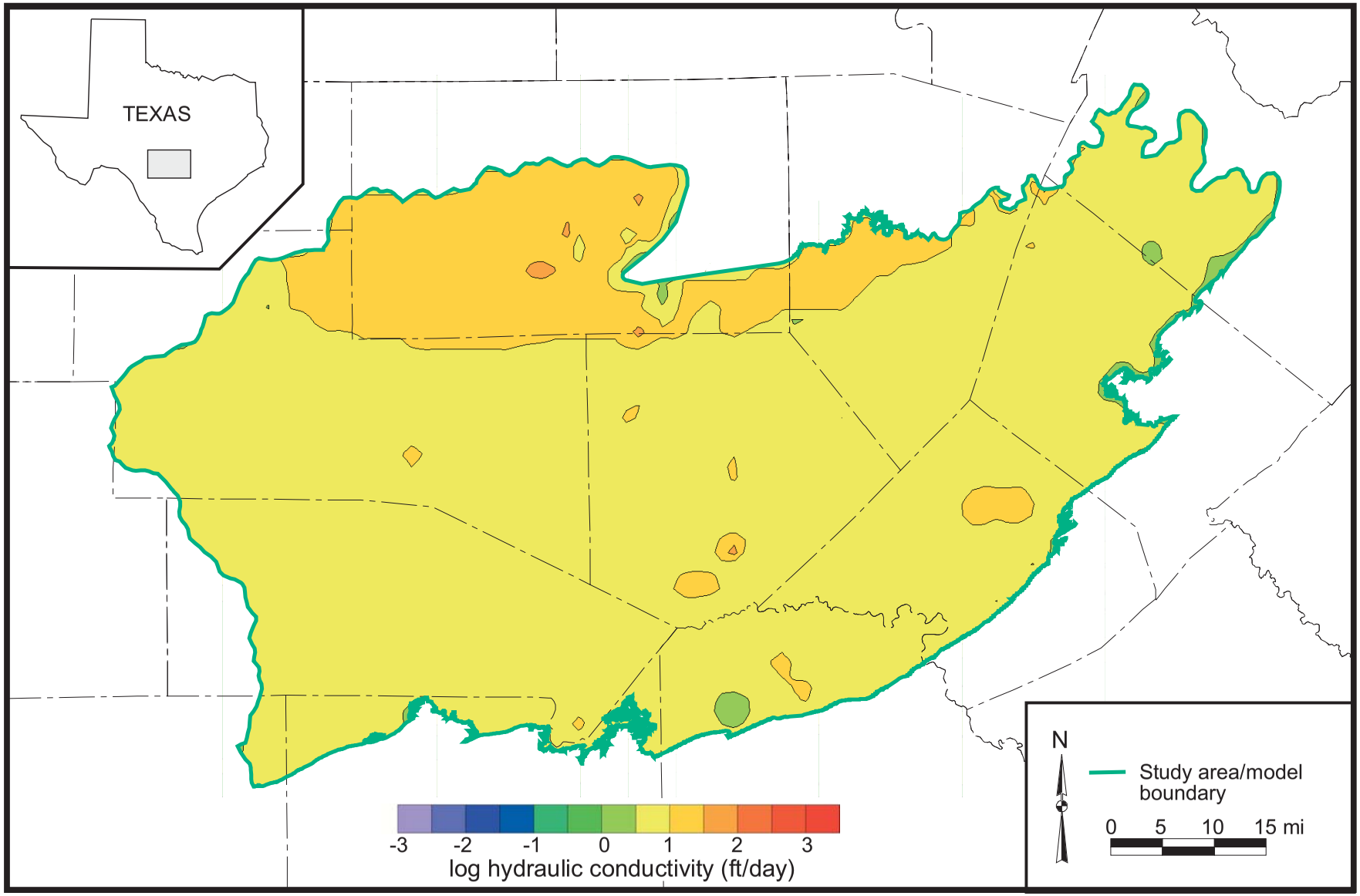

Figure 55. Calibrated distribution of hydraulic conductivity in the Middle Trinity aquifer.

aquifer pinches out against the Llano Uplift. This instability was probably due to the large size of the cells relative to the thickness of the layers and the uneven structural surface between Trinity and Pre-Cretaceous rocks. To increase the stability of the model, we smoothed the structure in this area.

The final, calibrated model does a good job of reproducing the spatial distribution of water levels in the Middle Trinity aquifer for the winter of 1975-1976 (fig. 56). The model reproduces the interpreted direction of groundwater flow and approximates water levels in most parts of the study area. The root-mean squared (RMS) error is 56-ft (fig. 57). The RMS error means that, on average, the simulated water level differs by about 56-ft. This RMS error is about 5 percent of the total hydraulic head drop across the modeled area, well within the 10 percent usually desired for model calibration. Errors are generally spread across the model area although there are some areas with consistently higher and some areas with consistently lower simulated water levels (fig. 58).

We included 19 springs in the model (table 2). We varied drain conductance values within reasonable bounds (50 to 100,000 ft2/day) to approximate measured springflow values (table 9). Higher conductance values (100,000 ft2/day) were needed to reproduce springflows in springs issuing from the Upper Member of the Glen Rose Limestone than in the Lower Member of the Glen Rose Limestone and the Edwards Group (200 to 10,000 ft^2/day). Higher conductance values in the Upper Member of the Glen Rose Limestone may be due to greater dissolution of limestone which locally developed highly conductive zones in an otherwise tight limestone unit.

We were not able to accurately simulate flow from three springs included in the model (springs 4, 18, and 19 in table 9 and fig. 37). Conductance values required to match springflow resulted in a water-balance error of -1.34 percent in the model. Water-balance error is defined as:

$$\frac{Q_{in} - Q_{out}}{(Q_{in} + Q_{out})/2} \qquad (3)$$

Table 9: Simulated and estimated flow for selected springs issuing from the Edwards and Trinity aquifers of the Hill Country included in the model.

Springs	Estimated flow (gpm)	Simulated flow (gpm)	Formation
1	150	146	EDRDA
2	100	128	EDRDA
3	100	110	EDRDA
4	2,500	612	EDRDA
5	310	356	EDRDA
6	480	447	EDRDA
7	100	24	EDRDA
8	20	23	GLRSU
9	75	107	GLRSL
10	50	108	GLRSL
11	150	171	GLRSL
12	300	318	GLRSL
13	300	280	CCRK
14	500	427	CCRK
15	25	20	GLRSL
16	50	54	GLSU
17	50	51	GLRSU
18	9,000	351	EDRDA
19	5,000	265	GLRSL

EDRDA = Edwards Group and associated limestone
GLRSL = Lower Member of the Glen Rose Limestone
GLRSU = Upper Member of the Glen Rose Limestone
CCRK = Cow Creek Limestone

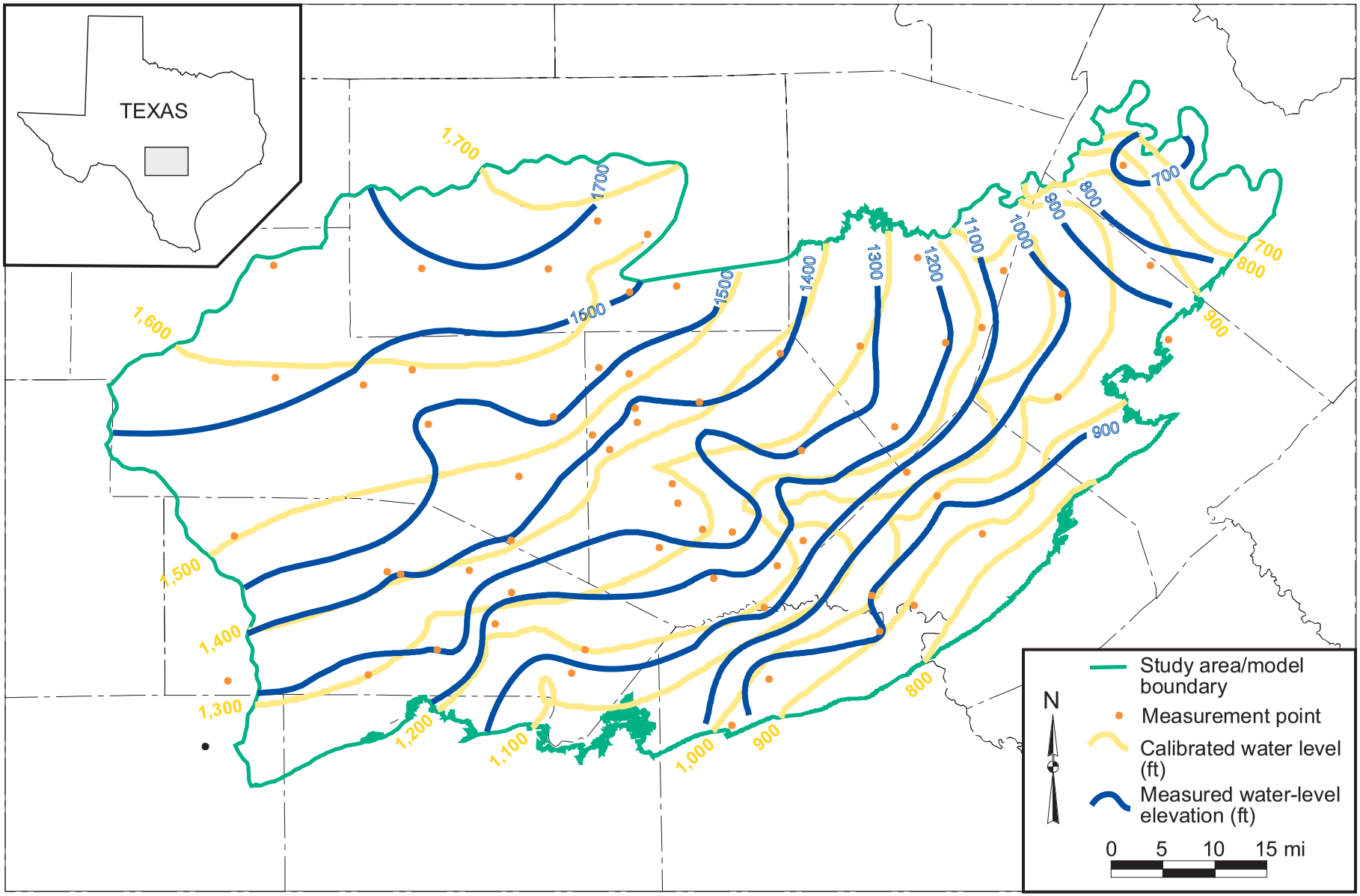

Figure 56. Comparison of simulated and measured water-level contours for the Middle Trinity aquifer for the 1975 steady-state model.

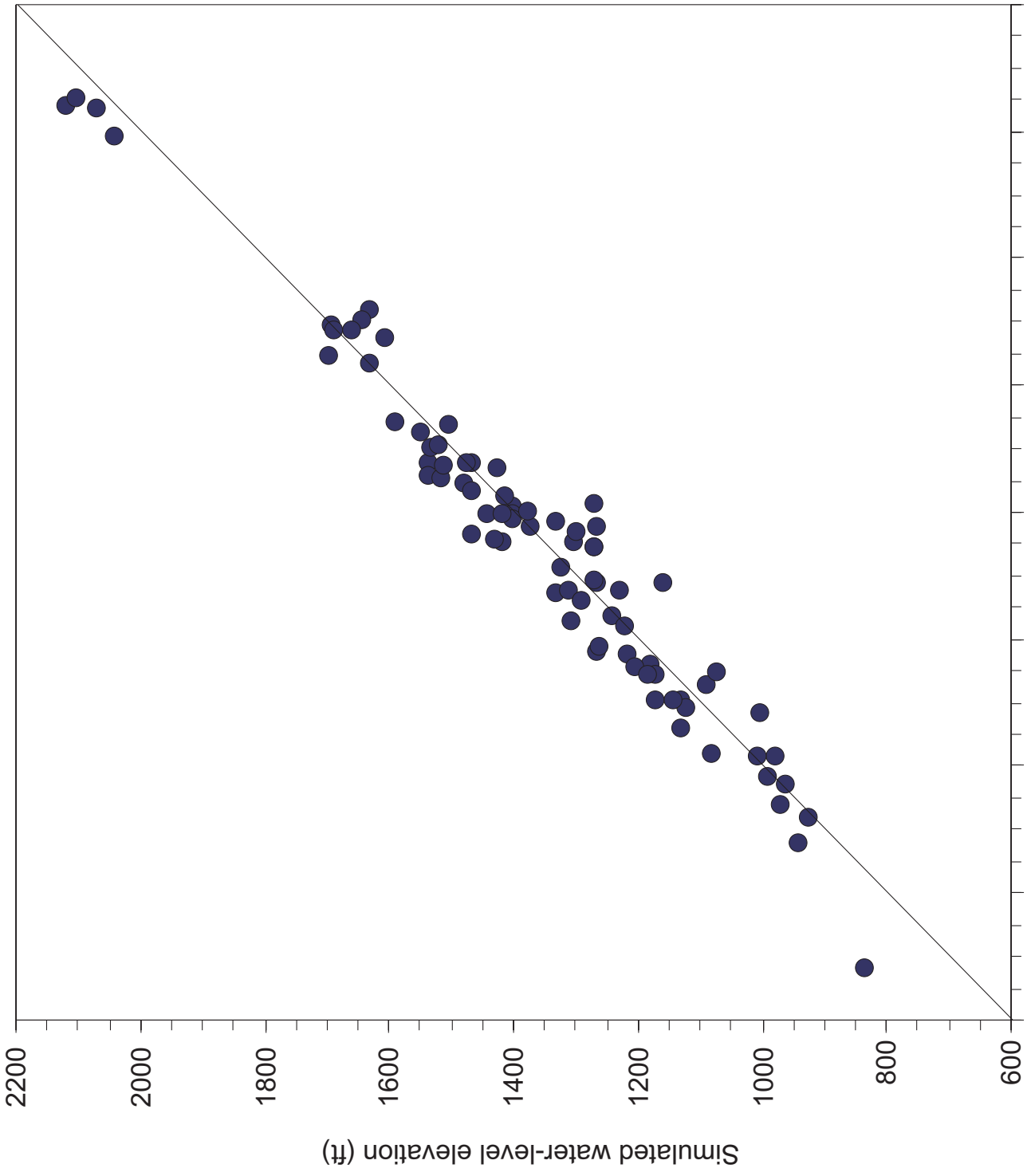

Figure 57. Comparison of simulated to measured water levels for the Middle Trinity aquifer for the 1975 steady-state model.

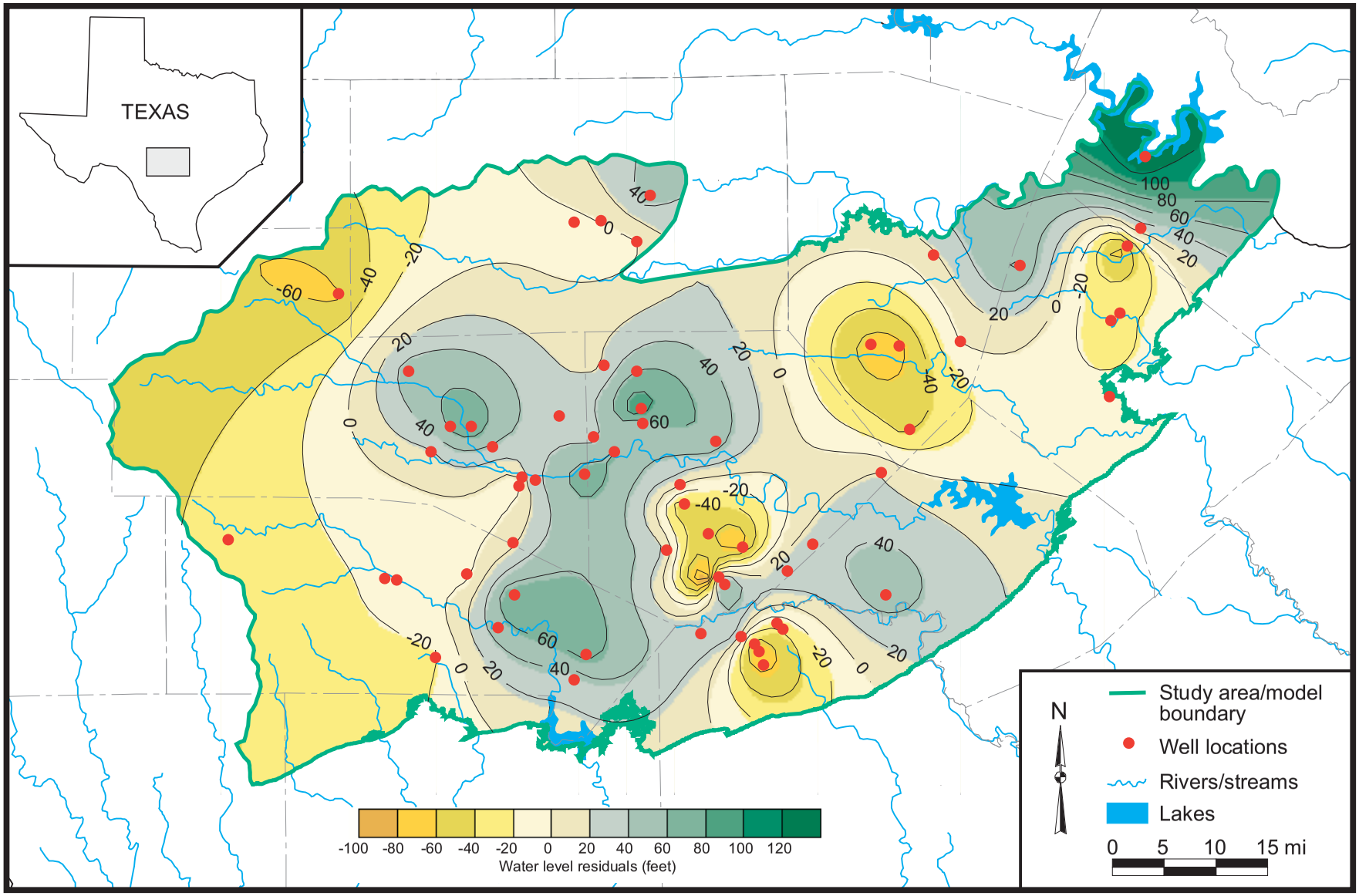

Figure 58. Water-level residuals (difference between the measured and simulated water-level elevations) for the calibrated steady-state model were attained without adjusting drain conductance. Subsequent sensitivity analysis showed that variations in the conductance had little effect on model results.

where Q_{in} is the simulated flow into the model and Q_{out} is the simulated flow out of the model. The water-balance error of the model dropped to 0.05 percent when we lowered calibrated drain conductances to 2×10^{9}, 5×10^{7} ft^2/day for springs 4, 18, and 19, respectively. Even at the lower values, these conductances are much higher than conductances used for other springs. These springs possibly have greater karstification than other springs, the spring discharge measurements are biased toward much wetter conditions, or the source area may be local and therefore not considered by the model. Because a water-balance error should ideally be less than 0.1 percent (Konikow, 1978), we used the lower conductances for these springs and maintained a lower overall water-balance error for the model. Water-balance errors in numerical modeling arise from truncation or discretization errors and round-off error (Anderson and Woessner, 1992, p. 219).

Simulated baseflow to the Guadalupe, Medina, and Blanco Rivers (table 10) are within about 25 percent of our estimated values of baseflow for the fall of 1975. Simulated baseflow for the Gualalupe, Medina, and Blanco Rivers are 59,800 acre-ft/yr, 29,200 acre-ft/yr, and 33,200 acre-ft/yr, respectively. Estimated baseflow based on baseflow analysis and climatic conditions in the winter of 1975 are 81,200 acre-ft/yr, 38,300 acre-ft/yr, and 29,500 acre-ft/yr, respectively. The simulated values of baseflow were attained without adjusting drain conductance. Subsequent sensitivity analysis showed that variations in the conductance had little affect on model results.

Water Budget

We used the calibrated model to investigate the volumes of water moving through the aquifers (table 11). In a steady-state model, flow into the model equals flow out of the model. According to the calibrated model, total flow through the aquifer is about 303,000 acre-ft/yr. Of this flow, about 57 percent discharges to rivers, 21 percent flows in the direction of the Edwards (BFZ) aquifer (out of the GHB boundary), 15 percent discharges to springs (including those along the escarpment of the Edwards Group in the plateau area), four percent discharges to lakes, and three percent is pumped to meet 1975 demands. Of the rivers included in the model, the Guadalupe, Blanco, and Medina Rivers have the largest groundwater discharges (table 10). Without any special parameter or boundary adjustments, the numerical model reproduced the observed behavior of Cibolo Creek: baseflow where the creek overlies the Upper Trinity aquifer and no baseflow where the creek overlies Middle Trinity aquifer (table 10).

Table 10: Simulated groundwater discharge to streams.

Feature:	Layer 1	Layer 2	Layer 3	Total discharge (acre-ft/yr)
Guadalupe River	10,300	16,400	33,100	59,800
Medina River	5,100	7,100	17,000	29,200
Balcones Creek/ Cibolo Creek	-	2,200	0	2,200
Blanco River		19,700	13,500	33,200
Onion Creek	-	9,500	-	9,500
Cypress Creek	-	6,200	-	6,200
Pedernales River	1,800	300	2,300	4,400
Quihi Creek	-	4,000	-	4,000
Hondo Creek	-	4,200	-	4,200
Middle Verde Creek	-	6,900	-	6,900
Total:	17,200	76,500	65,900	159,600

Values are rounded to the nearest 100 acre-ft

We also used the calibrated model to investigate the volume of recharge to and the volume of water moving between the different layers. The total volume of recharge to the aquifer due to precipitation falling on the land surface is about 303,000 acre-ft/yr. About 61 percent of the recharge in the study area occurs in the Upper Trinity aquifer with 19 percent in the Edwards Group and 20 percent in the Middle Trinity aquifer. About 10 percent of the water that recharges the Edwards Group flows into the Upper Trinity aquifer. Therefore, the total inflow of water to the Upper Trinity aquifer including infiltration of precipitation and cross-formational flow is about 190,000 acre-ft/yr under normal climatic conditions. About 37 percent of the water that recharges and flows into the Upper Trinity aquifer moves from the Upper Trinity aquifer into the Middle Trinity aquifer. Therefore, total recharge to the Middle Trinity aquifer is about 131,000 acre-ft/yr. According to the model, more water moves into the Middle Trinity aquifer through cross-formational flow than through direct infiltration on the outcrop.

The model shows that about 64,000 acre-ft/yr of water moves out of the GHB boundary along the eastern and southern ends of the model. This water moves from the Upper and Middle Trinity aquifer in the direction of the Edwards (BFZ) aquifer. Some of the water that moves in this direction flows directly from the Trinity aquifer into the Edwards (BFZ) aquifer

Table 11: Water budget for the calibrated steady-state model for 1975.

Budget item	Volume (acre-ft/yr)
Recharge	303,000
Recharge to Edwards Group	59,000
Recharge to the Upper Trinity aquifer	184,000
Recharge to the Middle Trinity aquifer	60,000
Cross-formational flow from the Edwards Group into the Upper Trinity aquifer	6,000
Cross-formational flow from the Upper Trinity aquifer into the Middle Trinity aquifer	71,000
Recharge + cross-formational flow to the Upper Trinity aquifer	190,000
Recharge + cross-formational flow to the Middle Trinity aquifer	131,000
Discharge	303,000
Rivers	173,000
GHB boundary at Edwards BFZ aquifer	64,000
GHB boundary in Travis and Hays counties	8,000
GHB boundary in Comal and Bexar counties	36,000
GHB boundary in Medina County	20,000
Springs	45,000
Edwards Group escarpment	35,000
Lakes	11,000
Pumping for 1975	10,000

Values are rounded to the nearest 1,000 acre-ft

and some continues to flow in the Trinity aquifer, but downdip beneath the Edwards aquifer (see Ashworth and Hopkins, 1995, p. 18-19 for the downdip limits of the Trinity aquifer). Presumably, water that moves downdip in the Trinity aquifer eventually discharges upward into the Edwards (BFZ) aquifer.

The average flow of water out of the 129 mile long GHB boundary is about 500 acre-ft/yr per mile of the boundary. Kuniansky and Holligan's (1994) model showed a flux of about 1,800 acre-ft/yr per mile of boundary. However, their model also includes the Lower Trinity aquifer and may also overestimate the flow of water from the Trinity aquifer to the Edwards (BFZ) aquifer (see earlier discussion in 'Discharge' section). LBG-Guyton Associates (1995) estimated that a flow of about 360 to 1,400 acre-ft/yr per mile may be transmitted along the Haby-Crossing fault from the Lower Member of the Glen Rose limestone to the Edwards aquifer.

The model shows that the flow of water across the GHB boundary is much less for the northeastern part of the boundary than the central and southwestern parts. The flow is 310 acre-ft/yr per mile for the boundary within Travis and Hays counties, 660 acre-ft/yr per mile for the boundary within Comal and Bexar counties, and 500 acre-ft/yr per mile for the boundary within Medina County. This numerical result is qualitatively supported by the measured potentiometric surface which shows groundwater generally flowing into the boundary in Comal, Bexar, and Medina counties and parallel to the boundary in Travis and Hays counties (fig. 20). Faults have greater displacements to the east and therefore may act as more effective barriers to flow.

Sensitivity Analysis

After we calibrated the model, we assessed the sensitivity of water levels in the model to different aquifer parameters. Sensitivity analysis quantifies the uncertainty of the calibrated model to the uncertainty in the estimates of aquifer parameters, stresses, and boundary conditions (Anderson and Woessner, 1992, p. 246) and is an essential step in modeling applications (Freeze and others, 1979). Sensitivity analysis assesses the adequacy of the model with respect to its intended purpose (ASTM, 1994) and can offer insight to the nonuniqueness of the calibrated model. Sensitivity analysis also identifies which hydrologic parameters most influence water levels and flows to springs, streams, and rivers and can identify parameters that require additional study.

We conducted sensitivity analyses on a number of model parameters including horizontal and vertical hydraulic conductivity for each of the layers, recharge, riverbed conductance, conductance of the general head boundary cells, and 1975 pumpage. Sensitivity analyses were performed by systematically varying a parameter value and noting the change in water levels from the values. We calculated the change in water levels at (1) the well locations used to calibrate the model and (2) each active cell in layer 3 in the model. This allowed us to determine if there was significant bias of the sensitivity analysis and the calibration between the calibration points and the entire layer. We quantified the change in water levels by calculating the mean difference, *MD*, according

$$MD = \frac{1}{n}\sum_{i=1}^{n}\left(h_{sen} - h_{cal}\right) \qquad (4)$$

where n is the number of points, h_{sen} is the simulated water level for the sensitivity analysis, and h_{cal} is the calibrated water level. The mean difference can be positive if water levels are higher than calibrated values and negative if lower than calibrated values.

We found that water levels in the model for the Middle Trinity aquifer were most sensitive to recharge, horizontal hydraulic conductivity of the Middle Trinity aquifer, and vertical hydraulic conductivity of the Upper Trinity aquifer (fig. 59). Recharge and horizontal hydraulic conductivity of the Middle Trinity aquifer affected water levels in the entire model

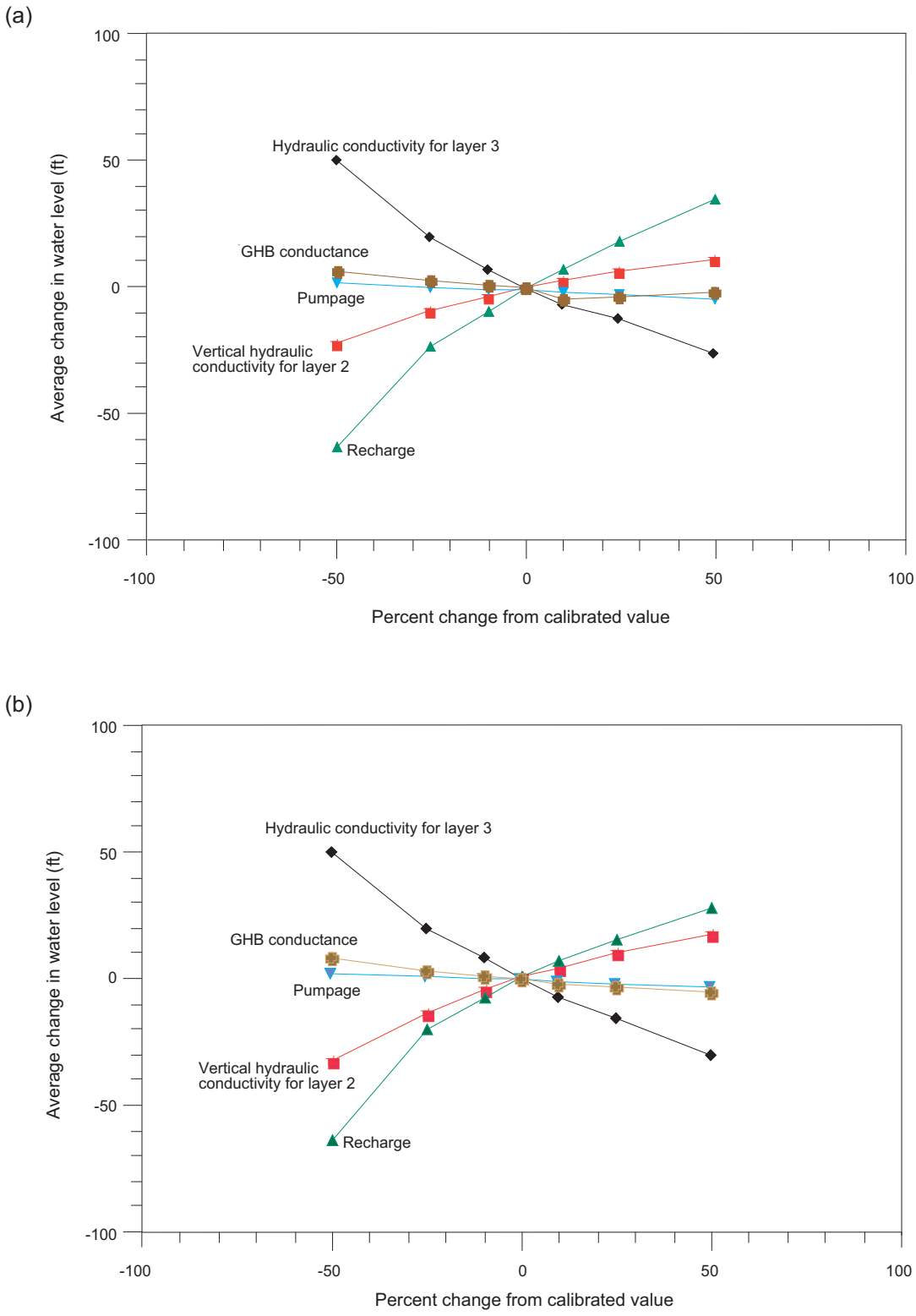

Figure 59. Sensitivity of numerically predicted water levels in layer 3 (Middle Trinity aquifer) of the steady-state model to changes in model parameters at (a) the calibration wells and (b) each active cell in the layer.

area while vertical hydraulic conductivity of the Upper Trinity aquifer mostly affected water levels in the western part of the model area. For the investigated ranges ($\pm$ 50 percent of calibrated values), water levels in the Middle Trinity aquifer were not sensitive to initially assigned values of riverbed conductance, conductance of the general-head boundary cells, horizontal hydraulic conductivity for Upper Trinity aquifer, vertical hydraulic conductivity for the Middle Trinity aquifer, and horizontal and vertical hydraulic conductivity for the Edwards Group in the plateau area. The mean differences calculated at the calibration locations and at each active cell in layer 3 in the model are similar (fig. 59) indicating that the calibration points probably do not bias the sensitivity analysis and are a good representation of the Middle Trinity aquifer.

Lower values of recharge and vertical hydraulic conductivity for the Upper Trinity aquifer resulted in lower water levels in the model while higher values resulted in higher water levels (fig. 59). Lower values of horizontal hydraulic conductivity for the Middle Trinity aquifer resulted in higher water levels in the model while higher values resulted in lower water levels. In all cases the sensitivity was asymmetric in that water levels in the model were slightly more sensitive to lower parameter values than to higher values.

Water levels in the model were less sensitive to 1975 pumping than to other model parameters. However, pumping volume comprised only about 3 percent of the modeled recharge volume in 1975. Therefore, we conducted additional sensitivity analyses on pumping rates where we (1) used the 1975 pumping distribution and increased total pumping volumes to predicted 2050 pumping volumes (about 70,000 acre-ft) and (2) entered the 1997 pumping distribution into the calibrated steady-state model and increased total pumping volumes to predicted 2050 volumes. This analysis showed that water levels in the model are sensitive to larger pumping rates in the Middle Trinity aquifer (fig. 60) and that the distribution of pumping does not affect the mean water-level change in the model.

We also did sensitivity analyses on the (1) lower boundary condition, (2) distribution of hydraulic conductivity in layer 3, and (3) distribution of recharge in the model. When we developed the model, we assumed no flow between the Middle and Lower Trinity aquifers due to the presence of the low permeability Hammett Shale. However, the Hammett Shale pinches out in the northwest part of the study area (fig. 8). Therefore, water that recharges the aquifer north of this area flows into the Upper and Middle Trinity aquifers as well as the Lower Trinity aquifer. Based on aquifer thickness, perhaps as much as half of the subsurface flow in the northwest part of the model moves into the Lower Trinity aquifer.

Because the model does not include the Lower Trinity aquifer, hydraulic conductivity may be overestimated in the model in order to remove the excess recharge, or recharge may be underestimated due to substantial leakage into the Lower Trinity aquifer. If the model included the Lower Trinity aquifer, it would take some of the flow from the Upper and Middle Trinity aquifers. Therefore, we raised the recharge rate in the northwestern part of the study area where the Hammett shale pinches out and investigated water levels in the rest of the model. We found that doubling the recharge in this area had little impact on water levels in the rest of the model because most of the added recharge discharged locally.

Cross-formational flow through the Hammett Shale could also affect model results. To address this issue, we calculated the potential for cross-formational flow based on the hydraulic head difference between the Middle and Lower Trinity aquifers and an estimated hydraulic conductivity of the Hammett Shale. Water levels suggest that there are downward hydraulic-head gradients in the western part of the study area and upward hydraulic-head gradients along the eastern and southern boundaries (Ashworth, 1983). Assuming a vertical

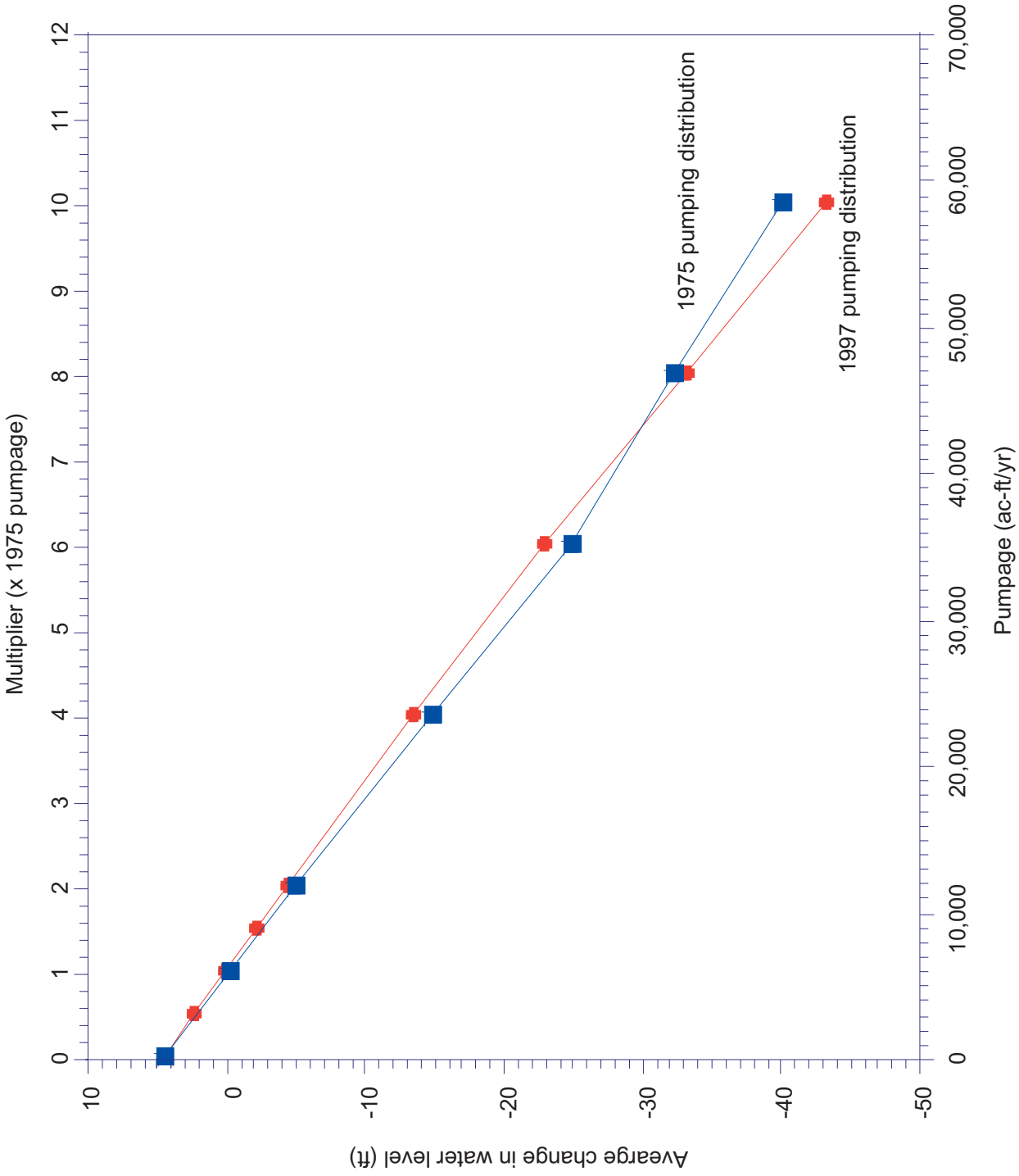

Figure 60. Sensitivity of water levels in layer 3 (Middle Trinity aquifer) to increases in pumping using the steady-state model and the pumping distribution for 1975 and 1997.

hydraulic head drop of 50-ft, an average thickness of 35-ft for the Hammett Shale, a vertical hydraulic conductivity of 0.00001 ft/day, and an area of 3,000 square miles, the total flow to the Lower Trinity aquifer might be 10,000 acre-ft/yr or about 3 percent of the total flow system. However, a large part of this flow may return to the Middle Trinity aquifer thus canceling any budget errors.

The model is not very sensitive to the distribution of hydraulic conductivity. We assessed the sensitivity of hydraulic heads in layer 3 to the distribution of horizontal hydraulic conductivity in layer 3 by (1) assigning a uniform geometric mean and (2) increasing hydraulic conductivity along an eight-mile buffer zone along the Balcones Fault zone. RMS error in the model only increased one foot when we used a uniform distribution of horizontal hydraulic conductivity for the Middle Trinity aquifer instead of the distributed values. This means that this model of the regional aquifer is not sensitive to the overall distribution of horizontal hydraulic conductivity in layer 3 as we have characterized it. This result does not suggest that water-level drawdowns around individual wells or groups of wells are not sensitive to the local or sub-regional distribution of hydraulic properties.

Because of faulting, the area near the Balcones Fault Zone may have greater hydraulic conductivity than the rest of the study area. Therefore, we doubled the calibrated horizontal hydraulic conductivity values for layer 3 within an eight-mile area near the fault zone. In response, the RMS error increased by four feet, indicating that the regional model is not very sensitive to hydraulic conductivity in this area.

The model is sensitive to the distribution of recharge. When we doubled calibrated recharge values in the western part of the model, RMS error for the model increased to 100-ft. When we halved recharge values in the western part of the model, RMS error increased to 69-ft.

Transient Model

Once we calibrated the steady-state model for conditions in the winter of 1975-1976, we then calibrated the model for transient conditions in 1996 and 1997. Because of the time gap between the end of 1975 and the beginning of 1996, we first developed an initial condition appropriate for the beginning of 1996. To develop this initial condition, we ran the calibrated steady-state model using recharge for 1995 and pumping for 1996 and comapred the resulting water levels to water levels measured in early 1996. Because the aquifer was not in equilibrium with 1996 pumping rates in Travis and Bexar counties, we artificially lowered pumping rates in these areas by trial-and-error to develop a more representative water-level surface for the beginning of our transient modeling (RMS error = 61-ft). This surface served as the initial condition for the 1996 to 1997 transient simulations.

Calibration and Verification

Using monthly stress periods, we simulated water-level fluctuations according to recharge and pumping variations in 1996 and 1997. To calibrate, we adjusted specific-storage values until the model approximately reproduced the range of water-level fluctuations observed in wells in the model area. We found that specific-storage values of 0.00001, 0.000001, and 0.0000001 per ft for layers 1, 2, and 3, respectively, and specific-yield values of 0.008, 0.0005, and 0.0008 for layers 1, 2, and 3, respectively, worked best for reproducing observed water-level fluctuations.

The model does a good job of matching observed water-level fluctuations in some areas and not as well in matching water-level fluctuations in other areas (fig. 61, note that baseline shift in water levels is due to error in the steady-state model). Differences may be due to the influence of local-scale conditions not represented in the regional model or errors in our parameterization of the aquifer data. Although

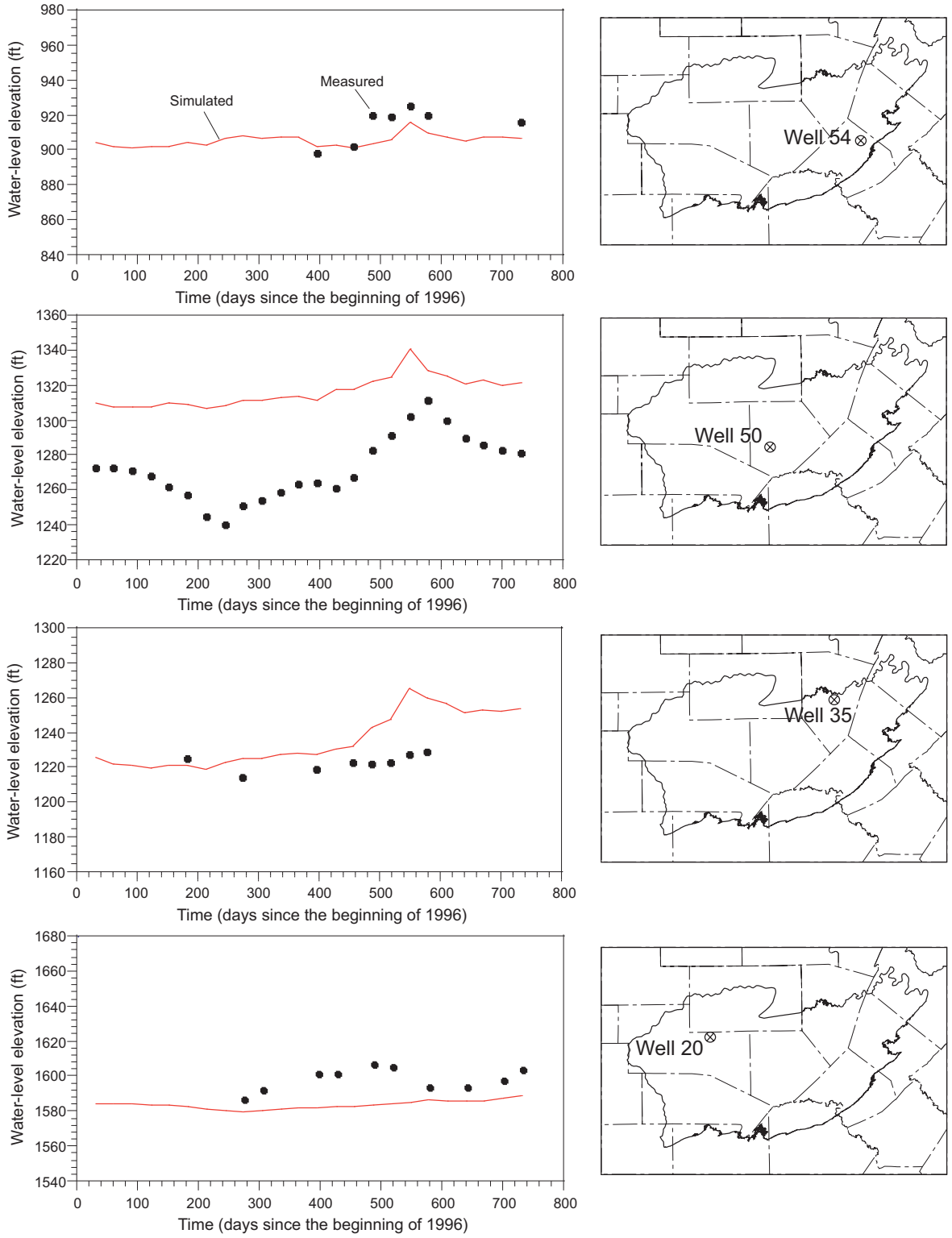

Figure 61. Comparison of simulated water-level fluctuations to measured water-level fluctuations in several wells in the Middle Trinity aquifer.

there are limitations, the model does a good job of reproducing seasonal and year-to-year water-level variations in most wells and accurately representing areas where water levels respond quickly and substantially to variations in recharge and areas where the water-level response is much more subdued.

A specific yield of 0.0008 may seem low for the Middle Trinity aquifer. However, when we increased specific yield ten times, simulated water-level variations were greatly dampened (fig. 62). A specific yield of 0.0008 is equivalent to a fracture porosity of about 0.1 percent, which is consistent with measured fracture porosities (0.01 to 1 percent [Freeze and Cherry, 1979, p. 408]). Smaller specific yields increase the magnitude of water-level fluctuations (fig. 62). The model was comparatively less sensitive to specific storage (fig. 63). Smaller values of specific storage had little affect on water levels while larger values generally had more affect depending on well location (fig. 63).

Predictions

To assess the future availability of groundwater in the Trinity aquifer for the Hill Country area, we used the calibrated model to predict future water levels under drought-of-record conditions using estimates of future groundwater demands based on demand numbers from the Regional Water Planning Groups. Senate Bill 1 requires water planning under drought-of-record conditions. The purpose of this planning is to ensure that the State's future water needs are met during times of severe drought. Before using the model to predict future water levels, we first assessed the drought of record for the study area and revisited the GHB boundary condition along the eastern and southern boundary of the model.

Drought of Record

In general, a drought is defined as an extended period of dry weather or a period of deficient rainfall (Wilson and Moore, 1998). In terms of its effects, a drought can be defined as a dry period of sufficient length to detrimentally affect crops and surface-water availability (Rogers, 1981, p. 118 as cited in Wilson and Moore, 1998). A drought of record is the most severe drought during the period of record in terms of duration and lack of rainfall.

Droughts are common in the Hill Country and vary in frequency, duration, and lack of rainfall. Based on measured precipitation for the last 100 years, the drought of record for the Hill Country occurred between 1950 and 1956 (fig. 64). During this 7-year drought period, the mean annual precipitation was about two thirds (22 inches) of the long-term 100-year mean annual precipitation of 33 inches. During the last three years of the drought, the mean annual precipitation was less than half (13.9 inches) of the long-term 100-year mean annual precipitation (fig. 64). An extreme storm event on September 10-11, 1952, provided a mild reprieve from the drought for the central northeastern part of the study area. This storm produced 12.0 inches of rain at the Boerne station, 21.1 inches at the Blanco station, and 23.3 inches at the Hye station (see fig. 25 for gage locations). Much of the rainfall from this event likely resulted in considerable runoff to streams and rivers and minimal recharge compared to the volume of rainfall.

We included the drought of record in the predictive simulations by using the mean annual precipitation data from 1950 through 1956 for each of the rainfall gaging stations within the study area. To calculate the rainfall for each grid-cell, we transformed these data into ArcInfo® TIN surfaces and intersected the surfaces with the centroid of each model cell. We multiplied these rainfall amounts by the recharge coefficient of each model cell (fig. 28) to create spatially distributed recharge estimates for the drought of record. We defined recharge for normal climatic conditions by using the average precipitation for the period 1960 to 1990.

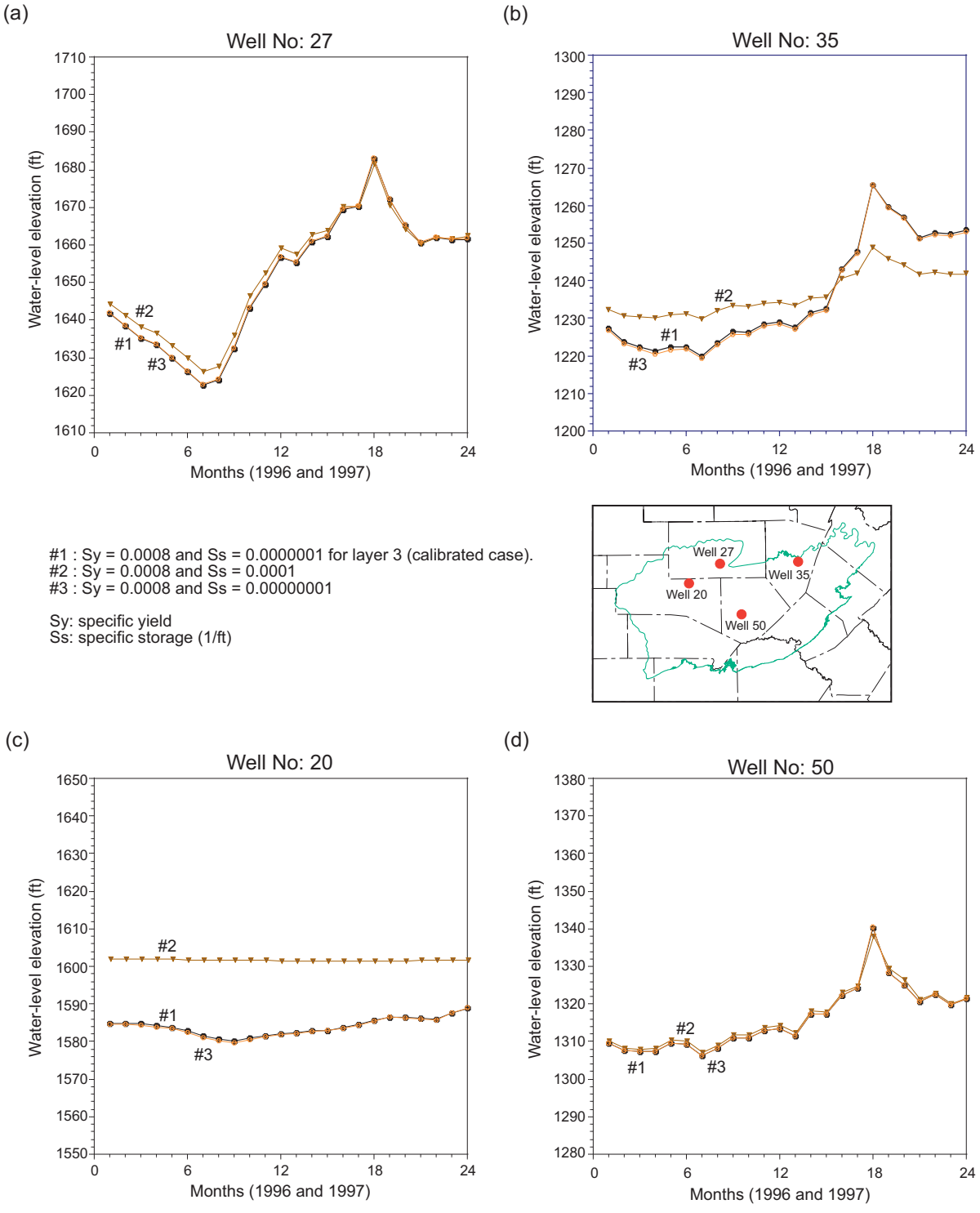

Figure 62. Sensitivity of the transient calibration to specific yield.

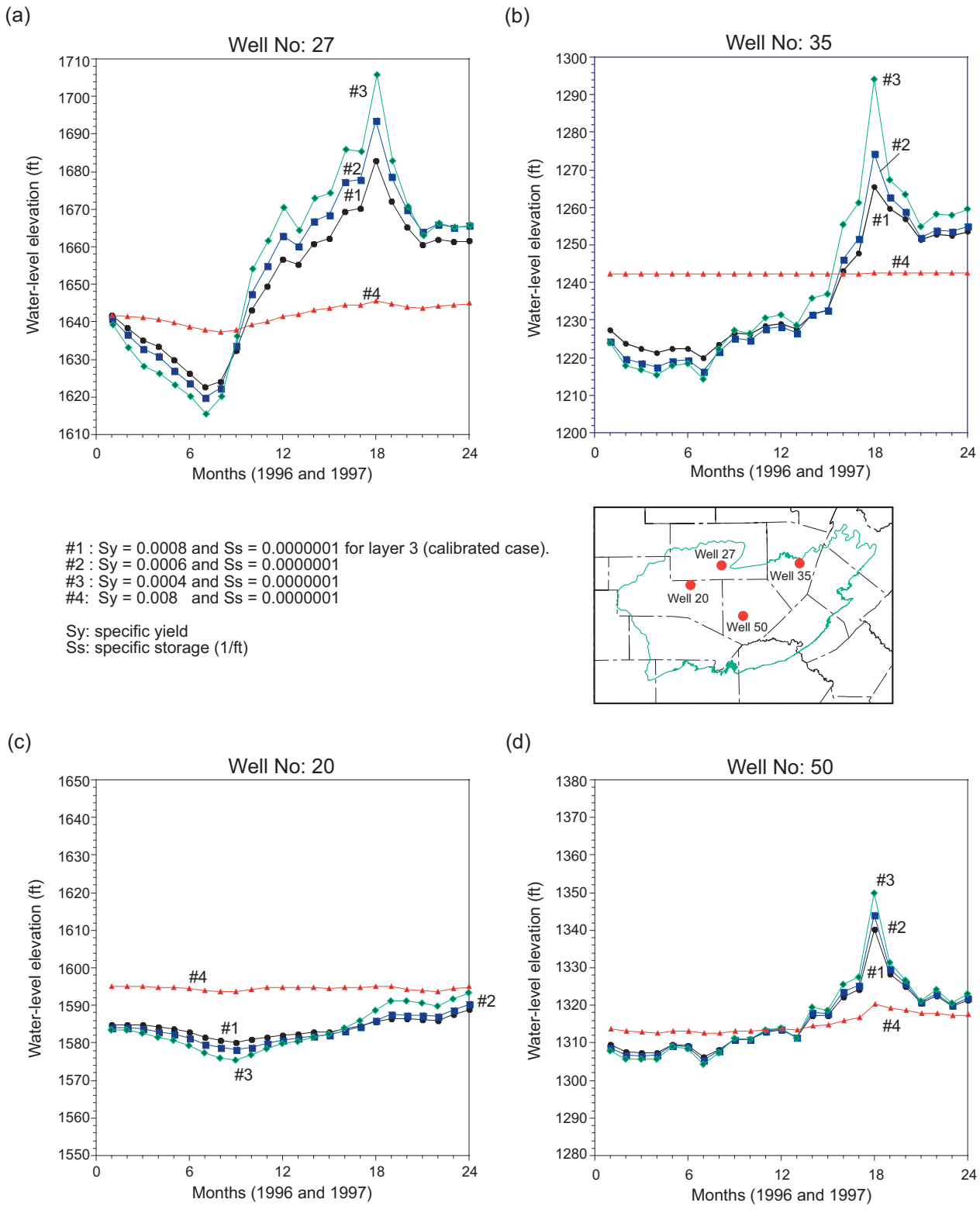

Figure 63. Sensitivity of the transient calibration to specific storage.

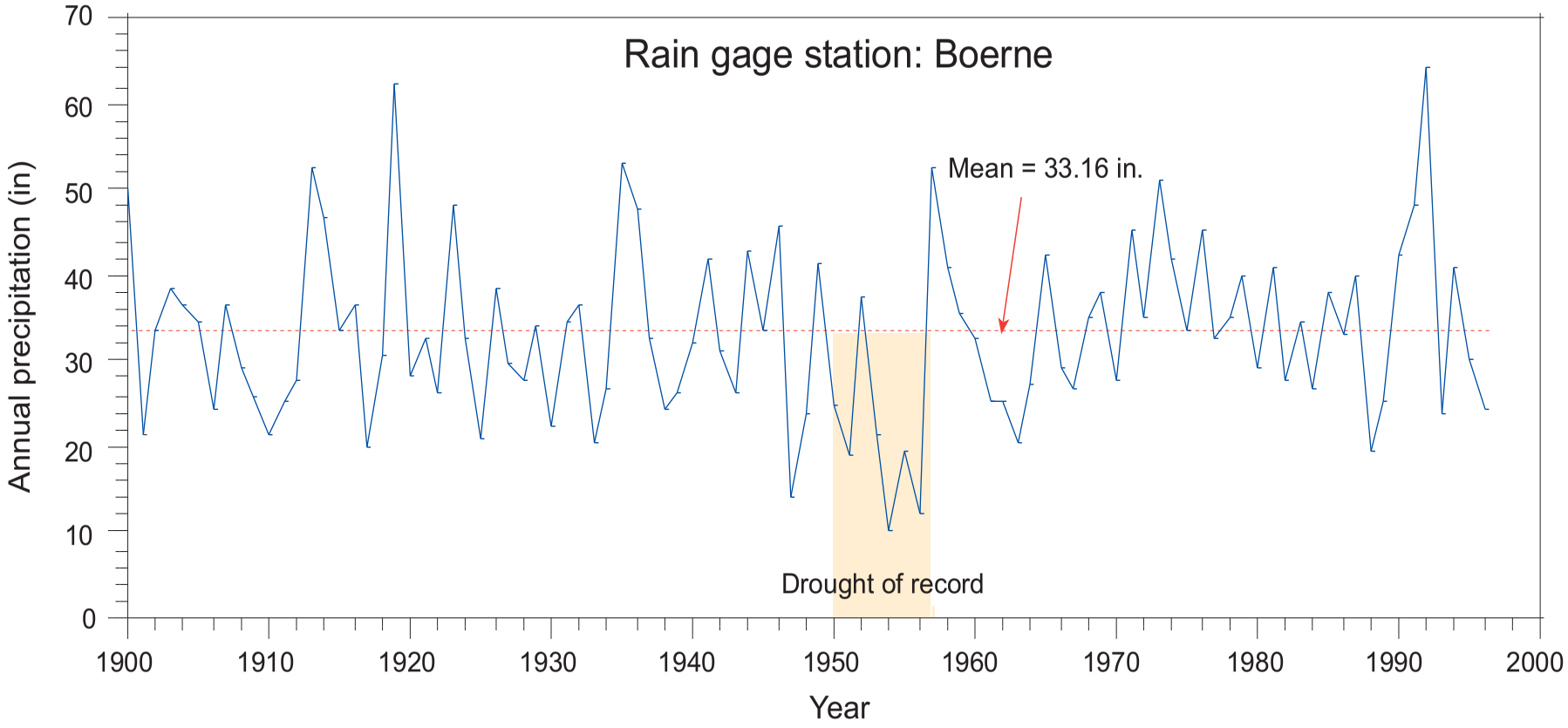

Figure 64. Precipitation from 1900 to 1997 measured at the rainfall gaging station at Boerne showing the drought of record during the 1950s. Gage location is shown in figure 25.

GHB Boundary Condition

After completing initial predictive simulations with the calibrated model, we noticed that drawdowns in the northern Bexar County area were reaching the GHB boundary to the southeast. For the calibrated model, we treated this boundary as a head-dependant flux boundary using the general-head boundary package in MODFLOW. Because the conductance in the general-head boundary was high enough to not resist flow from the model to the boundary, this general-head boundary behaves similar to a constant-head boundary. Therefore, water levels on the boundary remained the same no matter how much water levels declined in the nearby aquifer. In this case, water-level declines would be underestimated in this part of the model.

To more realistically simulate the southern and eastern boundary of the model under conditions with nearby water-level declines, we changed the assigned hydraulic head and conductance values in the general-head boundary to allow water levels to decline at the boundary while maintaining the calibration of the original model and the flow of water out of the boundary. We first assigned hydraulic head in the general-head boundary according to water levels in the Edwards (BFZ) aquifer along the boundary. These water levels were based on measurements from the TWDB water-well database. We then used Darcy's law, the hydraulic conductivity of the aquifer at the boundary (K_o), calibrated water level in the model at the boundary (h_m), hydraulic head in the original general-head boundary (h_{ghb}), hydraulic head in the Edwards aquifer along the boundary (h_{ed}), and a unit thickness (L_c) to estimate a conductance term, C_n, for the new general-head boundary:

$$C_n = K_o L_c \frac{h_m - h_{ghb}}{h_m - h_{ed}} \qquad (5)$$

We calculated new conductances for each cell along the boundary according the parameters listed above. After substituting the new hydraulic heads and conductances for layer 3, we ran the model, compared the results to the previous model, and found no difference in model results.

Predicted Groundwater Availability

Using the adjustment to the GHB boundary discussed above, we made six predictive runs with the calibrated model:

- Baseline Run: average recharge through 2050;
- 2010 Run: average recharge through 2003 and drought-of-record recharge for the remaining seven years;
- 2020 Run: average recharge through 2013 and drought-of-record recharge for the remaining seven years;
- 2030 Run: average recharge through 2023 and drought-of-record recharge for the remaining seven years;
- 2040 Run: average recharge through 2033 and drought-of-record recharge for the remaining seven years; and
- 2050 Run: average recharge through 2043 and drought-of-record recharge for the remaining seven years.

We calculated the water-level declines at each decade (2010, 2020, 2030, 2040, and 2050) by subtracting the predicted water levels at the end of the decade from the water levels at the end of 1997, the end of the transient calibration.

Predictive simulations show that water levels decline in response to increased groundwater pumping and to drought-of-record conditions and that water-level declines increase with time (figs. 65-69). The largest water-level declines occur in the Cibolo Creek area (northern Bexar, western Comal, and southern Kendall counties) and in Hays and Travis counties (figs.

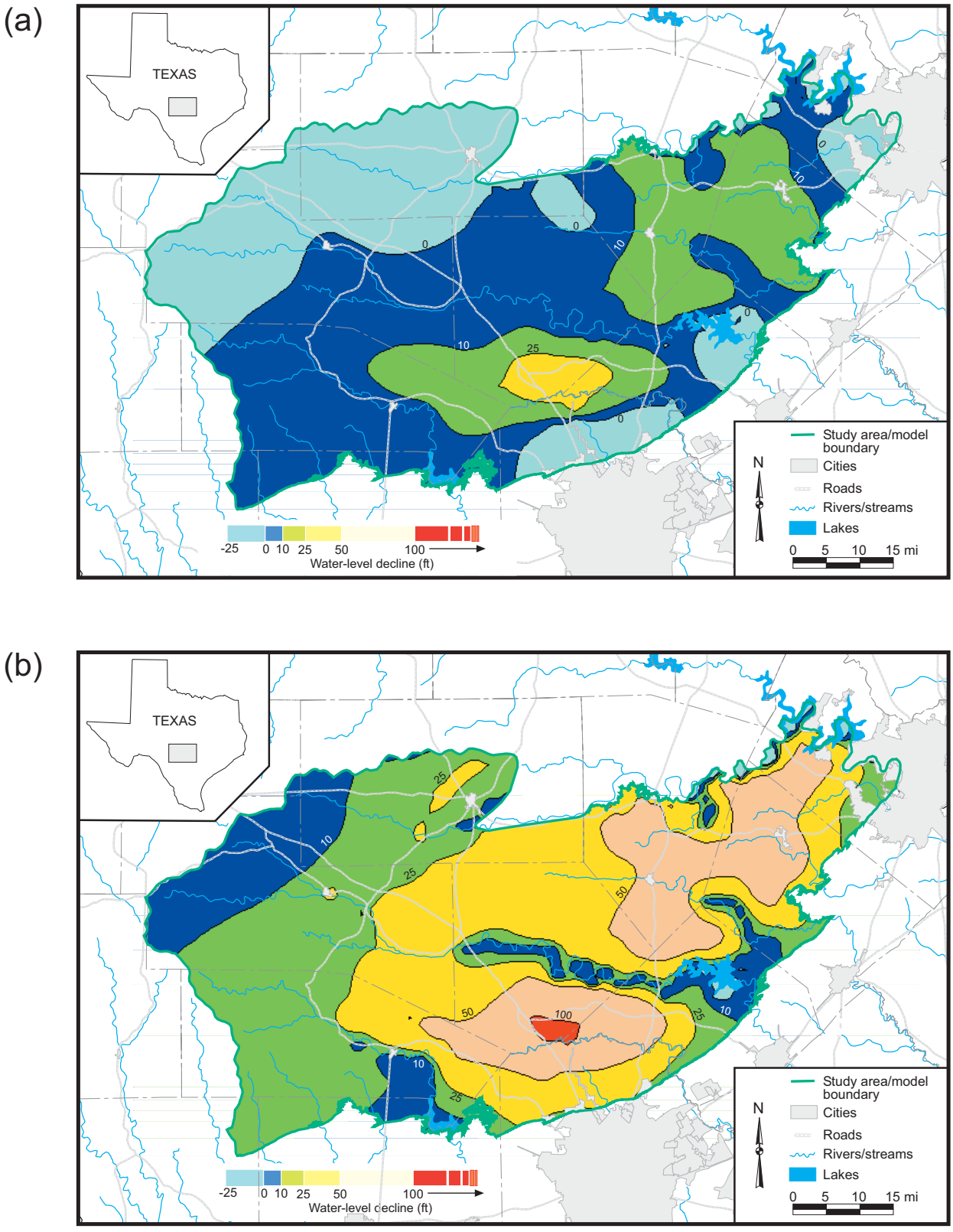

Figure 65. Simulated water-level declines in 2010 (relative to water levels in 1997) using (a) average recharge conditions through 2010 and (b) average recharge conditions through 2003 and drought-of-record recharge conditions from 2004 to 2010.

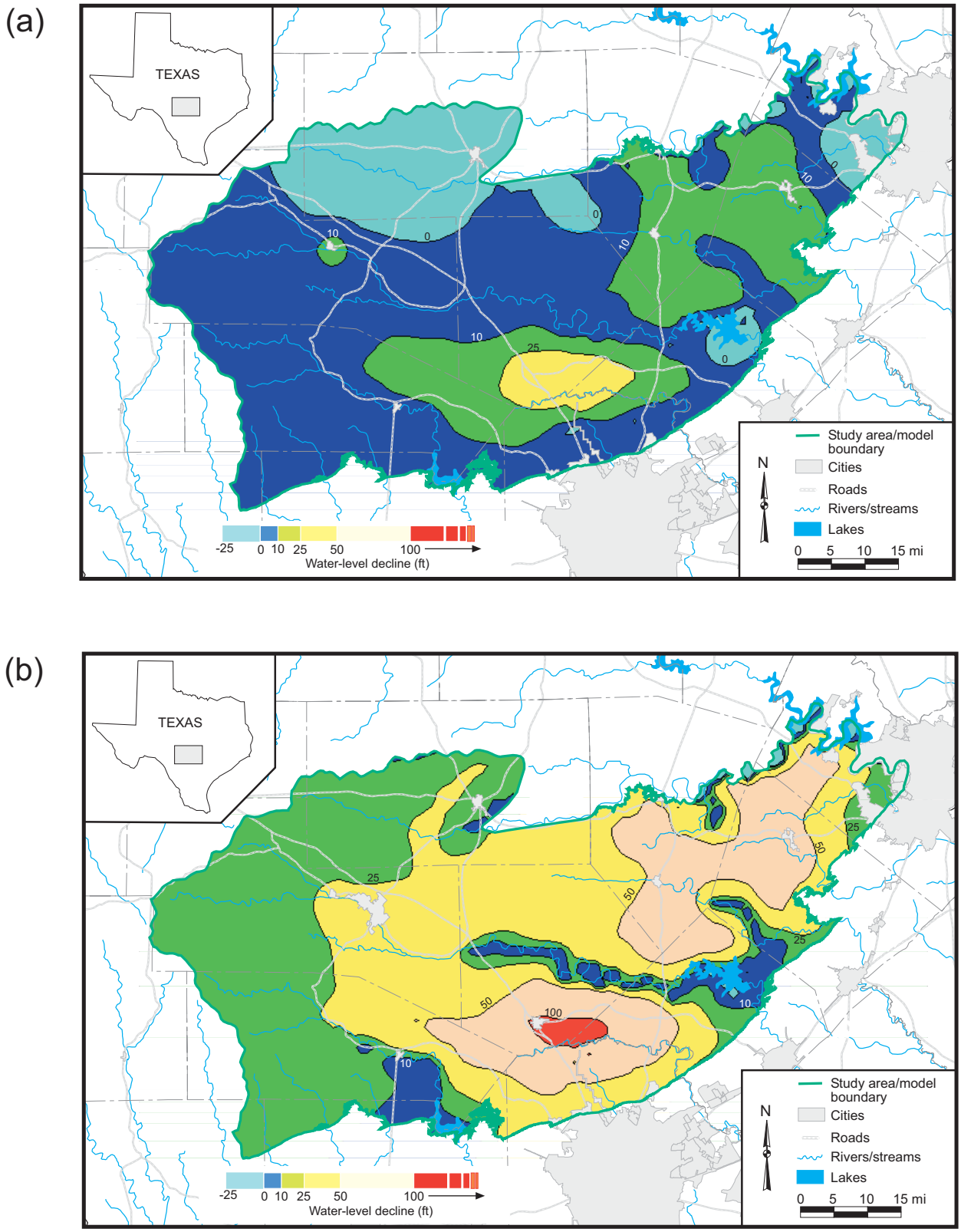

Figure 66. Simulated water-level declines in 2020 (relative to water levels in 1997) using (a) average recharge conditions through 2020 and (b) average recharge conditions through 2013 and drought-of-record recharge conditions from 2014 to 2020.

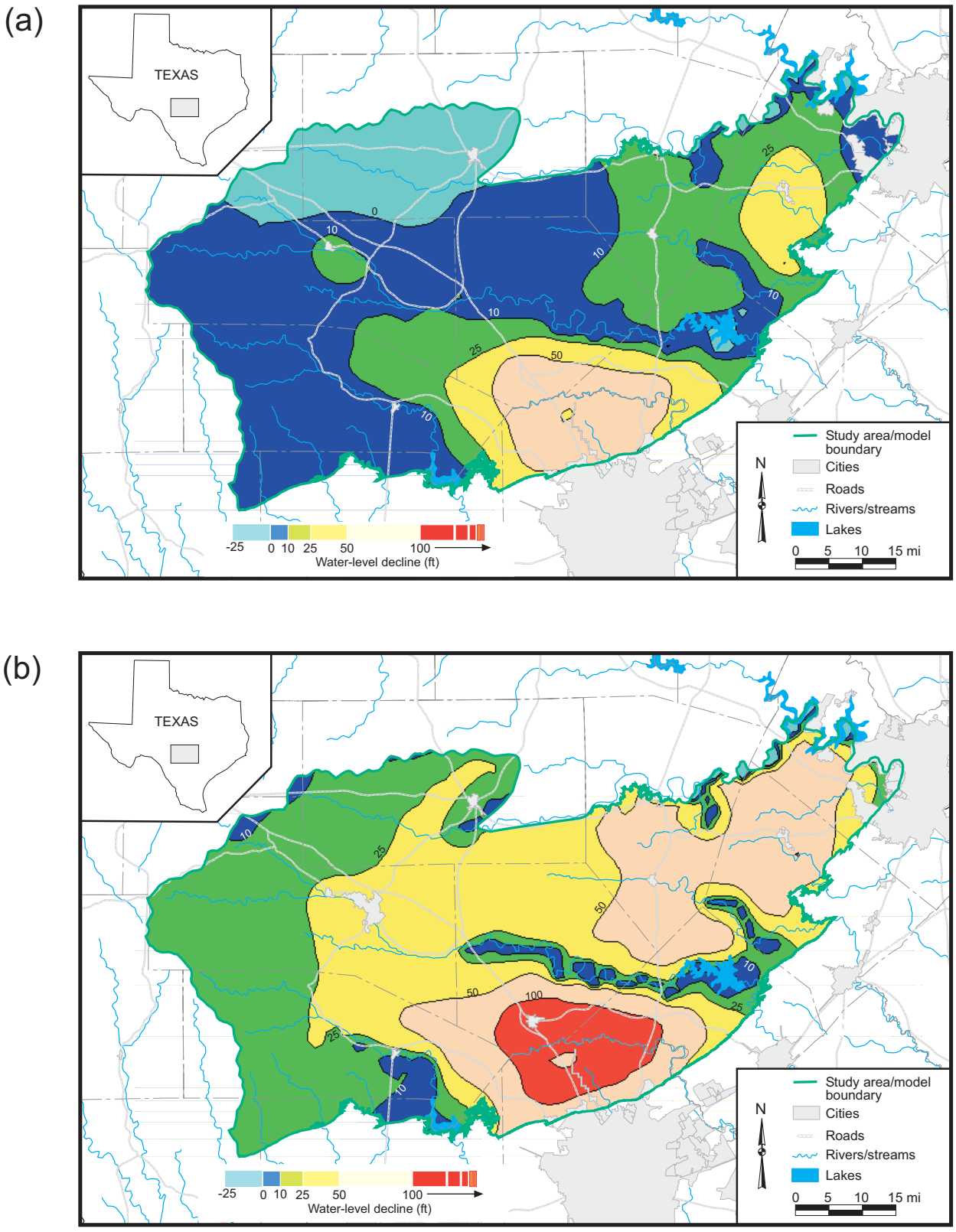

Figure 67. Simulated water-level declines in 2030 (relative to water levels in 1997) using (a) average recharge conditions through 2030 and (b) average recharge conditions through 2023 and drought-of-record recharge conditions from 2024 to 2030.

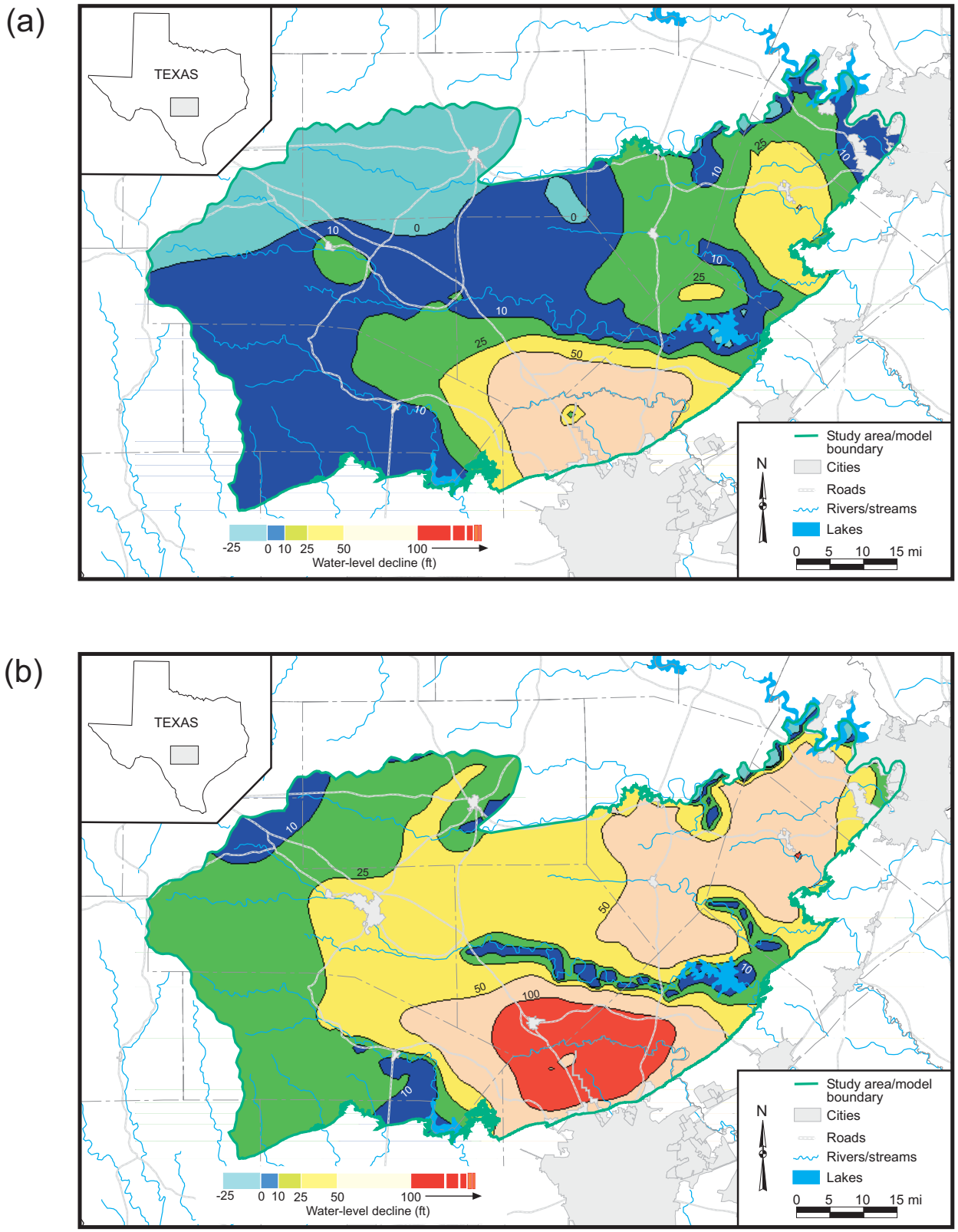

Figure 68. Simulated water-level declines in 2040 (relative to water levels in 1997) using (a) average recharge conditions through 2040 and (b) average recharge conditions through 2033 and drought-of-record recharge conditions from 2034 to 2040.

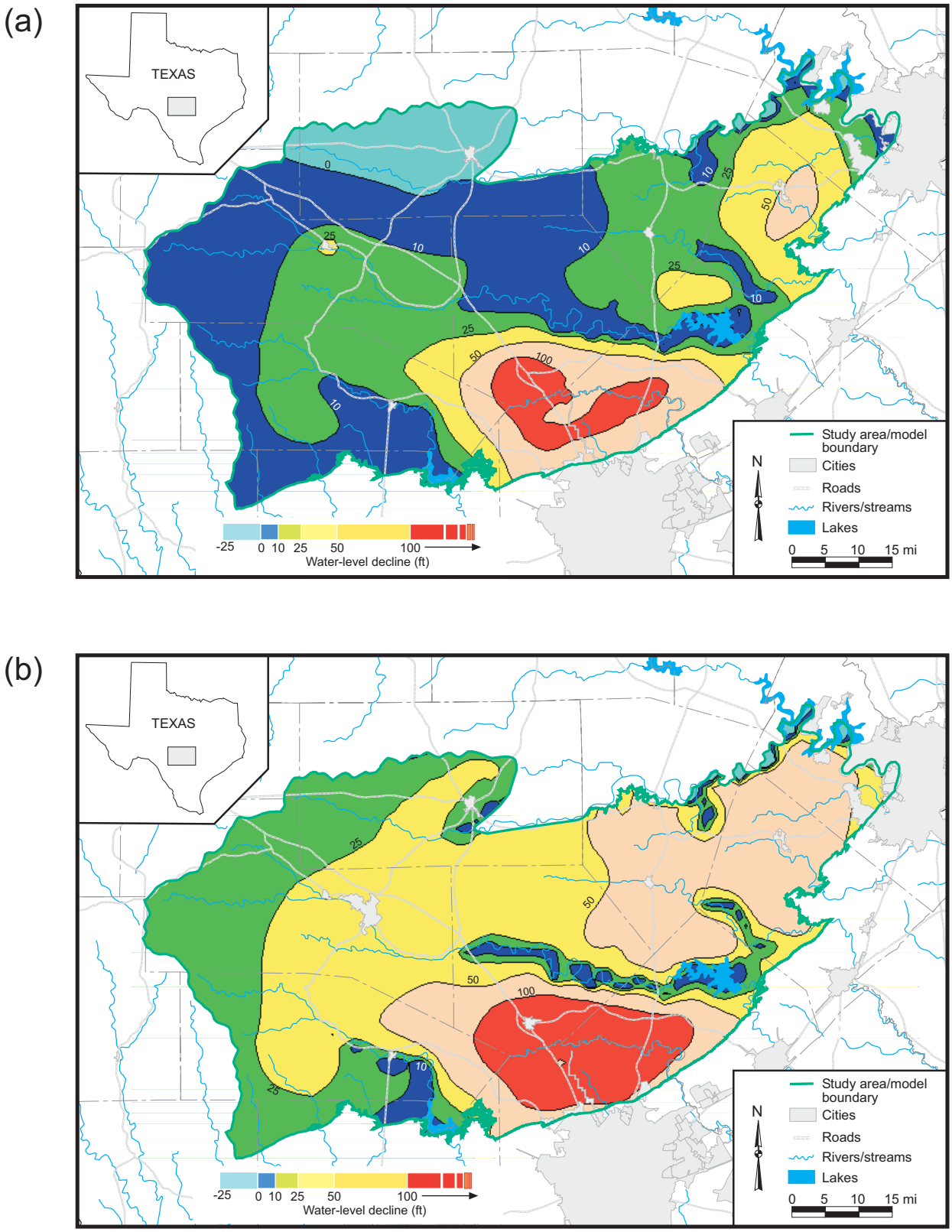

Figure 69. Simulated water-level declines in 2050 (relative to water levels in 1997) using (a) average recharge conditions through 2050 and (b) average recharge conditions through 2043 and drought-of-record recharge conditions from 2044 to 2050.

65-69). Declines greater than 100-ft occur in the Cibolo Creek area and first make an appearance in 2050 for normal recharge condition (fig. 69a) and in 2010 for drought-of-record conditions (fig. 65b). Water-level declines greater than 100-ft under drought-of-record conditions grows from a small area in southern Kendall County in 2010 (fig. 65b) to a much larger area in northern Bexar, western Comal, eastern Bandera, and southern Kendall counties by 2050 (fig. 69b).

Under drought-of-record conditions, much of the study area is affected by declining water levels (fig. 69b). Exceptions include the northwestern part of the study area in Kerr County before 2050 and the major rivers and streams in the study area including the Guadalupe, Blanco, Pedernales, and Medina Rivers and Miller Creek in Blanco County. Small water-level declines in the vicinity of rivers and creeks imply that these surface-water features will continue to flow, although at much lower rates, during droughts. These rivers continued to flow during most of the drought of the 1950s (figs. 29-34).

Comparisons between simulations with no drought and simulations with drought show that water-level declines are considerably larger under drought-of-record conditions. However, these simulations also show that in the unlikely case where there is no drought, water-level declines in the aquifer may still be substantial due solely to increases in pumping (for example, see fig. 58a).

We used the model to investigate how increased demands and droughts might affect flows in the aquifer (table 12). According to the model, groundwater flow to rivers might decrease 60 to 65 percent, discharge to the Edwards aquifer might decrease 50 to 67 percent, discharge to springs might decrease 55 percent, and discharge to lakes might decrease 70 to 95 percent in time of drought compared to 1975 flows (table 12). During a time of drought, the removal of water from aquifer storage (inducing a water-level decline) can be substantial (table 12).

The saturated thickness in 1997 ranges from less than 100-ft along the northern edge of the model to more than 500-ft along the Balcones Fault Zone (fig. 70). With a drought-of-record, the saturated thickness in 2010 has decreased along the northern edge where the saturated thickness is thin and where there are large amounts of pumping in the eastern parts of the study area (fig. 71). With a drought of record, the saturated thickness in 2020 is less than in 2010, especially in the pumping areas in the eastern parts of the study area (fig. 72). There are also localized areas where, according to the model, the aquifer has been drained (fig. 72). In MODFLOW, when a cell goes dry, it removes the pumping from the system and remains dry for the rest of the simulation. The saturated thickness decreases more for droughts-of-record that occur at later times (figs. 73, 74, and 75).

Given the uncertainty in model calibration, groundwater demand numbers, and recharge, we conducted sensitivity analyses on the predictive water-level declines by varying the specific yield, hydraulic conductivity, recharge, and pumping. Increasing the specific yield results in producing more water from the aquifer when it is pumped. When we increased specific yield in the Middle Trinity aquifer ten times from 0.0008 to 0.008, the model shows less water-level decline in the aquifer. However, water-level declines greater than 100-ft remain in the southern Kendall County area, and water level declines greater than 50 feet remain in the Dripping Springs area.

Recent aquifer testing suggests that the hydraulic conductivity may be locally much greater than average in northern Bexar County (William Stein, LBG-Guyton, personal communication, 2000). However, doubling horizontal hydraulic conductivity in Bexar County has little effect on water-level declines in the model. There has been some debate on how development on the aquifer affects recharge. On one hand, development increases impervious cover, which increases runoff and decreases recharge. On the other hand, many homes use

Table 12: Water budget for the calibrated steady-state, calibrated transient, and predictive runs. All values are in acre-ft/yr.

Year	Layer	Recharge	Rivers	GHB	Springs	Lakes	Wells	X-flow[1]	Storage
1975	1	59,100	-14,400	0	-37,400	0	-1,200	-6,300	-200
	2	184,400	-79,700	-34,700	-2,800	-1,100	-1,400	-64,800	-100
	3	60,200	-78,500	-29,800	-5,200	-10,200	-7,400	71,100	100
	All	303,700	-172,600	-64,500	-45,400	-11,300	-9,900	0	-200
1996	1	45,900	-12,500	0	-32,100	0	-3,500	-6,000	-8,200
	2	135,200	-64,600	-28,500	-2,100	-900	-3,500	-60,600	-24,800
	3	55,600	-60,300	-18,900	-3,100	-5,500	-28,400	66,600	5,800
	All	236,700	-137,400	-47,400	-37,300	-6,300	-35,400	0	-27,300
1997	1	54,700	-13,400	0	-35,900	0	-3,700	-6,100	-4,400
	2	214,400	-87,900	-37,900	-2,900	-1,400	-3,300	-73,300	7,800
	3	73,500	-78,000	-22,000	-4,100	-7,200	-30,800	79,400	10,700
	All	342,600	-179,300	-59,900	-42,900	-8,600	-37,800	0	14,100
2010	1	24,900	-8,900	0	-19,900	0	-5,400	-5,500	-14,900
	2	76,700	-30,500	-16,900	-1,000	-200	-3,800	-37,700	-13,500
	3	27,300	-32,600	-15,200	-1,800	-2,200	-32,100	43,300	-13,100
	All	128,900	-71,900	-32,100	-22,700	-2,400	-41,400	0	-41,500
2020	1	24,900	-8,800	0	-19,700	0	-5,700	-5,500	-14,900
	2	76,600	-30,300	-16,600	-1,000	-200	-4,600	-37,500	-13,500
	3	27,400	-32,000	-14,100	-1,800	-1,800	-37,900	43,000	-17,000
	All	128,900	-71,100	-30,700	-22,400	-1,900	-48,200	0	-45,400
2030	1	24,900	-8,800	0	-19,400	0	-6,300	-5,500	-15,100
	2	76,500	-30,000	-15,900	-1,000	-100	-5,500	-37,600	-13,500
	3	27,300	-28,500	-8,800	-1,700	-500	-45,000	43,100	-14,100
	All	128,700	-67,300	-24,700	-22,100	-600	-56,800	0	-42,700
2040	1	24,800	-8,500	0	-19,300	0	-6,700	-5,500	-15,300
	2	76,500	-29,700	-15,200	-1,000	-100	-6,400	-37,500	-13,400
	3	27,100	-26,200	-5,600	-1,800	500	-51,000	43,000	-13,900
	All	128,400	-64,400	-20,800	-22,100	400	-64,200	0	-42,600
2050	1	24,500	-8,500	0	-19,000	0	-6,900	-5,500	-15,400
	2	76,800	-29,500	-15,300	-1,000	-100	-6,600	-37,300	-13,100
	3	26,600	-24,900	-5,700	-1,600	1,500	-51,200	42,800	-12,500
	All	127,900	-62,900	-21,000	-21,600	1,400	-64,800	0	-41,000
2050*	1	59,100	-12,700	0	-33,100	0	-7,700	-6,100	-500
	2	175,100	-69,900	-31,700	-2,200	-900	-6,900	-63,500	0
	3	60,400	-55,300	-11,100	-3,500	-4,100	-56,900	69,700	-700
	All	294,700	-137,900	-42,900	-38,700	-5,100	-71,500	0	-1,200

[1] Net cross-formational flow

* Predictive run with no drought.

A positive sign indicates additions to the water budget and negative signs indicate removals. Storage in 1997 is positive because water levels rebounded after a dry spell in 1996. Numbers are all rounded to the nearest 100 acre-ft. Numbers represent fluxes for the specific year listed.

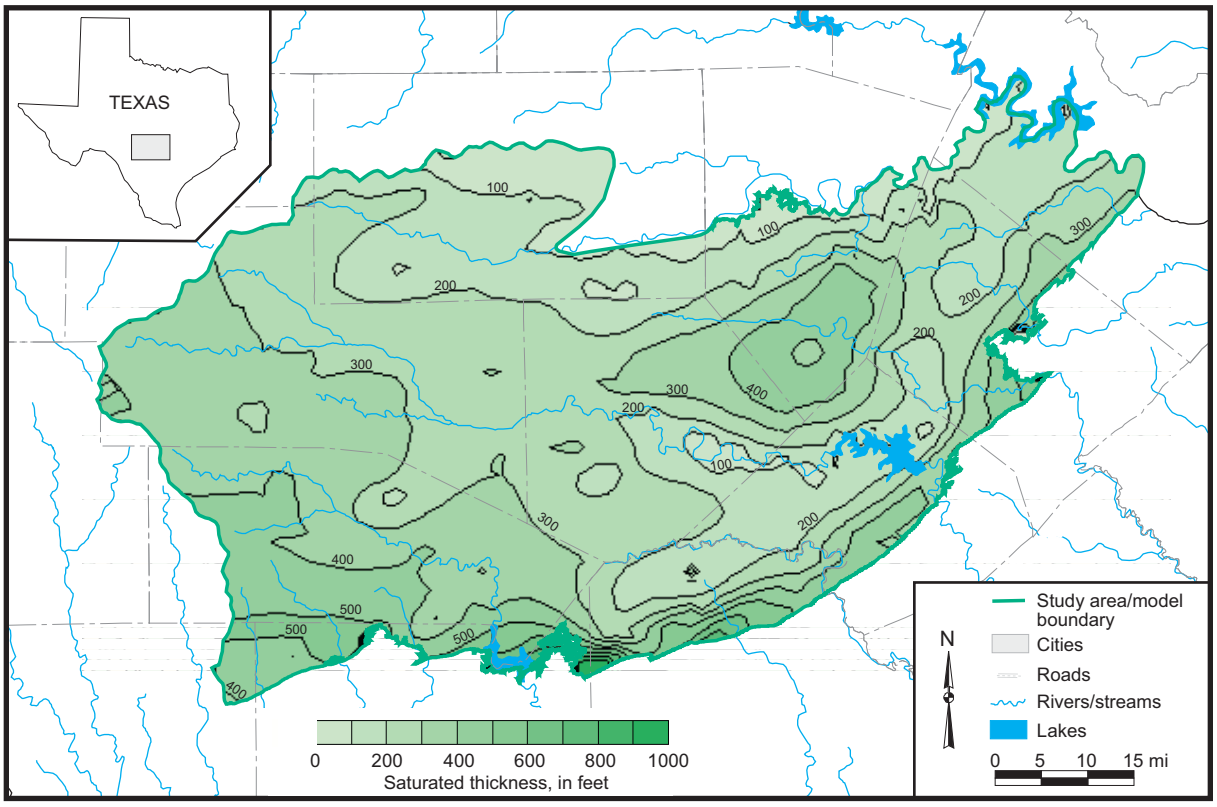

Figure 70. Simulated saturated thickness of the Middle Trinity aquifer in 1997.

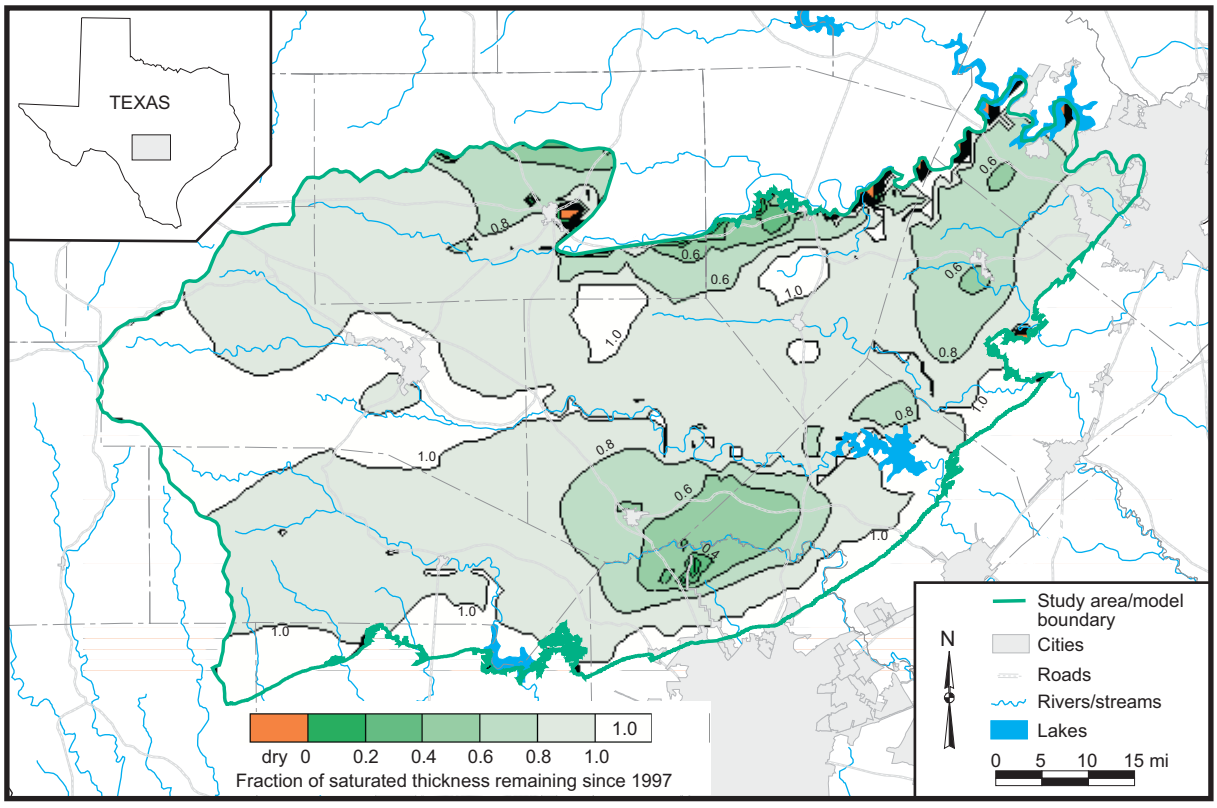

Figure 71. Fraction of saturated thickness of the Middle Trinity aquifer remaining in 2010 with a drought-of-record compared to the saturated thickness in 1997.

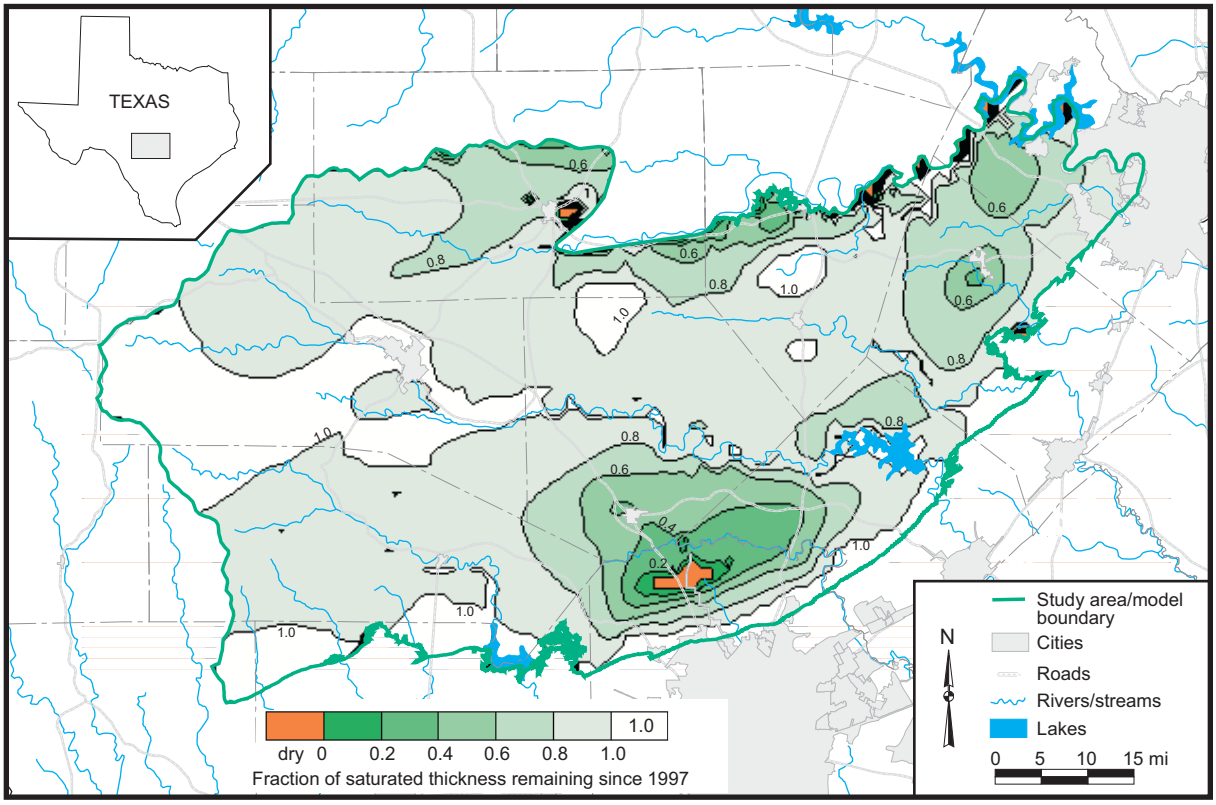

Figure 72. Fraction of saturated thickness of the Middle Trinity aquifer remaining in 2020 with a drought-of-record compared to the saturated thickness in 1997.

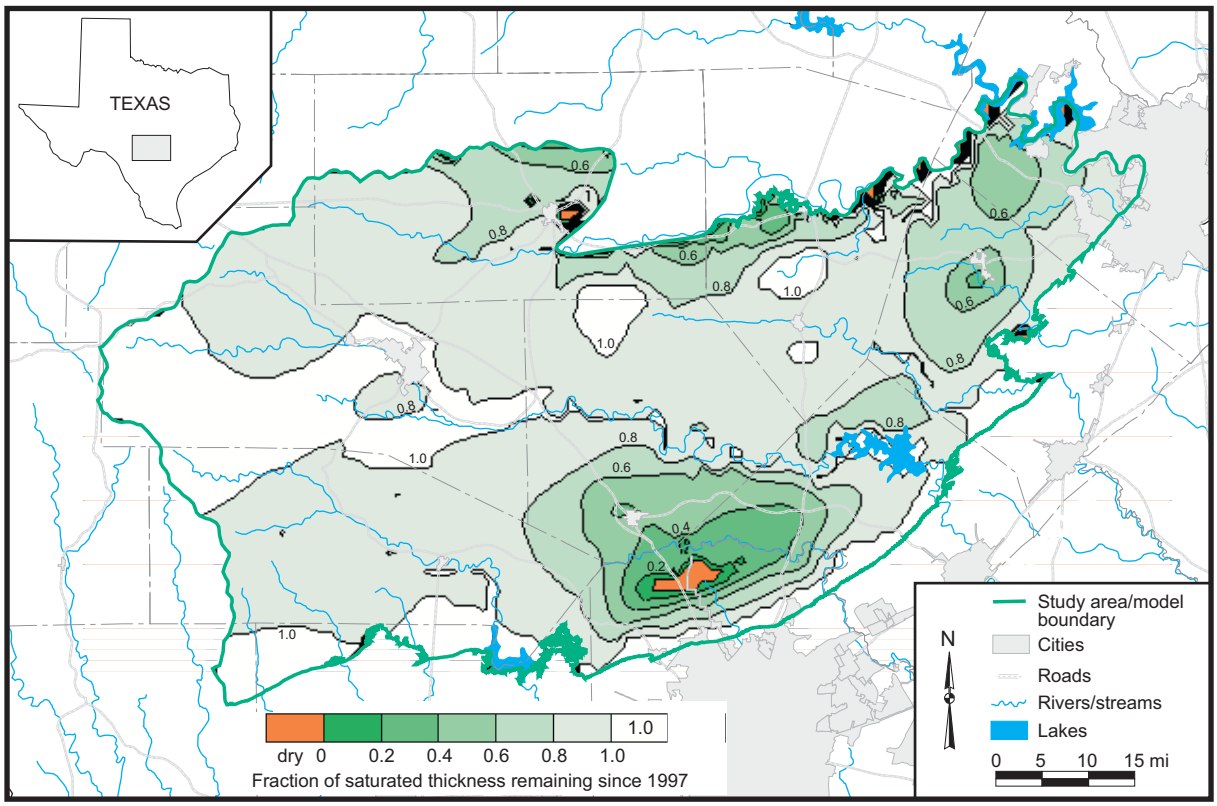

Figure 73. Fraction of saturated thickness of the Middle Trinity aquifer remaining in 2030 with a drought-of-record compared to the saturated thickness in 1997.

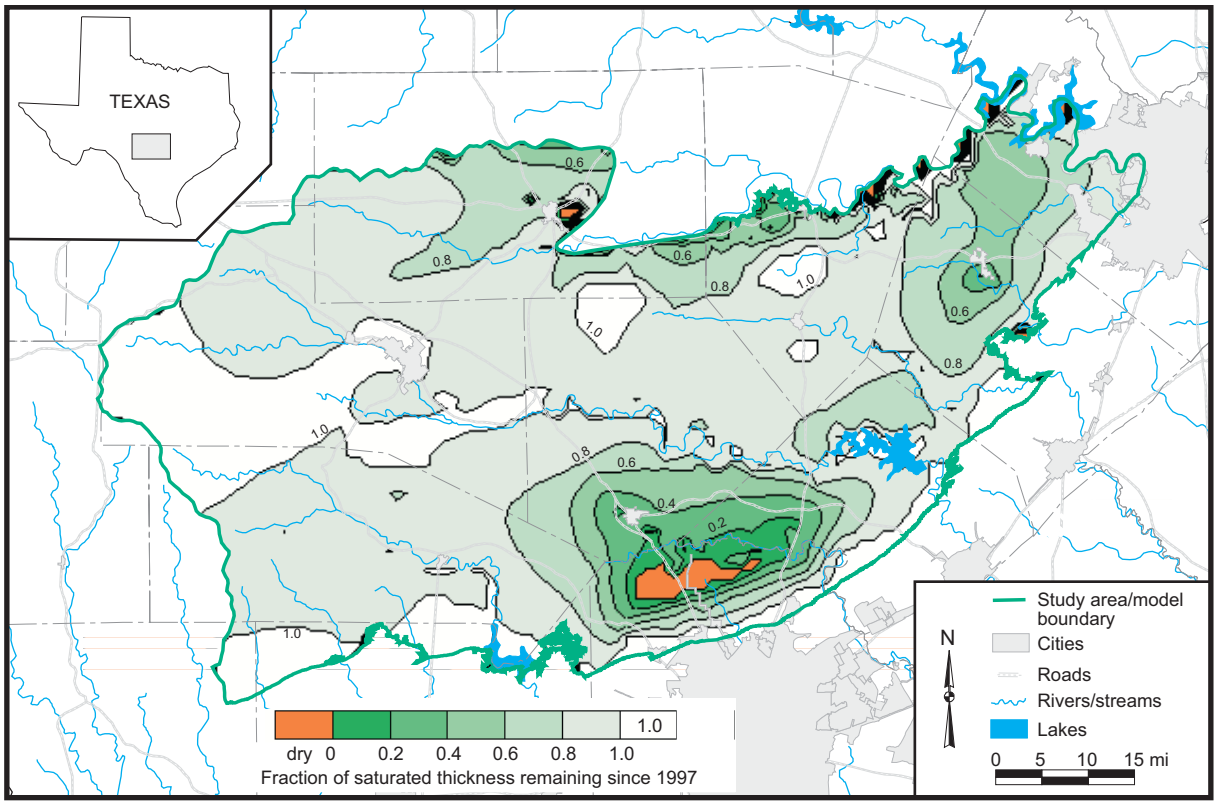

Figure 74. Fraction of saturated thickness of the Middle Trinity aquifer remaining in 2040 with a drought-of-record compared to the saturated thickness in 1997.

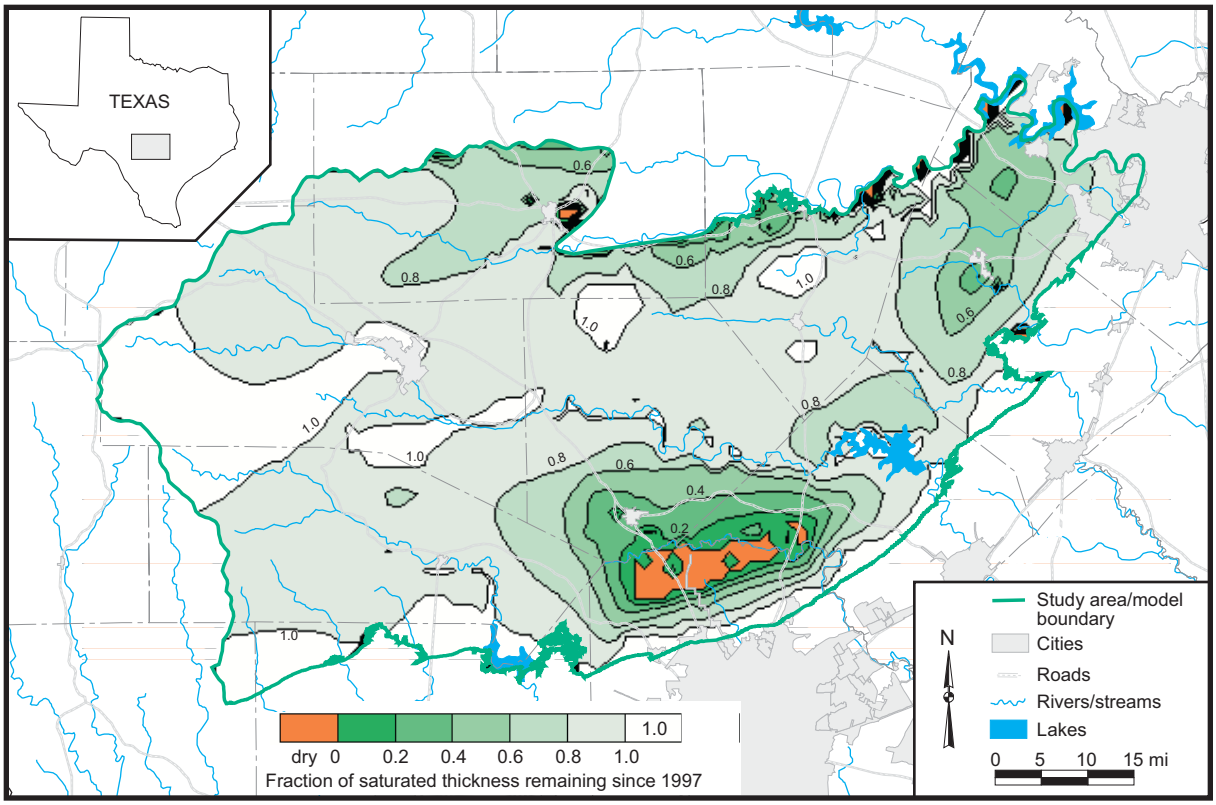

Figure 75. Fraction of saturated thickness of the Middle Trinity aquifer remaining in 2050 with a drought-of-record compared to the saturated thickness in 1997.

septic tank systems, which may leak and recharge the aquifer. Properly designed septic tanks should not allow septic tank effluent to move into the aquifer except during natural recharge events. However, septic tanks can fail to operate as designed and leak effluent into the aquifer. In northern Bexar County, most of these fluids would discharge to the Upper Member of the Glen Rose Limestone, which has a low vertical hydraulic conductivity. Septic-tank effluent could also migrate to the Middle Trinity aquifer through improperly cased wells. Greater recharge in Northern Bexar County (equal to the amount of pumping) results in lower water-level declines in the southern part of the county, but declines greater than 100-ft still result in the Cibolo Creek area.

Water demands developed by the RWPGs are for dry conditions. Therefore, pumping may be overpredicted in the predictive runs for normal conditions. In past State water plans, dry demands were about 2 to 20 percent greater than normal demands with an average difference of about 6 percent (TWDB, 1997). In order to investigate water-level declines with more realistic demands during periods of normal precipitation, we lowered the dry demands by 20 percent. We found that although water-level declines are lower than if we used dry demands, there are still large water-level declines in the aquifer.

Lakes are simulated in the model using constant heads, which assume that the lake level remains the same through time. In reality, lake levels vary with climate and can change substantially (for example, fig. 36). To assess the effect of lake levels on predicted water levels, we removed Medina Lake from the model and found that Medina Lake did not have much influence on water levels in the Middle Trinity aquifer. This is probably because Medina Lake is in contact with the Upper Member of the Glen Rose Limestone, which has a low vertical hydraulic conductivity. However, because Medina Lake is in direct contact with the Upper Member of the Glen Rose Limestone, local groundwater levels in wells completed in the Upper Trinity aquifer can vary concurrently with lake levels.

The Lower Member of the Glen Rose Limestone is highly karstified in the immediate area around Cibolo Creek where it is exposed at land surface between Boerne and Bulverde. Water that flows in Cibolo Creek downstream of Boerne leaks into this karstified zone and flows through this zone to the Edwards (BFZ) aquifer. Because the aquifer in this zone behaves similar to the Edwards (BFZ) aquifer and groundwater in this zone flows into the Edwards (BFZ) aquifer, George (1947), Pearson and others (1975), and Veni (1994, 1995) believe that this karstified zone may be part of the Edwards (BFZ) aquifer. Current maps published by the Edwards Aquifer Authority (EAA) show Cibolo Creek and its immediate area to be part of the recharge zone of the Edwards (BFZ) aquifer (EAA, 1998, exhibit 1.1). Because flow through the karstified zone at Cibolo Creek appears to be part of the Edwards (BFZ) aquifer system, we did not model groundwater flow through this zone. Not including this zone simplified our model because including the zone would have required much more detailed modeling in the area and a dynamic interaction with surface water.

The model predicts that water levels in the Middle Trinity aquifer in the Cibolo Creek area will decrease substantially and potentially deplete the aquifer. In this case, it may be possible that groundwater that flows in the karstified zone could recharge the Trinity aquifer and decrease potential water-level declines. We believe that the amount of recharge to the Trinity aquifer from the karstified zone would be small owing to the large contrast in hydraulic conductivity. Furthermore, recharge to the Trinity aquifer from the karstified zone would only have a local and transient benefit to water levels.

To assess the potential effect of greater recharge in the Cibolo Creek area, we used the River Package with a high conductance to allow

water to move into the aquifer. By using the River Package, we allowed the greatest possible amount of water to recharge the aquifer from the karstified zone during normal climatic conditions. For the drought of record, we decreased the conductance to remove the recharge from the karstified zone (Cibolo Creek rarely flowed during the drought of the 1950s [fig. 34]). The model showed that increased recharge from the karstified zone in the Cibolo Creek area does not affect model predictions for 2050 under drought-of-record conditions.

Limitations of the Model

All numerical groundwater flow models have limitations. These limitations are usually associated with (1) the quality and quantity of input data, (2) assumptions and simplifications used to develop the conceptual and numerical models, and (3) the scale of application of the model.

Input Data

Several of the input data sets for the model are based on limited information. Hydraulic properties, especially for layers 1 and 2, are limited. Although the current information may be fine for the regional model, it may not be applicable for local-scale conditions.

Recharge rates, both the amount and the areal distribution, are limited because they are based on a baseflow analysis that does not cover the entire model area and represents a 26-month period. Because of the relatively short period of baseflow analysis, the recharge coefficients likely represent localized variations specific to the analysis period for baseflow and precipitation and may not represent the long-term distribution of recharge potential. In addition, we assume that the relationship between precipitation and recharge is linear. This relationship may actually be nonlinear. Therefore, we may be underestimating or overestimating recharge in years with different amounts of precipitation. Our current distribution of recharge is based on basins and the distribution of precipitation in 1975. Local attributes, such as soil type and topography, may control recharge at a smaller-than-basin scale. A more accurate distribution of recharge rates could be determined by using more long-term information on baseflow and precipitation and more local attributes of the geology, soils, and topography.

Our structure maps simplify faulting on the southeastern side of the model and smooth out the base of the Middle Trinity aquifer in the northern part of the model. This simplification causes the model to not accurately represent structural control on local groundwater flow in these areas. Greater structural control could be attained with more detailed maps and a finer model grid in this area.

Water-level maps, and therefore the calibration of the model, are affected by limited information, especially in layers 1 and 2 where there are few measurements. Layer 3 has the greatest number of measurements, but not many in the western and northeastern parts of the model. Limited water-level measurements bias model calibration to areas where water levels have been measured.

We were only able to assemble pumping information for two years for the transient calibration. A longer time period for transient calibration would increase confidence in the predictive abilities of the model. Because the calibration of the transient model ends at the end of 1997, the model could be run to see how well it predicts water-level declines from 1997 to present. This post-audit would also offer insight into the accuracy of model predictions.

Assumptions

We used several assumptions to simplify construction of the model. The most important assumptions are: (1) there is no flow between the Middle and Lower Trinity aquifers and (2) the Drain Package of MODFLOW can be used to simulate discharge to streams and rivers.

Most of the bottom of the model is under-

lain by the Hammett Shale (Amsbury, 1974; Barker and Ardis, 1996), which is relatively impermeable and serves as a hydrologic barrier between the Lower and Middle Trinity aquifers (Ashworth, 1983, p. 27). However groundwater flow between the Middle and Lower Trinity aquifers occurs in some parts of the study area. In the outcrop area of the Middle Trinity aquifer in Gillespie County, some of the recharge moves into the Lower Trinity aquifer. We tested the sensitivity of the model to increased recharge (a part of which would move into the Lower Trinity aquifer) and found that the model was not sensitive to increased recharge in this area. Some groundwater likely moves from the Middle Trinity aquifer into the Lower Trinity aquifer through the Hammett Shale. However, the volume of flow is probably small compared to flow through the rest of the aquifer.

We used the Drain Package of MODFLOW to simulate streams and rivers in the study area. The Drain Package allows water to move from the aquifer to the streams and rivers but not from the streams and rivers into the aquifer. Therefore, we assumed that the streams and rivers are gaining and will remain gaining in the future. Predictive simulations though 2050 under drought-of-record conditions show that streams and rivers in the study area may remain gaining streams, although with less flow. Therefore, the Drain Package appears to accurately model surface-water/groundwater interaction. As discussed earlier, the River Package appeared to add too much water to the aquifer under certain conditions. Future updates of this model might include the Stream-flow Routing Package (Prudic, 1988) which would limit the amount of water rivers and streams could leak into the aquifer.

Scale of Application

The limitations described above and the inherent nature of regional groundwater flow models affect the scale of application of the model. This model is most accurate in assessing regional-scale groundwater issues such as predicting aquifer-wide water-level declines over the next fifty years and the relative comparison of water management scenarios. Accuracy and applicability of the model decreases when moving from the regional to the local scale. This is due to limitations of the information in the model (described above) and the 1-mile by 1-mile size of the cells in the model. For example, the model will not likely accurately predict water-level declines in and around a single well in a community. These water-level declines are too dependent on site-specific hydraulic properties: information the model does not include. The model is more likely to accurately predict water-level declines of a group of wells in a general, multiple square mile area. Such local-scale issues need to be addressed with a more detailed numerical model with local estimates of hydraulic properties or analytical equations. The model predicts declines in ambient water levels in the aquifer due to pumping, not the actual water-level decline in an individual well (which will be much larger).

Conclusions

We developed a numerical groundwater flow model using MODFLOW that can be used to predict water-level changes in response to pumping and potential future droughts. The model has three layers (Edwards Group in the plateau area, the Upper Trinity aquifer, and the Lower Trinity aquifer) and 9,262 active cells. We developed the conceptual model of groundwater flow and defined aquifer properties based on a review of previous work and studies we conducted on water levels, structure, recharge, and hydraulic properties. Our modeling approach included (1) calibrating a steady-state model for 1975 hydrologic conditions when the aquifer was near steady-state, (2) calibrating a transient model for 1996 and 1997 when the climate transitioned from a dry to a wet period, and (3) using the calibrated model to predict groundwater availability through 2050 under drought conditions.

The calibrated model does a reasonable job of matching the water-level distribution and water-level fluctuations in the aquifer (RMS error is 56-ft, about five percent of the hydraulic-head drop across the study area). Calibration of the steady-state model resulted in an average recharge rate of about four percent of mean annual precipitation and a geometric mean hydraulic conductivity of 7.5 ft/day for the Middle Trinity aquifer. Water levels in the model are most sensitive to changes in (1) recharge, (2) horizontal hydraulic conductivity of the Middle Trinity aquifer, and (3) vertical hydraulic conductivity of the Upper Trinity aquifer. The model predicts that about 64,000 acre-ft/yr of water moves from the Upper and Middle Trinity aquifers to the Edwards (BFZ) aquifer. We also calibrated values of vertical hydraulic conductivity, specific storage, and specific yield for the aquifer.

To assess the future availability of groundwater in the Trinity aquifer for the Hill Country area, we used the calibrated model to predict future water levels under drought-of-record conditions using estimates of future groundwater demands based on demand numbers from the Regional Water Planning Groups. The model predicts that water levels will decline in response to increased groundwater pumping and to drought-of-record conditions. According to the model, the largest water-level declines (>100-ft) occur in the Cibolo Creek area in northern Bexar, western Comal, and southern Kendall counties. The model also predicts that water levels could decline nearly 100 ft in the Dripping Springs area. The model shows moderate water-level declines (50 to 100 ft) in response to greater demands and potential drought in parts of Hays, Blanco, Travis, southeastern Kerr, and eastern Bandera counties. Under drought-of-record conditions, much of the study area is affected by declining water levels. However, the model suggests relatively smaller water-level declines in low-lying areas near historically gaining streams. Even in the unlikely event that the Hill Country does not experience a drought over the next 50 years, the model indicates that there may still be large water-level declines in the aquifer.

A numerical groundwater flow model is an approximation of the actual aquifer. The accuracy and applicability of the model is affected by limited information on the aquifer, simplifying assumptions used to develop the model, and the size of cells in the model. Furthermore, model predictions are limited by assumptions of future climate and future pumping. This model is meant to simulate regional groundwater flow and predict regional effects of increased pumping and drought. The model should not be expected to reproduce water-level declines in and around individual wells or localized groups of wells. Additional aquifer studies and subsequent recalibration of the model will improve model performance and increase its accuracy.

Even with the limitations inherent in developing groundwater models, we believe that the predictive results of the model are reasonable. Conclusions based on model results agree with observations and predictions made by Ashworth (1983), Bluntzer (1992), Simpson and others (1993), and Kalaswed and Mills (2000). Furthermore, since model results were presented in March of 2000 (TWDB, 2000), an ongoing drought in the Hill Country coupled with increased pumping has (1) resulted in wells going dry in Sunset Canyon east of Dripping Springs (Scheibal and Kelley, 2000), (2) lowered water levels 80 ft below normal in Boerne (MacCormack, 2000), and (3) caused Jacob's Well, an artesian spring in Wimberley, to stop flowing in August (Scheibal, 2000) for the first time in recorded history.

Acknowledgments

In any major modeling effort, there are many people to acknowledge for their assistance. First and foremost, we thank the members of the Trinity Aquifer Advisory Committee assembled for this project, which includes members of the Plateau, Lower Colorado, and South Central Texas Regional Water Planning Groups, for

their support, interest, assistance, and suggestions during the modeling effort. We also thank Pam Hodges of the Guadalupe-Blanco River Authority for organizing opportunities for us to present results of the modeling efforts and Dr. Weldon Hammond of The University of Texas at San Antonio for providing facilities to present results and train people on how to use the model.

A number of TWDB staff members have been very helpful in assembling the needed information for the model: Cindy Ridgeway, Ted Angle, and Teresa Howard on pumping; Randy Williams on structure; Wayne Tschirhart and Nadira Kabir on surface water; Mike Harren on hydraulic properties; Tom Culhane on water levels and boundary conditions; Doug Coker, Steve Moore, and John Derton on aquifer testing; Ann Omoegbele on administrative duties; Zelphia Bloodworth and Mike McCathern for layout and printing of the final document. We thank Paul Tybor of the Hill Country Groundwater Conservation District, Cameron Cornett of the Springhills Water Management District, and John Ashworth of LBG Guyton Associates for data and many helpful discussions. The support of our management, including Harald Petrini, William Mullican, Tommy Knowles, and Craig Pedersen, has been very helpful in ensuring the successful completion of this project.

Acronyms

BFZ	Balcones Fault Zone
DEM	Digital elevation model
GHB	General-head boundary
GIS	Geographical Information System
RMS	Root-mean squared
TIN	Triangulated irregular network
TNRCC	Texas Natural Resource Conservation Commission
TWDB	Texas Water Development Board
USGS	United States Geological Survey
WUD	Water Use Division
WUS	Water Use Survey

References

Amsbury, D. L., 1974, Stratigraphic petrology of Lower and Middle Trinity rocks on the San Marcos platform, south-central Texas: *in* Perkins, B. F., ed., Aspects of Trinity division geology - a symposium: Louisiana State University, Geoscience and Man, v. 8, p. 1-35.

Anderson, M. P., and Woessner, W. W., 1992, Applied groundwater modeling - Simulation of flow and advective transport: Academic Press, Inc., San Diego, 381 p.

Ardis, A. F., and Barker, R. A., 1993, Historical saturated thickness of the Edwards-Trinity aquifer system and selected contiguous hydraulically connected units, west-central Texas: U.S. Geological Survey Water-Resources Investigation Report 92-4125, 2 plates.

Arnold, J. G., Allen, P. M., Muttiah, R., and Bernhardt, G., 1995, Automated base flow separation and recession analysis techniques: Ground Water, v. 33, no. 6, p. 1010-1018.

Ashworth, J. B., 1983, Ground-water availability of the Lower Cretaceous formations in the Hill Country of south-central Texas: Texas Department of Water Resources Report 273, 173 p.

Ashworth, J. B., and Hopkins, Janie, 1995, Aquifers of Texas: Texas Water Development Board Report 345, 69 p.

ASTM, 1994, Standard guide for conducting a sensitivity analysis for a ground-water flow model application: American Society for Testing and Materials Standard D5611-94e1, 6 p.

Autodesk, 1997, AutoCad Map 2.0, Autodesk, Inc., San Rafael, CA.

Barker, R. A. and Ardis, A. F., 1992, Configuration of the base of the Edwards-Trinity aquifer system and hydrogeology of the underlying pre-Cretaceous rocks, west central Texas: U.S. Geological Survey Water Resources Investigation Report 91-4071, 25 p.

Barker, R. A., and Ardis, A. F., 1996, Hydrogeologic framework of the Edwards-Trinity aquifer system, west-central Texas: U.S. Geological Survey Professional Paper 1421-B, 61 p. with plates.

Barker, R. A., Bush, P. W., and Baker, E. T., Jr., 1994, Geologic history and hydrogeologic setting of the Edwards-Trinity aquifer system, west central Texas: U.S. Geological Survey Water Resources Investigation Report 94-4039, 50 p.

Barnes, V. E., 1981, Geologic Atlas of Texas - Llano Sheet: Bureau of Economic Geology, The University of Texas at Austin.

Barrett, M. E., and Charbeneau, R. J., 1996, A parsimonious model for simulation of flow and transport in a karst aquifer: Center for Research in Water Resources, The University of Texas at Austin, Technical Report CRWR 269, 149 p.

Bluntzer, R. L., 1992, Evaluation of Ground-water Resources of the Paleozoic and Cretaceous Aquifers in the Hill Country of Central Texas: Texas Water Development Board Report 339, 130 p.

Bradley, R. G., Coker, D. B., and Moore, S. W., 1997, Data and results from an aquifer test performed at the Medina Water Supply Corporation well field, Medina, Texas: Texas Water Development Board Open-File Report 97-02, 25p.

Brown, T. E., Waechter, N. B., and Barnes, V. E., 1974, Geologic Atlas of Texas - San Antonio Sheet: Bureau of Economic Geology, The University of Texas at Austin.

Brune, Gunnar, 1981, Springs of Texas, Volume 1: Branch-Smith Inc., Fort Worth, Texas, 566 p.

Bush, P. W., Ardis, A. F., and Wynn, K. H., 1993, Historical potentiometric surface of the Edwards-Trinity aquifer system and contiguous hydraulically connected units, west-central Texas: U.S. Geological Survey Water-Resources Investigations Report 92-4055, 3 sheets.

Carr, J. T., Jr., 1967, The climate and physiography of Texas: Texas Water Development Board Report 53, 27 p.

Chiang, W.-H., and Kinzelbach, Wolfgang, 1998, Processing Modflow- A simulation system for modeling groundwater flow and pollution: software manual, 325 p.

Clark, Isobel, 1979, Practical geostatistics: Applied Science Publishers, Limited, London, 129 p.

Cooper, H. H., Jr., and Jacob, C. E., 1946, A generalized graphical method for evaluating formation constants and summarizing well field history: American Geophysical Union Transactions, v. 27, p. 526-534.

EAA, 1998, Groundwater management plan- 1998-2008: San Antonio, Texas, Edwards Aquifer Authority.

Elliot, W. R., and Veni, G., 1994, The Caves and Karst of Texas- A guidebook for the 1994 Convention of the National Speleological Society with Emphasis on the Southwestern Edwards Plateau: National Speleological Society, 342 p.

Espey, Huston, and Associates, 1989, Medina Lake hydrology study: Report to the Edwards Underground Water District, 56 p.

Espey, Huston, and Associates, 1982, Feasibility study of recharge facilities on Cibolo Creek: Draft consulting report to the Edwards Underground Water District, 56 p.

ESRI, 1991, ARC/INFO, Version 6.0: Environmental Systems Research Institute, Inc., Redlands, California.

Feinstein, D. T., and Anderson, M. P., 1987, Recharge to and potential for contamination of an aquifer system in northeastern Wisconsin: Wisconsin Water Resources Center, Technical Report 87-01, 173 p.

Freeze, R. A., and Cherry, J. A., 1979, Groundwater: Prentice-Hall, Inc., Englewood Cliffs, New Jersey, 604 p.

George, W. O. ,1947, Geology and ground-water resources of Comal County, Texas: Texas Board of Water Engineers, 142 p.

Golden Software, 1995, Surfer for Windows, Version 6, Contouring and 3D surface mapping: Golden Software, Inc., Golden, Colorado, variously paginated.

Guyton, W. F. , and Associates, 1958, Memorandum on ground-water gains in upper Cibolo Creek area: Consulting report to the San Antonio City Water Board, 8 p.

Guyton, W. F. , and Associates, 1970, Memorandum on Cibolo Creek studies: Consulting report to the San Antonio City Water Board, 17 p.

Guyton, W. F. and Associates, 1993, Northern Bexar County water resources study for the Edwards Underground Water District- Volume 1: Ground water: final report to the Edwards Underground Water District, San Antonio, Texas, 66 p., tables and figures.

Halihan T., Sharp, J. M., Jr., and Mace, R. E., 1999, Interpreting flow using permeability at multiple scales: in Karst Modeling: Karst Water Institute Special Publication 5, p. 82-96.

Hammond, W. W., 1984, Hydrogeology of the Lower Glen Rose Aquifer, South-Central Texas: Ph.D. dissertation, The University of Texas at Austin. 243 p.

Harbaugh, A.W., and McDonald, M.G., 1996, User's documentation for MODFLOW-96, an update to the U.S. Geological Survey modular finite-difference ground-water flow model: U.S. Geological Survey Open-File Report 96-485, 56 p.

Hubert, Martin, 1999, Senate Bill 1 - The first big bold step toward meeting Texas's future water needs: Texas Tech Law Review, v. 30, no. 1, p. 53-70.

Huntoon, P. W., 1995, Is it appropriate to apply porous media ground water circulation models to karstic aquifers? *in* El-Kadi, A. I., ed., Assessment of models for groundwater resource analysis and management: Boca Raton, Lewis Publishers, p. 339–358.

Kalaswad, Sanjeev, and Mills, K. W., 2000, Evaluation of northern Bexar County for inclusion in the Hill Country Priority Groundwater Management Area: Austin, Texas, Priority Groundwater Management Area Report, Texas Natural Resource Conservation Commission, 82 p.

Kastning, E. H., 1986, Cavern development in the New Braunfels area, central Texas: *in* Abbott, P. L., and Woodruff, C. M., Jr., eds., The Balcones escarpment, geology, hydrology, ecology and social development in central Texas: Geological Society of America, p. 91-100.

Klemt, W. B., Knowles, T. R., Elder, G. R., and Sieh, T. W., 1979, Ground-water resources and model applications for the Edwards (Balcones Fault Zone) aquifer in the San Antonio region, Texas: Texas Department of Water Resources Report 239, 88 p.

Konikow, L. F., 1978, Calibration of ground-water models: *in* Verification of Mathematical and Physical Models in Hydraulic Engineering, American Society of Civil Engineers, N.Y., p. 87-93.

Kruseman, G. P., and de Ridder, N. A., 1994, Analysis and evaluation of pumping test data, second edition: International Institute for Land Reclamation and Improvement, The Netherlands, 377 p.

Kuniansky, E.L., 1989, Precipitation, streamflow, and baseflow, in west-central Texas, December 1974 through March 1977: U.S. Geological Survey Water-Resources Investigations Report 89-4208, 2 sheets.

Kuniansky, E. L., 1990, Potentiometric surface of the Edwards-Trinity aquifer system and contiguous hydraulically connected units, west-central Texas, winter 1974-75: U.S. Geological Survey Water-Resources Report 89-4208, 2 sheets.

Kuniansky, E. L., and Holligan, K. Q.,1994, Simulations of flow in the Edwards–Trinity aquifer system and contiguous hydraulically connected units, west-central Texas: U. S. Geological Survey Water-Resources Investigations Report 93-4039, 40 p.

LBG-Guyton Associates, 1995, Edwards/Glen Rose hydrologic communication, San Antonio region, Texas: final report submitted to the Edwards Underground Water District, 38 p. with 7 tables, 13 figures and 4 appendices.

Long, A. T., 1962, Ground-water geology of Edwards County, Texas: Texas Water Commission Bulletin 6208, 123 p.

Lowry, R. L., 1955, Recharge to Edwards ground-water reservoir: Consulting report to the San Antonio City Water Board, 66 p.

Lurry, D. L., and Pavlicek, D. J., 1991, Withdrawals from the Edwards-Trinity aquifer system and contiguous hydraulically connected units, west-central Texas, December 1974 through March 1977: U.S. Geological Survey Water-Resources Investigations Report 91-4021, 1 sheet.

MacCormack, Zeke, 2000, Boerne restricts water use: San Antonio Express-News, July, 19, 2000.

Mace, R. E., Chowdury, A. H., Anaya, R., and Way, S.-C., 2000, A numerical groundwater flow model of the Upper and Middle Trinity aquifer, Hill Country area: Texas Water Development Board Open File Report 00-02, 62 p.

Maclay, R. W., and Land, L. F., 1988, Simulation of flow in the Edwards aquifer, San Antonio Region, Texas, and refinements of storage and flow concepts: U. S. Geological Survey Report Water-Supply Paper 2336, 48 p.

Maclay, R. W., and Small, T. A., 1986, Carbonate geology and hydrology of the Edwards aquifer in the San Antonio area, Texas: Texas Water Development Board Report 296, 90 p.

McCuen, R. H., and Snyder, W. M., 1986, Hydrologic modeling - statistical methods and applications: Prentice Hall, Englewood Cliffs, New Jersey, 568 p.

McDonald, M. G. and A. W. Harbaugh, 1988, A modular three-dimensional finite-difference ground-water flow model: U.S. Geological Survey Techniques of Water-Resources Investigations, book 6, variously paginated.

Meyers, B.N., 1969, Compilation of results of aquifer tests in Texas: Texas Water Development Board Report 98, 532 p.

Muller, D. A. and Price, R. D., 1979, Ground-water Availability in Texas, Estimates and Projections Through 2030: Texas Department of Water Resources Report 238, 77 p.

Nathan, R. J., and McMahon, T. A., 1990, Evaluation of automated techniques for baseflow and recession analysis: Water Resources Research, v. 26, no. 7, p. 1465-1473.

Pearson, F. J., Jr., Rettman, P. L., and Wyerman, T. A., 1975, Environmental tritium in the Edwards Aquifer, central Texas, 1963-71: U.S. Geological Survey Open-File Report 74-362, 32 p.

Proctor, C. V., Jr., Brown, T. E., McGowen, J. H., Waechter, N. B., and Barnes, V. E., 1974a, Geologic Atlas of Texas - Austin Sheet: Bureau of Economic Geology, The University of Texas at Austin.

Proctor, C. V., Jr., Brown, Waechter, N. B., Aronow, S., and Barnes, V. E., 1974b, Geologic Atlas of Texas - Seguin Sheet: Bureau of Economic Geology, The University of Texas at Austin.

Prudic, D. E., 1988. Documentation of a computer program to simulate stream-aquifer relations using a modular, finite-difference, ground-water flow model, U.S. Geological Survey, Open-File Report 88-729, Carson City, Nevada.

Riggio, R. F., Bomar, G. W., and Larkin, T. J., 1987, Texas drought- its recent history (1931-1985): Texas Water Commission LP 87-04, 74 p.

Rogers, B. G., 1981, Glossary- Water and wastewater control engineering: Washington, D.C. American Public Health Association, 441 p.

Rovey, C. W., II, 1994, Assessing flow systems in carbonate aquifers using scale effects in hydraulic conductivity: Environmental Geology, v. 24, p. 244–253.

Scheibal, S., 2000, Austin's hottest day ever: Austin American-Statesman, September 5, 2000.

Scheibal, S., and Kelley, M., 2000, Some wells in Central Texas already running dry as drought predicted to extend into summer: Austin American-Statesman, April 29, 2000.

Senger, R. K., and Kreitler, C. W., 1984, Hydrogeology of the Edwards Aquifer, Austin area, Central Texas: The University of Texas at Austin, Bureau of Economic Geology Report of Investigations No. 141, 35 p.

Simpson and others, 1993, North Bexar County water resources study for the Edwards Underground Water District- Executive summary: San Antonio, Texas, final report by W. E. Simpson Company, Inc. in association with William F. Guyton and Associates, Inc. for the Edwards Underground Water District, variously paginated.

Slade, R. M., Jr., Ruiz, Linda, and Slagle, Diana, 1985, Simulation of the flow system of Barton Springs and associated Edwards Aquifer in the Austin area, Texas: U.S. Geological Survey Water-Resources Investigations Report 85-4299.

Stein, E. G., and Klemt, W. B., 1995, Edwards/Glen Rose hydrologic communication, San Antonio region, Texas: report prepared for the Edwards Underground Water District by LBG-Guyton Associates, Austin, TX, variously paginated.

Stoertz, M. W., and Bradbury, K. R., 1989, Mapping recharge areas using a ground-water flow model - a case study: Ground Water, v. 27, no. 2, p. 220-229.

Teutsch, Georg, and Sauter, Martin, 1991, Groundwater modeling in karst terranes—scale effects, data acquisition, and field validation: Proceedings of the Third Conference on Hydrology, Ecology, Monitoring, and Management of Ground Water in Karst Terranes, Nashville: U.S. Environmental Protection Agency and National Ground Water Association, p. 17–34.

Theis, C. V., 1935, The relation between the lowering of the piezometric surface and the rate and duration of discharge of a well using groundwater storage: American Geophysical Union Transaction, v. 16, p. 519–524.

Theis, C. V., 1963, Estimating the transmissivity of a water-table aquifer from the specific capacity of a well: U.S. Geological Survey Water Supply Paper 1536-I, p. 332-336.

TWDB, 1997, Water for Texas: Texas Water Development Board, document No. GP-6-2, variously paginated.

TWDB, 2000, Texas Water Development Board presents results of computer model of the Trinity aquifer in the Hill Country area: Texas Water Development Board, March 17, 2000, press release, 1 p. with attachment.

Veni, G., 1994, Geomorphology, hydrology, geochemistry, and evolution of karstic Lower Glen Rose aquifer, south-central Texas: Pennsylvania State University, Ph.D. Dissertation, 712 p.

Veni, G., 1995, Revising the boundaries of the Edwards (Balcones Fault Zone) aquifer recharge zone: Water for Texas, Proceedings of the 24th Water for Texas Conference, p. 99-107.

Walker, L. E., 1979, Occurrence, availability, and chemical quality of ground water in the Edwards Plateau Region of Texas: Texas Department of Water Resources Report 235, 336 p.

Wanakule, Nisai, and Anaya, Roberto, 1993, A lumped parameter model for the Edwards aquifer: Texas A&M University, Texas Water Resources Institute, Technical Report No. 163, 84 p.

Waterreus, P. A., 1992, Hydrogeology of the Camp Bullis area, northern Bexar County, Texas: Master's thesis, The University of Texas at San Antonio, 186 p.

W.E. Simpson Company, Inc. and W.F. Guyton Associates, Inc., 1993, North Bexar County Water Resources Study for the Edwards Underground Water District: v. 1 and 2, unpaginated.

Wilson, W. E., and Moore, J. E., 1998, Glossary of hydrology: American Geological Institute, Alexandria, Virginia, 248 p.

Woodruff, C. M., Jr., and Abbott, P. L., 1986, Stream piracy and evolution of the Edwards aquifer along the Balcones escarpment, Central Texas: in Abbott, P. L., and Woodruff, C. M., Jr., The Balcones Escarpment, Central Texas: Geological Society of America, p. 77-90.

Young, K., 1972, Mesozoic history, Llano region: in Barnes, V. E., Bell, W. C., Clabaugh, S. E., and Cloud, P. E., eds., Geology of the Llano region and Austin area, field excursion, The University of Texas at Austin, Bureau of Economic Geology Guidebook 13, 77 p.